23-26th November 2021, IMPT, Lyon, France

Detection, dynamics and impact of landslides

Anne Mangeney[1,1']

with specialists in seismology (C. Hibert, E. Stutzmann, Y. Capdeville, C. Levy, J. P. Montagner, etc.), mathematics (F. Bouchut, E. Fernandez-Nieto, G. Narbona-Reina, J. Sainte-Marie, J. Garres, J. Delgado-Sanchez), acoustics (J. De Rosny, X. Jia, R. Toussaint), etc.

[1] Institut de Physique du Globe de Paris, Université de Paris

[1'] Equipe ANGE INRIA-Laboratoire Jacques Louis Lions

Outline

I – Introduction : Natural landslides and their simulation

Ia – Geophysics and mathematics
Ib – Complexity and variability of natural landslides
Ic – Examples of landslide simulations for hazard assessment
Id – Challenges in geophysics and landslide modelling

II – Thin layer depth-averaged models for field-scale simulation

IIa – Thin layer approximation for granular flows
IIb – Accounting for complex topography
IIc – Need of two different reference frames for landslide tsunamis
IId – Application to real landslides : unexplained high mobility

III – Back to lab-scale experiments and simulation

IIIa – Granular column collapse on rigid and erodible beds
IIIb – $\mu(I)$ rheology in 2D models, comparison with other models (DEM, thin-layer)
IIIc – Static-flowing interface (erosion/deposition)
IIId – Grain-fluid mixture model

IV – Landslide detection/characterization from generated seismic waves

IVa – Inversion/simulation of low frequency landslide forces
IVb – Insight from high frequency data through lab-experiments
IVc – Monitoring landslide activity in link with volcanic activity
IVd – Similar approach for glacial earthquakes and ice-mass loss quantification

Key elements to address geophysical problems

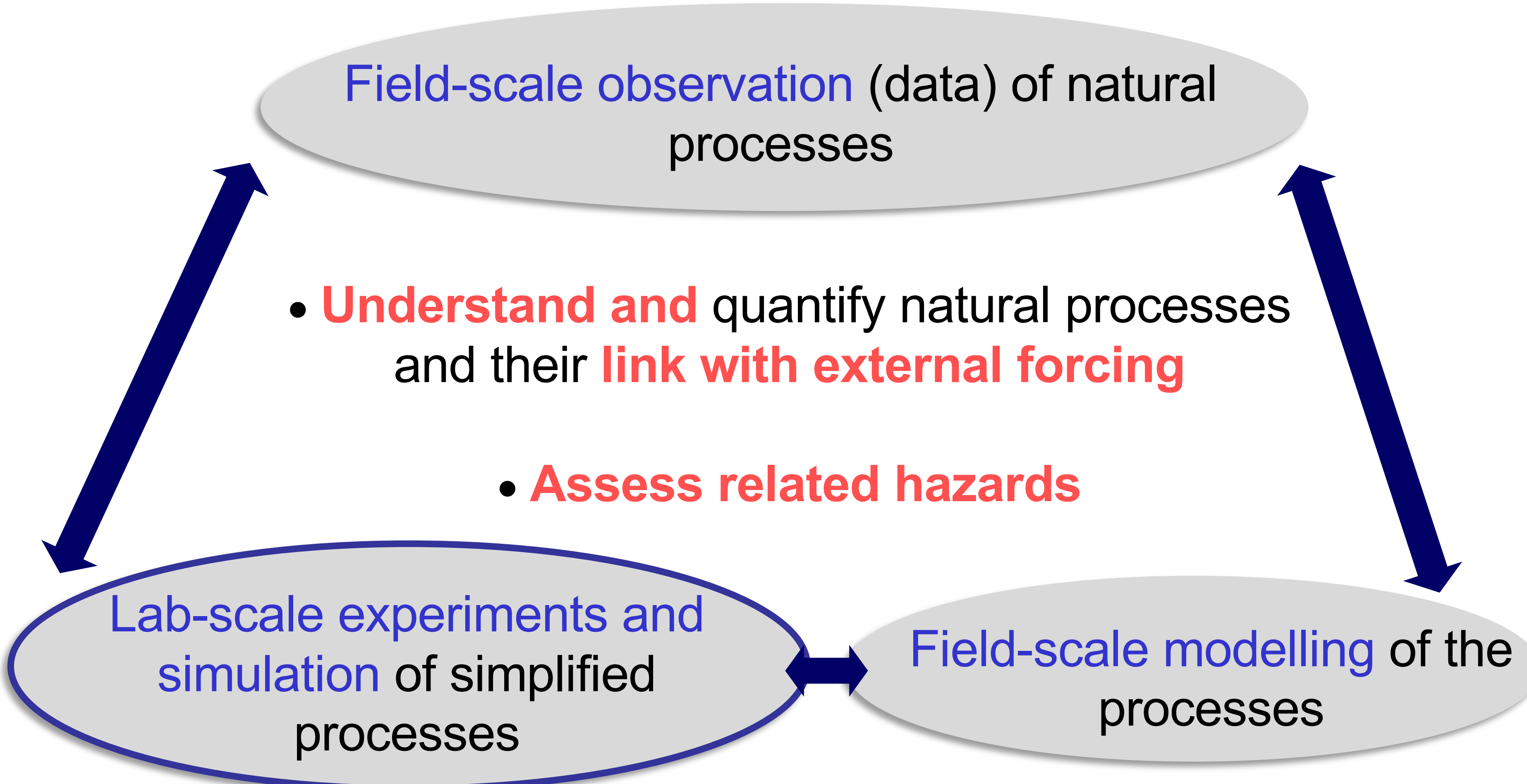

Strong need of mathematical modelling, numerical methods, data analysis, signal processing, Machine Learning, statistics, surrogate models, uncertainty quantification, data assimilation, etc.

Different physical processes

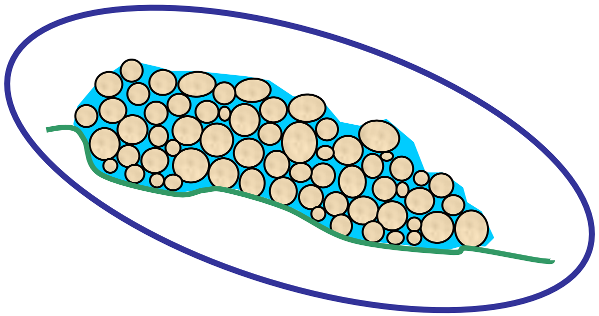

Fluid phase
(water, mud)

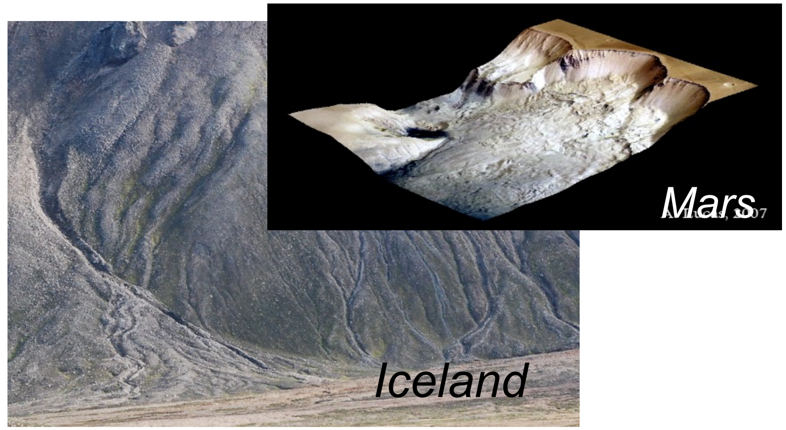

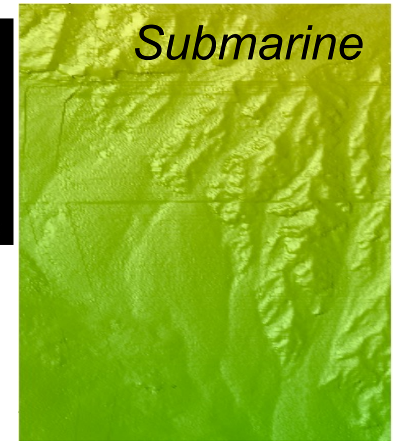

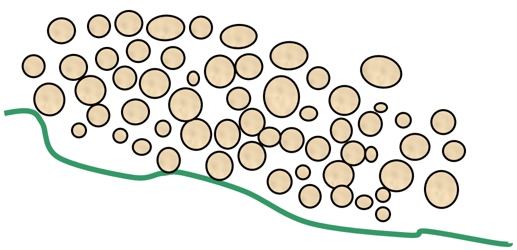

Fluidisation (gas, air)

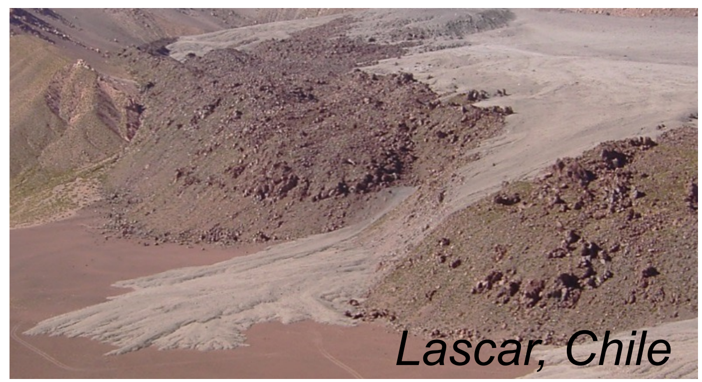

// snow avalanches

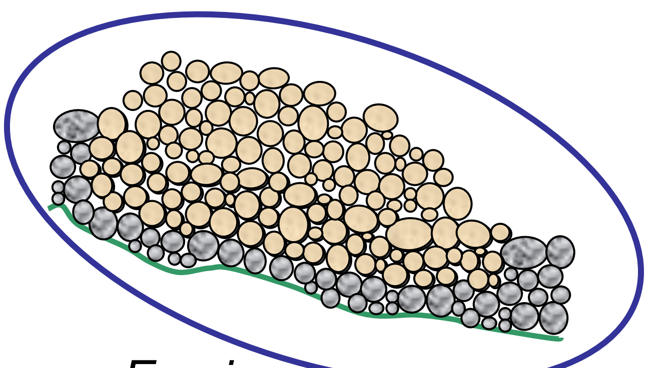

Erosion

// rivers,
glaciers

From field to laboratory scale

Natural flows
km^3

Same physical processes ?

Laboratory granular flows
cm^3

Heterogeneous materials
Few **field data**

Numerical simulation

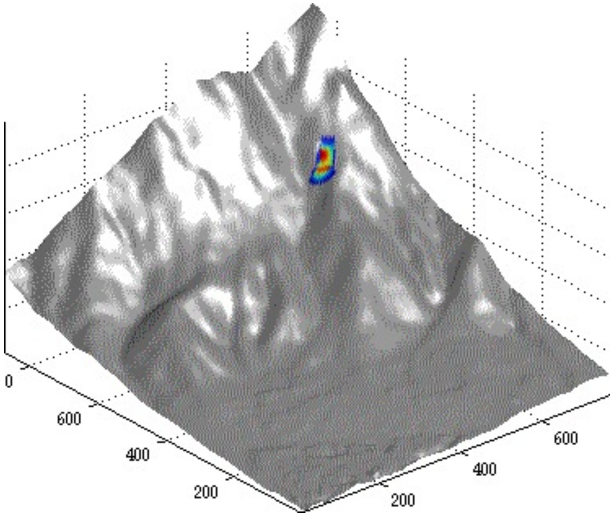

Velocity and thickness
measurements

A lot of laboratory experiments !

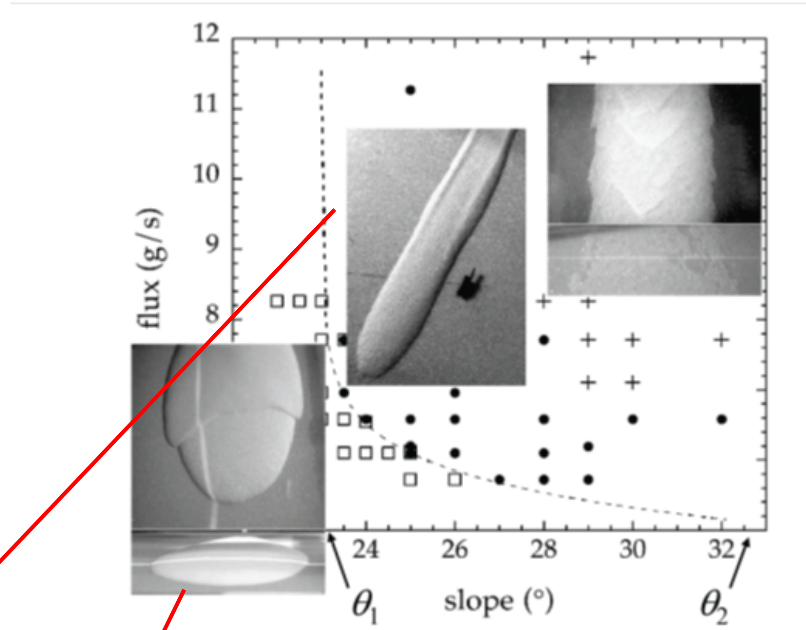

Laboratory experiments

Félix and Thomas, 2007

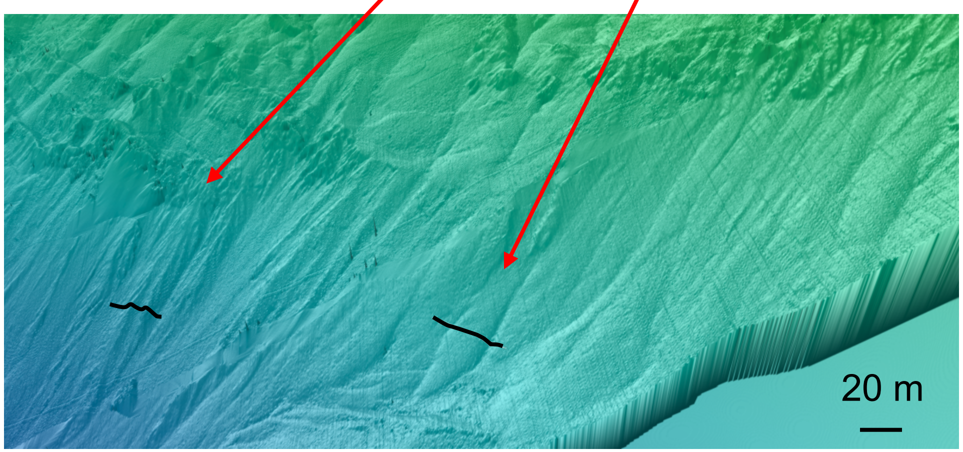

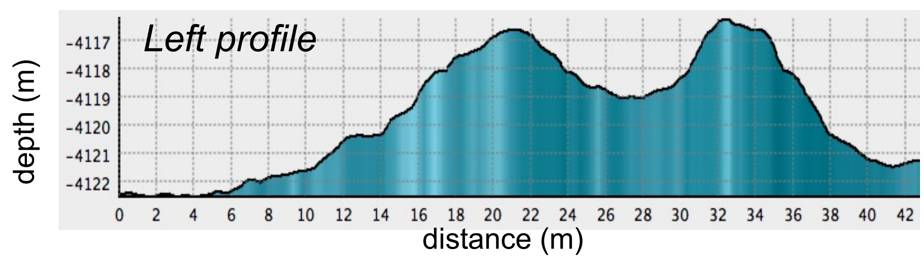

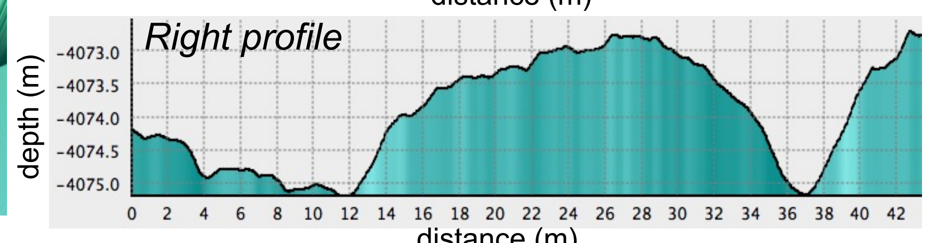

Submarine deposits, *Cannat et al., 2013*

A lot of laboratory experiments !

Role of particle size in erosion processes

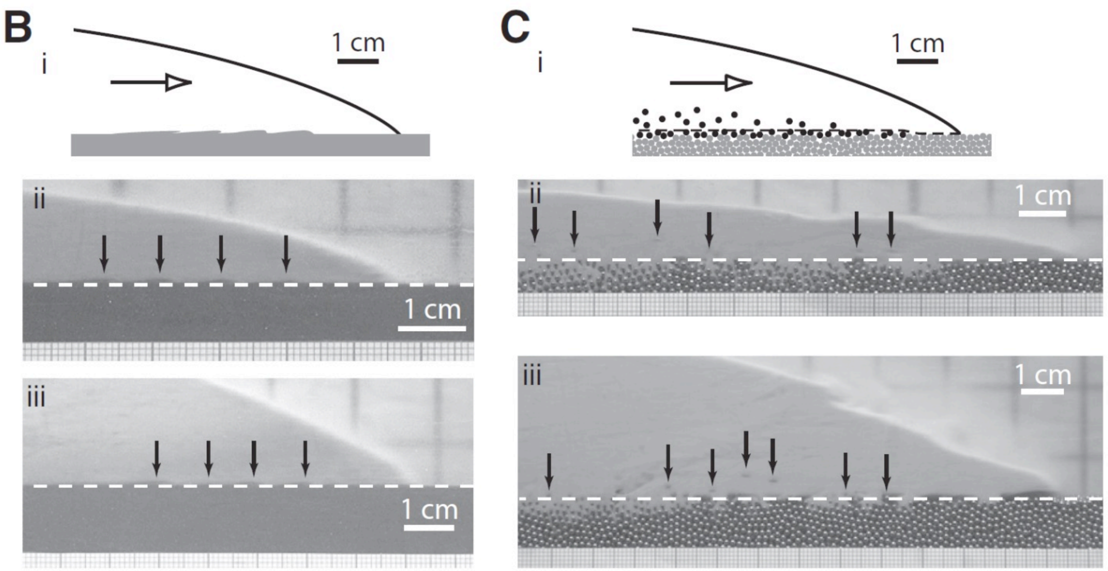

Roche et al., 2013

Segregation in self-channeling flows

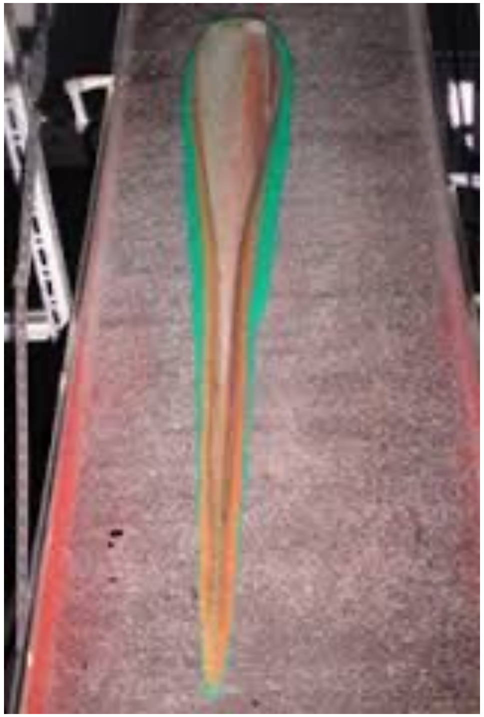

Félix and Thomas, 2004

Johnson et al., 2012

...

Unsteady flows on inclined planes

Measurement of velocity profiles

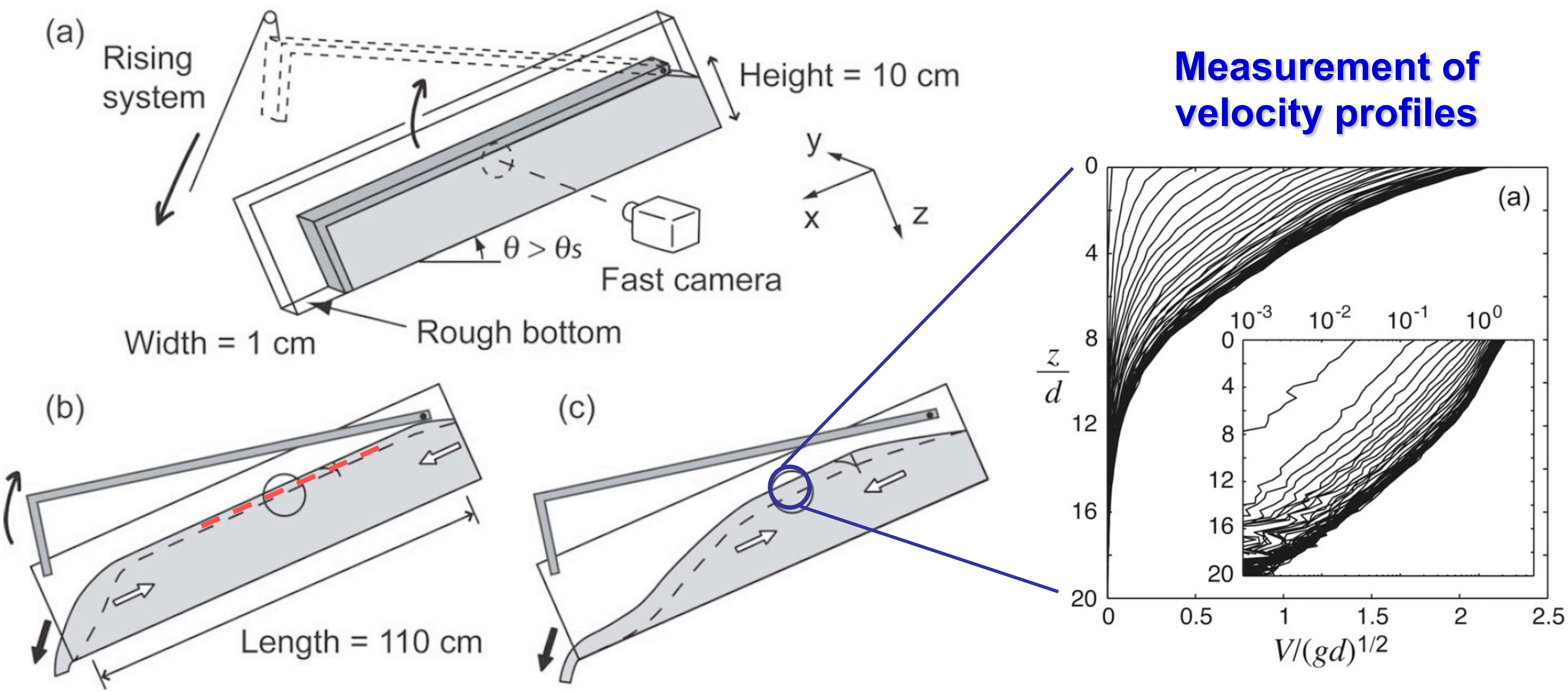

Jop, Forterre, Pouliquen, 2007

Main questions in physics

- How to describe the grains/fluid coupling, taking into account in particular dilatation/compression effects?
- Can we obtain constitutive relations giving a complete description of the granular flows and of their transitions (jammed, dense, dilute)?
- How can the boundary conditions be captured and how do they affect the flow? This includes mobile interfaces related to erosion/deposition
- How to quantify and describe theoretically the evolution of granular size distribution in space and time (segregation, fragmentation processes) and its coupling with the flow?

Physics and Geophysics

- How to measure granular and fluid stresses, particle volume fraction, etc. in both experimental and natural flows?

Review paper: *Delannay, Valance, Mangeney, Roche, Richard, 2017*

Outline

III – Back to lab-scale experiments and simulation

IIIa – Granular column collapse on rigid and erodible beds

IIIb – *μ*(I) rheology in 2D models, comparison with other models (DEM, thin-layer)

IIIc – Static-flowing interface (erosion/deposition)

IIId – Grain-fluid mixture model

Granular flow experiments

Granular column collapse over an inclined channel

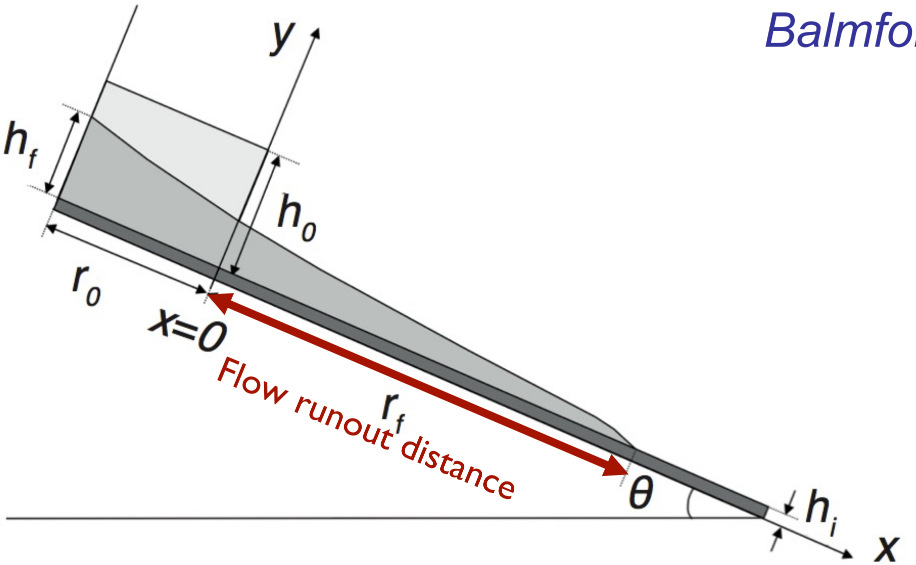

Balmforth and Kerswell 2005, Lube et al. 2005, Hogg, 2007, Farin et al., 2014

Control parameters:
- slope angle: $0° < \theta < \delta$
- volume $V = h_0\, r_0\, W$
- aspect ratio $a = h_0 / r_0$
- column shape
- channel width

Friction angles:
repose $\delta_r \approx 23° \pm 0.5°$, avalanche $\delta_a \approx 25° \pm 0.5°$

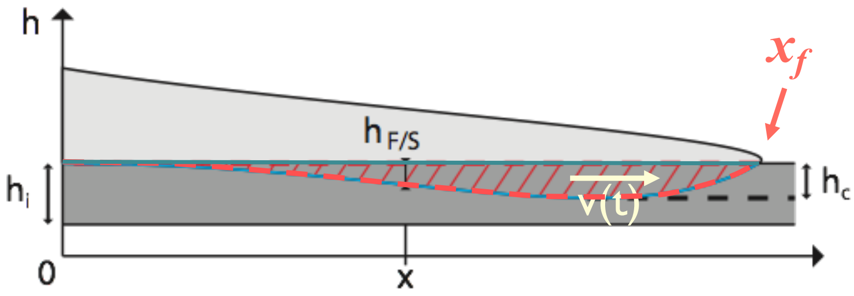

Mangeney, Roche, Hungr, Mangold, Faccanoni, Lucas, 2010
Farin, Mangeney, Roche, 2014

Granular collapse over a rigid bed

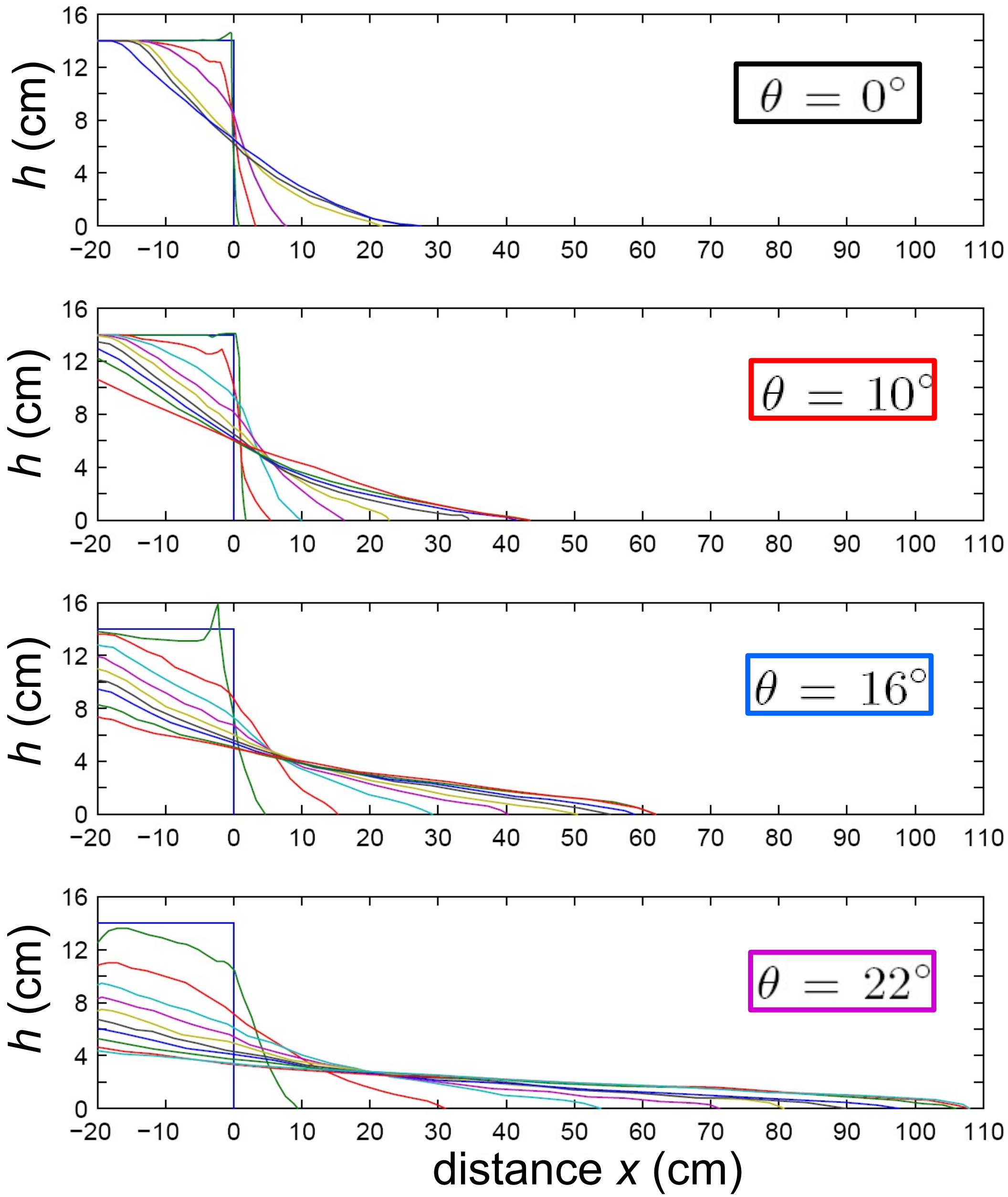

Measurement of front velocity

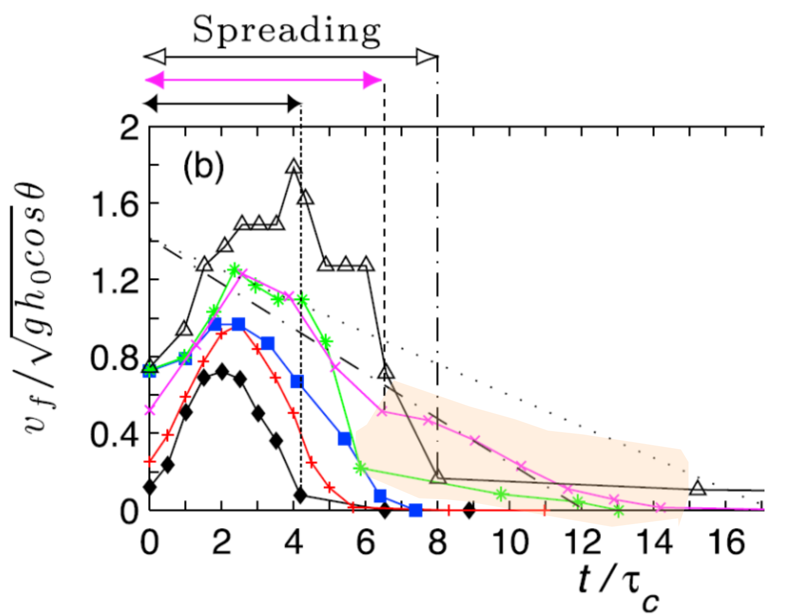

Granular collapse over an erodible bed

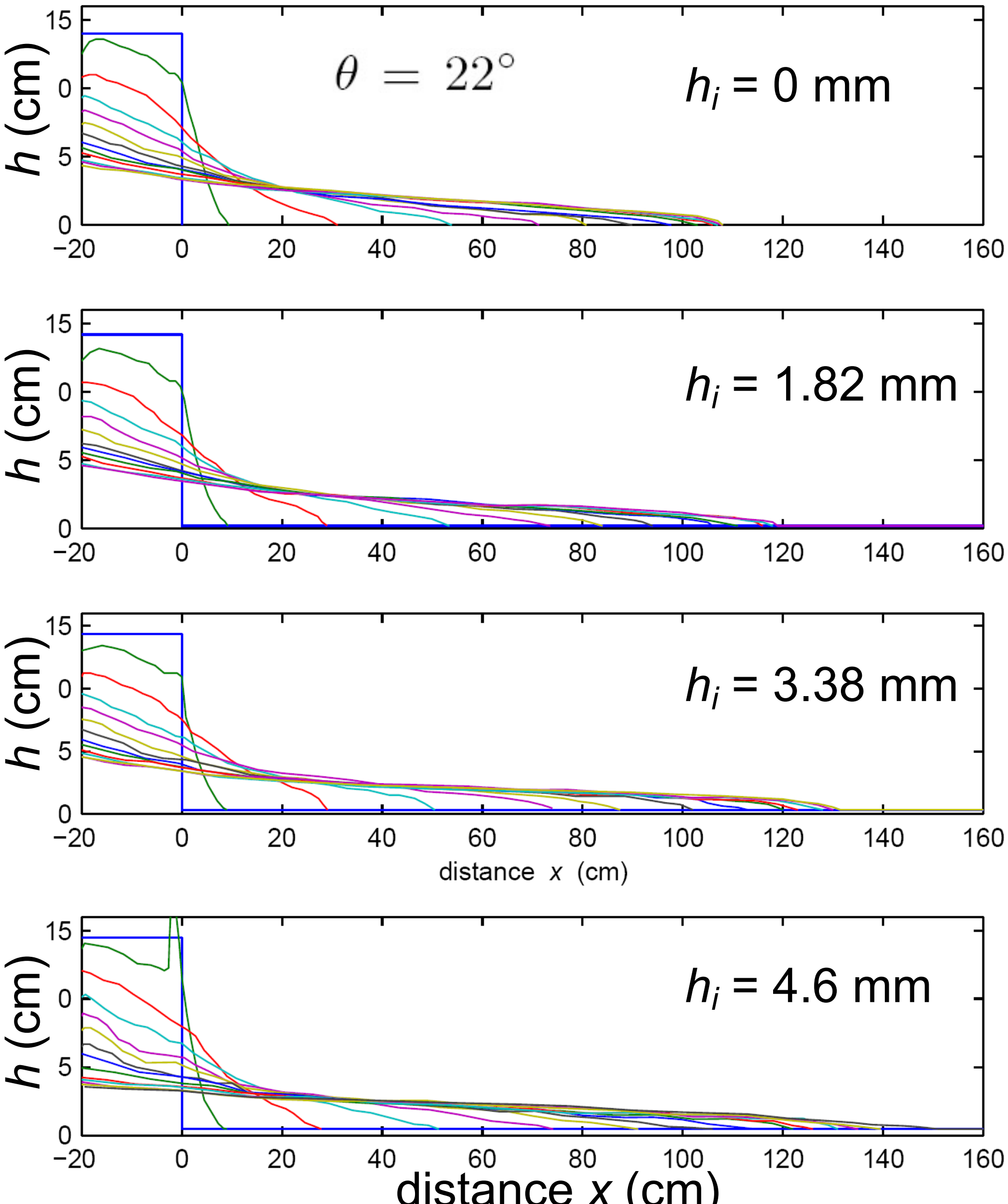

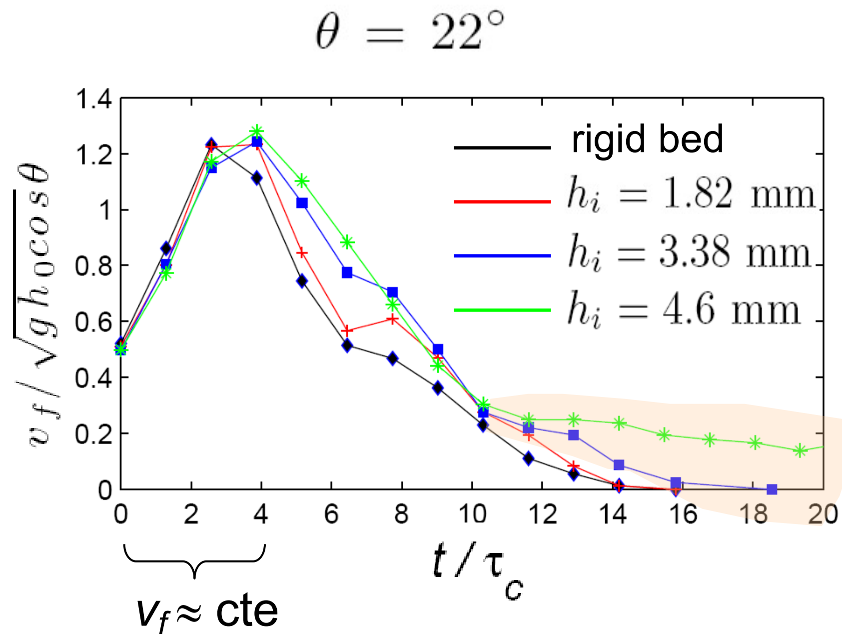

$t \geq 4 - 5\tau_c$, $v_f \nearrow$ if $h_i \nearrow$

For $t \geq 10\tau_c$ and $h_i = 4.6$ mm

Slow flow

Outline

III – Back to lab-scale experiments and simulation

IIIa – Granular column collapse on rigid and erodible beds

IIIb – μ(I) rheology in 2D models, comparison with other models (DEM, thin-layer)

IIIc – Static-flowing interface (erosion/deposition)

IIId – Grain-fluid mixture model

2D granular flow modelling

- Momentum equation: $$\rho\left(\frac{\partial \boldsymbol{u}}{\partial t}+\nabla\cdot(\boldsymbol{u}\otimes\boldsymbol{u})\right)=\nabla\cdot\boldsymbol{\sigma}+\rho\boldsymbol{g}$$
- Incompressibility: $$\nabla\cdot\boldsymbol{u}=0$$

$$\boldsymbol{\sigma}=-p\mathrm{Id}+\boldsymbol{\sigma}'$$, pressure: $p=-\mathrm{trace}(\boldsymbol{\sigma})/3$

Strain rate tensor: $$\boldsymbol{D}(\boldsymbol{u})=\frac{1}{2}(\boldsymbol{\nabla}\boldsymbol{u}+\boldsymbol{\nabla}^T\boldsymbol{u})$$

Constitutive relation

$$\boldsymbol{\sigma}' = \mu(I)p\frac{\boldsymbol{D}}{\|\boldsymbol{D}\|} \qquad \|\boldsymbol{D}\| = \sqrt{\tfrac{1}{2}\mathrm{tr}\,\boldsymbol{D}^2}$$

can be called viscosity

Jop et al. 2005, 2006

$$\mu(I) = \mu_s + \frac{\mu_2 - \mu_s}{1 + I_0/I} \quad \text{with} \quad I = \frac{2\|\boldsymbol{D}\|d}{\sqrt{p/\rho_s}}$$

$$\boldsymbol{\sigma}' = \mu_s p\frac{\boldsymbol{D}}{\|\boldsymbol{D}\|} + 2\frac{(\mu_2 - \mu_s)p}{2\|\boldsymbol{D}\| + I_0\sqrt{p}/k}\boldsymbol{D} \qquad k = d\sqrt{\rho_s}$$

can be called viscosity η

Drücker-Prager yield stress

Constitutive relation

$$\begin{cases} \boldsymbol{\sigma}' = 2\eta(|\boldsymbol{D}|, p)\boldsymbol{D} + \mu_s p \dfrac{\boldsymbol{D}}{|\boldsymbol{D}|} & \text{if } |\boldsymbol{D}| \neq 0, \\ |\boldsymbol{\sigma}'| \leq \mu_s p & \text{if } |\boldsymbol{D}| = 0. \end{cases}$$

Plasticity (flow/no flow) criterion

Constant viscosity: $\eta(|\boldsymbol{D}|, p) =$ Cte

$\mu(I)$ rheology : $2\eta(|\boldsymbol{D}|, p) = \dfrac{k(\mu_2 - \mu_s)p}{k|\boldsymbol{D}| + I_0\sqrt{p}}$

Ionescu, Mangeney, Bouchut, Roche 2015

Boundary conditions

- At the free surface : $\mathcal{D}(t)$

characteristic function of the domain

$$\boldsymbol{\sigma n} = 0 \qquad \text{on} \quad \Gamma_s(t),$$

$$\mathrm{St}\frac{\partial 1_{\mathcal{D}(t)}}{\partial t} + \boldsymbol{u}\cdot\nabla 1_{\mathcal{D}(t)} = 0,$$

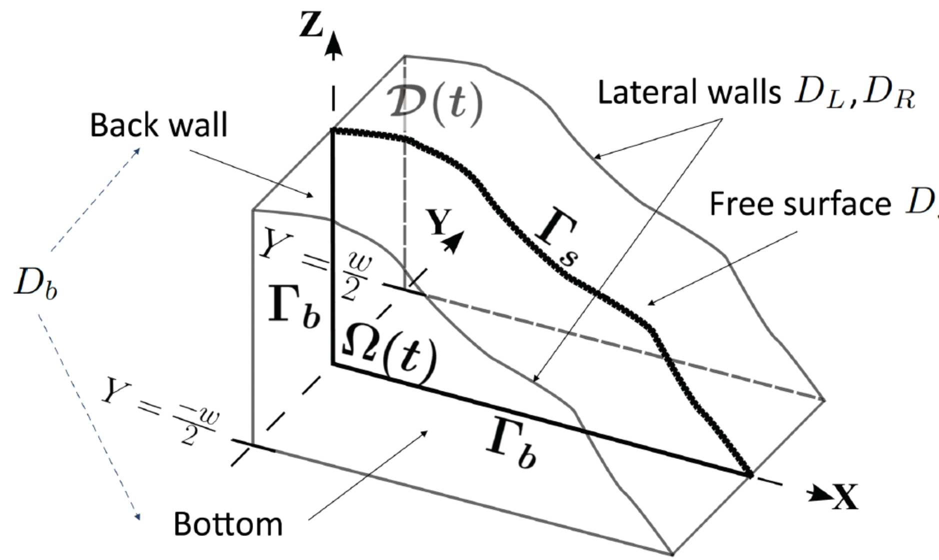

- At the base and walls: Coulomb friction

$$\boldsymbol{u}\cdot\boldsymbol{n} = 0, \qquad \boldsymbol{\sigma}_T = \boldsymbol{F}^f$$

$$\begin{cases} \boldsymbol{F}^f = -\mu^f[-\sigma_n]_+ \dfrac{\boldsymbol{u}_T}{|\boldsymbol{u}_T|} \text{ if } \boldsymbol{u}_T \neq 0, \\ |\boldsymbol{F}^f| \leq \mu^f[-\sigma_n]_+ \text{ if } \boldsymbol{u}_T = 0. \end{cases}$$

$$\mu^f = \begin{cases} \mu^f_w \text{ on the back wall and on the lateral walls,} \\ \mu^f_b \text{ on the rough bottom.} \end{cases}$$

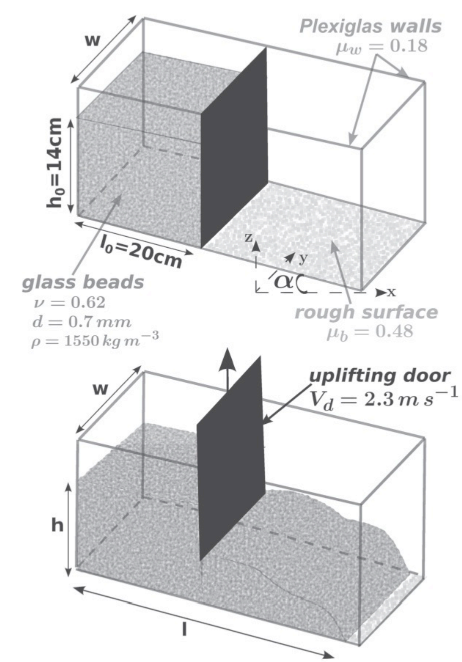

Side wall effects

$$\rho\,(\partial_t \boldsymbol{u} + (\boldsymbol{u}\cdot\nabla)\boldsymbol{u}) + \nabla p - \operatorname{div}(\boldsymbol{\sigma}') = \frac{2}{w}\boldsymbol{F}^f_w + \rho\boldsymbol{g}$$

$$\begin{cases} \boldsymbol{F}^f_w = -\mu^f_w[p]_+ \dfrac{\boldsymbol{u}}{|\boldsymbol{u}|} \text{ if } \boldsymbol{u} \neq 0, \\ |\boldsymbol{F}^f_w| \leq \mu^f_w\,[p]_+ \text{if } \boldsymbol{u} = 0, \end{cases}$$

For a laminar shear flow with hydrostatic pressure, equivalent to:

Taberlet et al., 2003; Jop et al., 2005

$$\mu(I) = \mu_s + \frac{\mu_2 - \mu_s}{I_0 + I} I + \mu_w \frac{H - z}{W}$$

Martin, Ionescu, Mangeney, Bouchut, Farin, 2017

Granular collapses

ALE (Arbitrary Lagrangian-Eulerian) description to compute the evolution of the fluid domain
- iterative decomposition-coordination formulation, coupled with the augmented Lagrangian method: *Ionescu, Mangeney, Bouchut, Roche, 2014*

or

-regularization method: *Lusso, Ern, Bouchut, Mangeney, Farin, Roche, 2017*

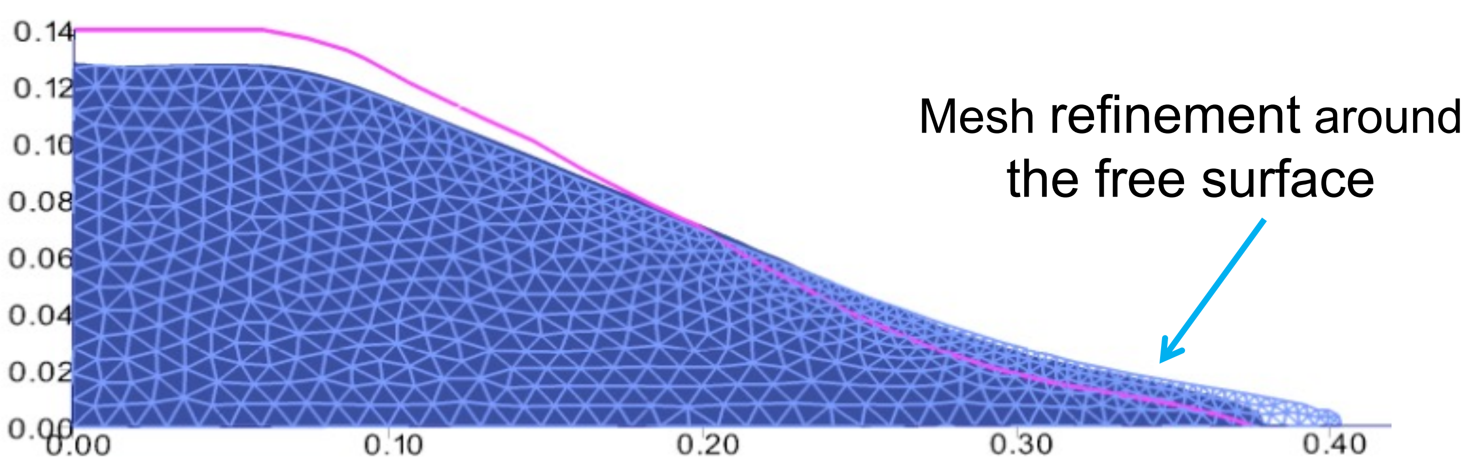

Crosta et al. 2009, Lagrée et al. 2011

Parameters deduced from the experiments

Grain diameter: $d = 0.7 \pm 0.1\mathrm{mm}$

Density: $\rho_s = 2500 \ \mathrm{kg\ m^{-3}}$, $\nu = 0.62$ $\Rightarrow$ $\rho = 1550 \ \mathrm{kg\ m^{-3}}$

Repose angle: $\theta_r = 23.5^o \pm 0.5^o \ (\mu_r = 0.43 \pm 0.01)$

Avalanche angle: $\theta_a = 25.5^o \pm 0.5^o \ (\mu_a = 0.48 \pm 0.01)$

Wall friction: $\mu_w = \tan(10.5^o) = 0.18$ *Pouliquen and Forterre 2002*

Additional friction due to the wall: + $\mu_w h/W$ *Jop et al. 2005*

$\Downarrow$

Constant viscosity: $\mu = \mu_s = \tan(25.5^\circ)$,

$\mu(I)$ rheology : $\mu_s = \tan(25.5^o)$, $\mu_2 = \tan(36^o)$, $I_0 = 0.279$

Friction at the base: $\mu_b = \mu = \tan(25.5^\circ)$

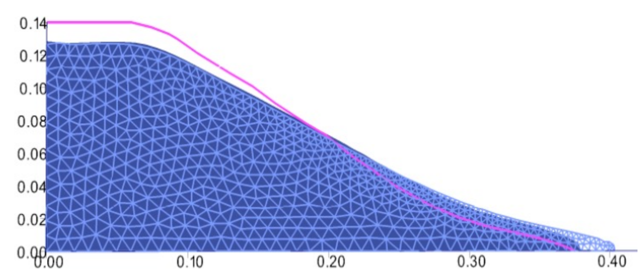

Simulation with the variable viscosity (μ (I))

Granular collapse over an horizontal plane: $\theta = 0°$

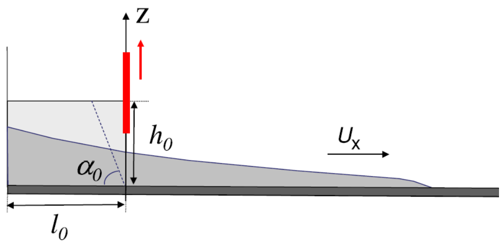

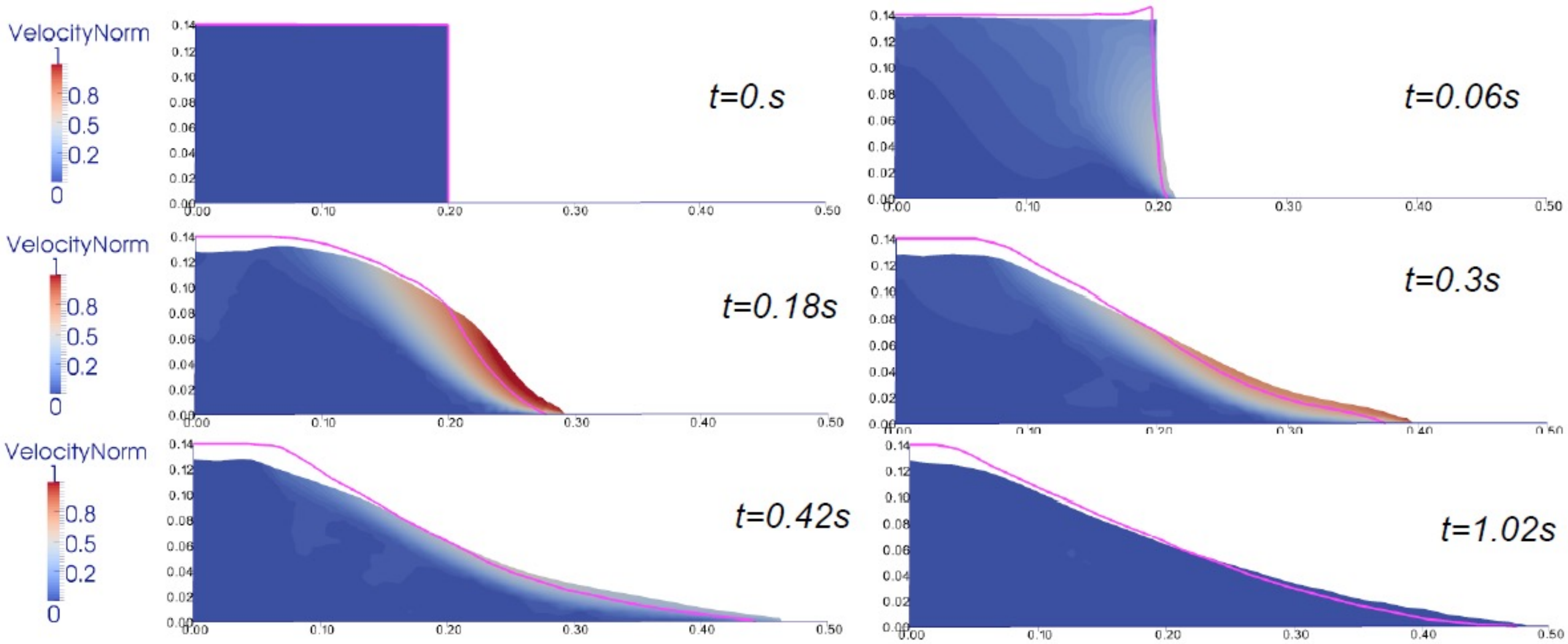

Well reproduces the dynamics

The gate has to be taken into account !

Effect of the gate

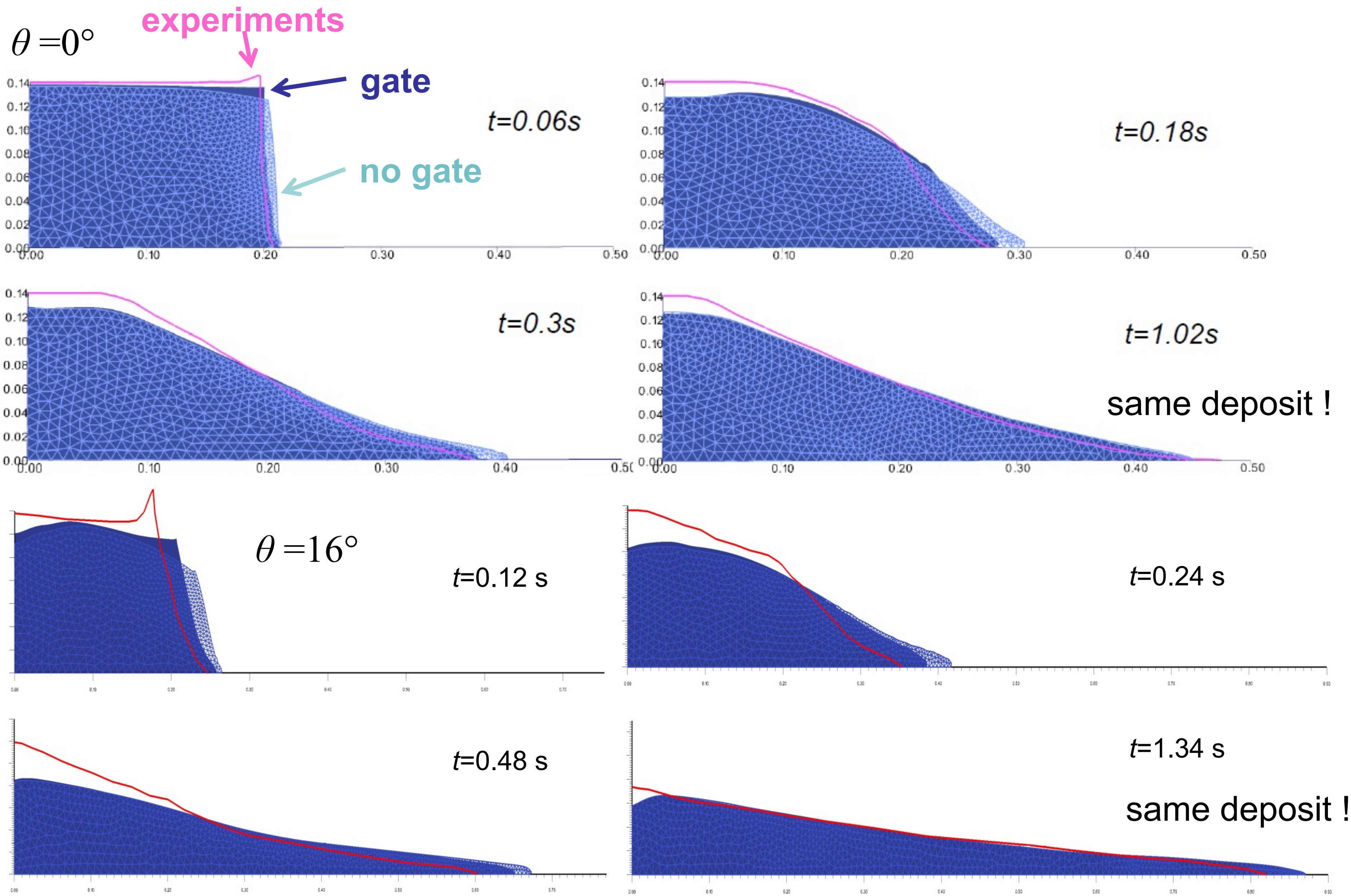

Effect of the side walls

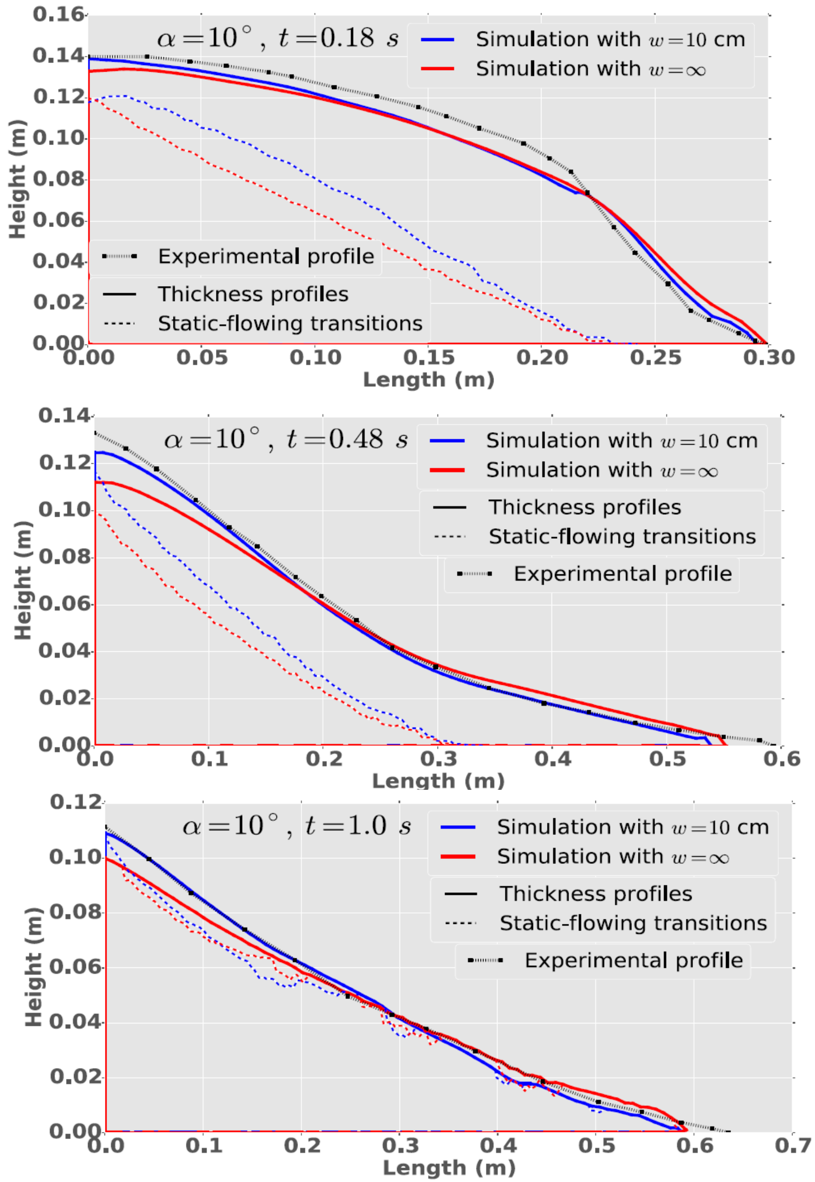

Side wall friction: the static-flowing interface closer to the free surface

Effect of the side walls

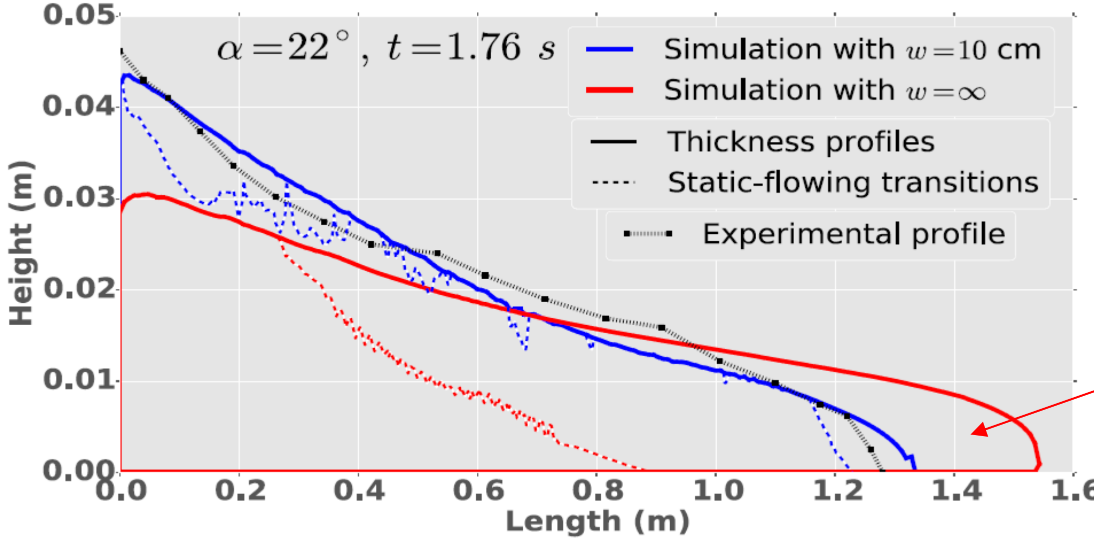

The material still flows

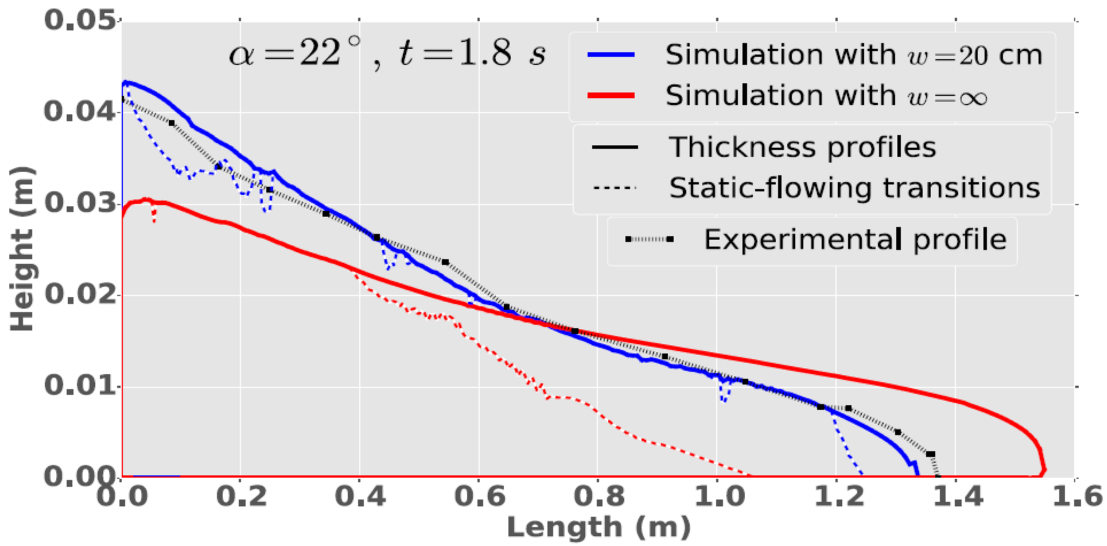

Martin, Ionescu, Mangeney, Bouchut, Farin, 2017

Horizontal velocity field and profiles

$\theta = 0°$

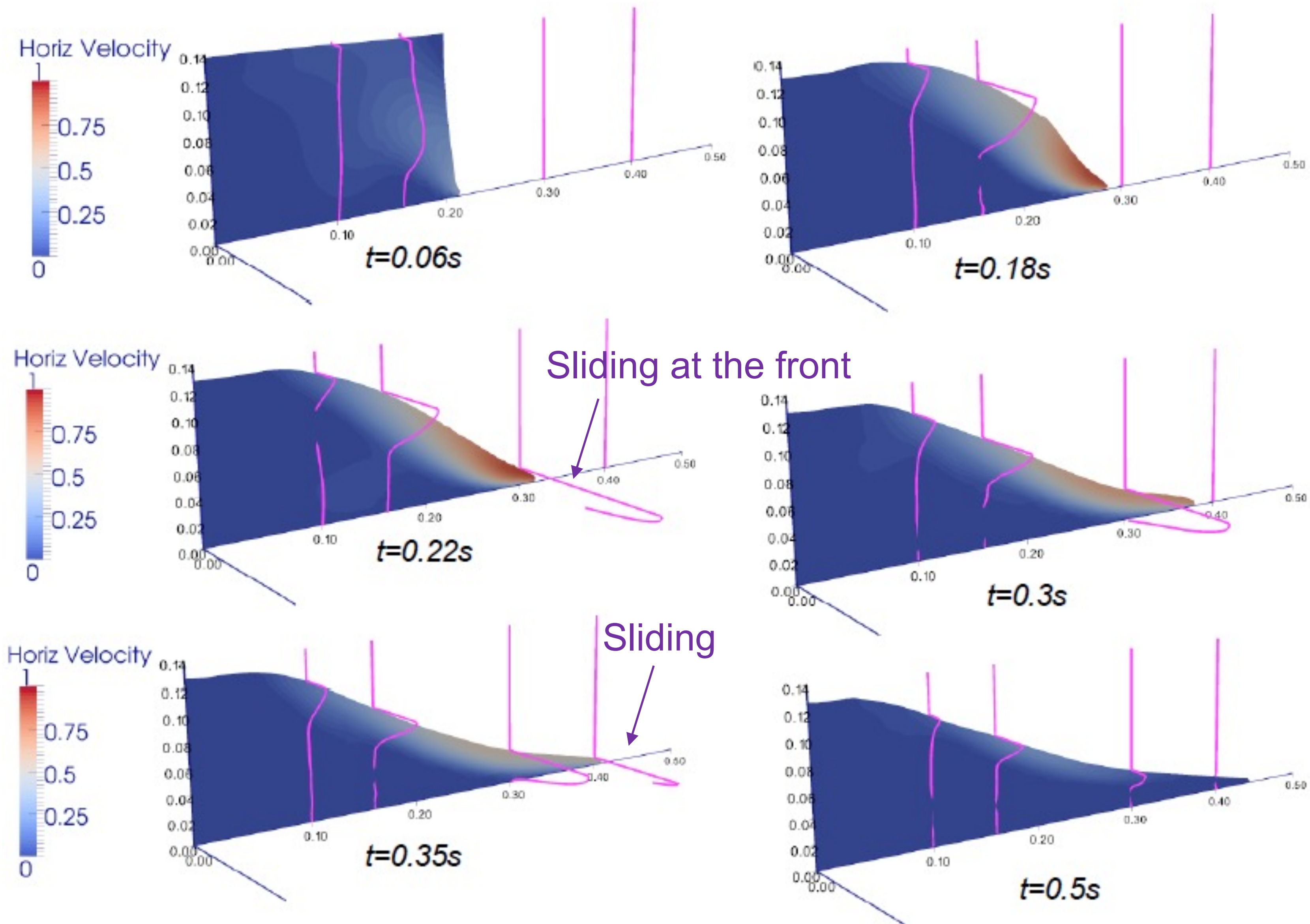

Slip at the front

Insight into the flow dynamics

Strain rate (s^{-1})

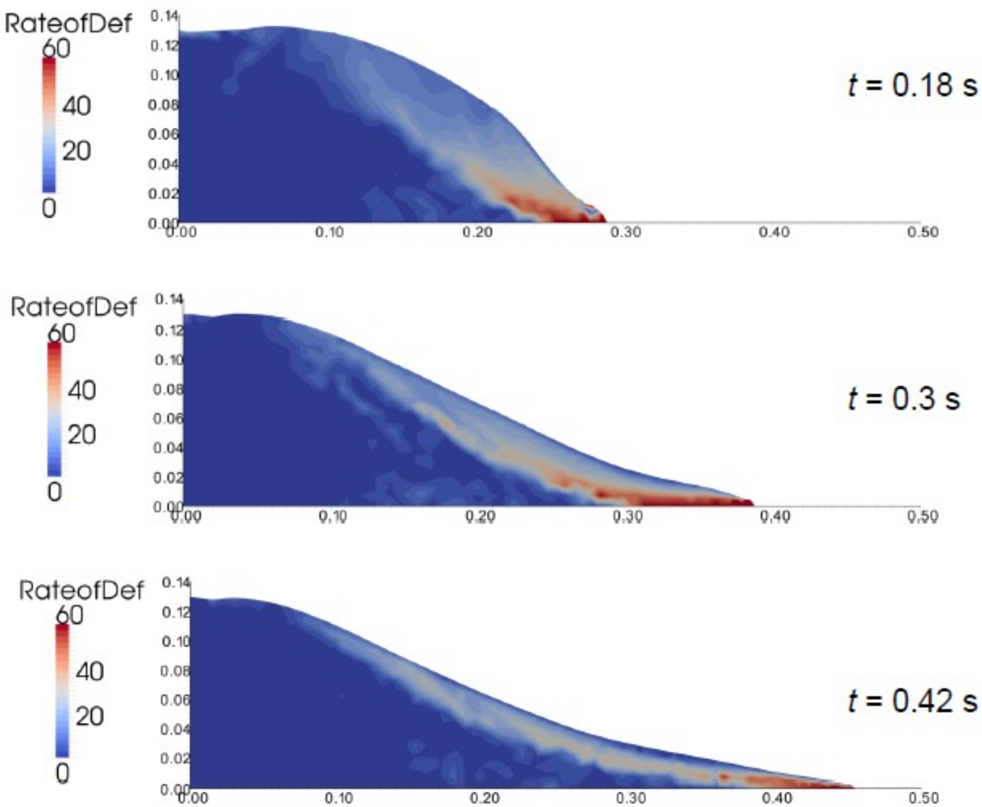

Pressure (Pa)

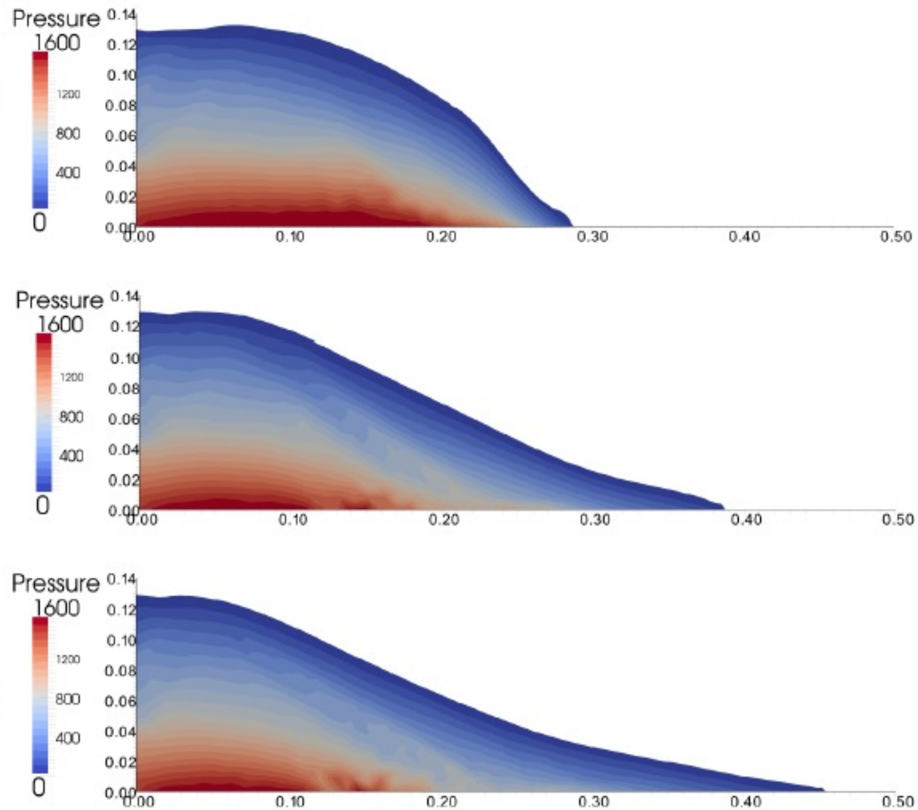

Strain rate localization

$$2\eta(|\boldsymbol{D}|,p) = \frac{k(\mu_2-\mu_s)p}{k|\boldsymbol{D}|+I_0\sqrt{p}},$$

Viscosity η in the $\mu(I)$ rheology

$$2\eta_I(|\boldsymbol{D}|, p) = \frac{k(\mu_2 - \mu_s)p}{k|\boldsymbol{D}| + I_0\sqrt{p}},$$

Pa.s

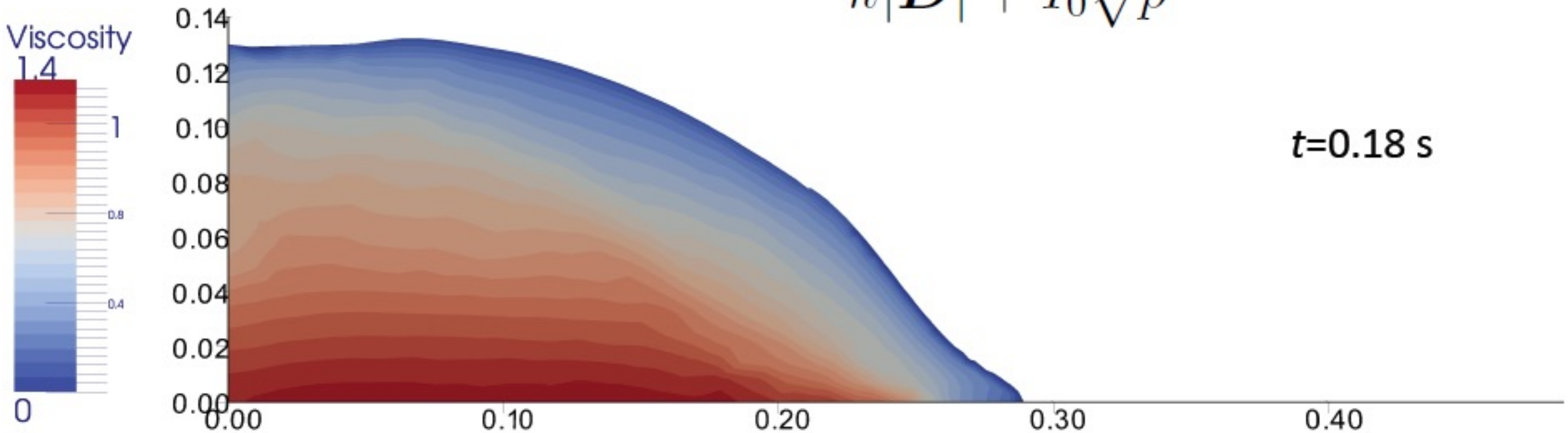

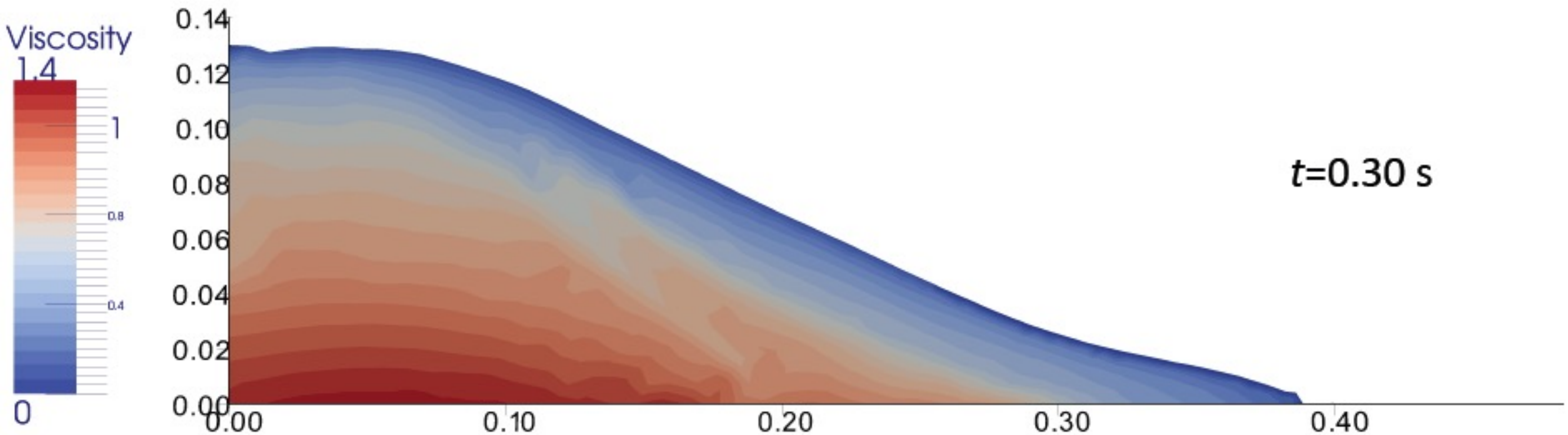

η ~ 1 Pa.s

Very similar results with η = 1 Pa.s

Drucker- Praguer $\eta = 1$ Pa.s versus $\mu(I)$

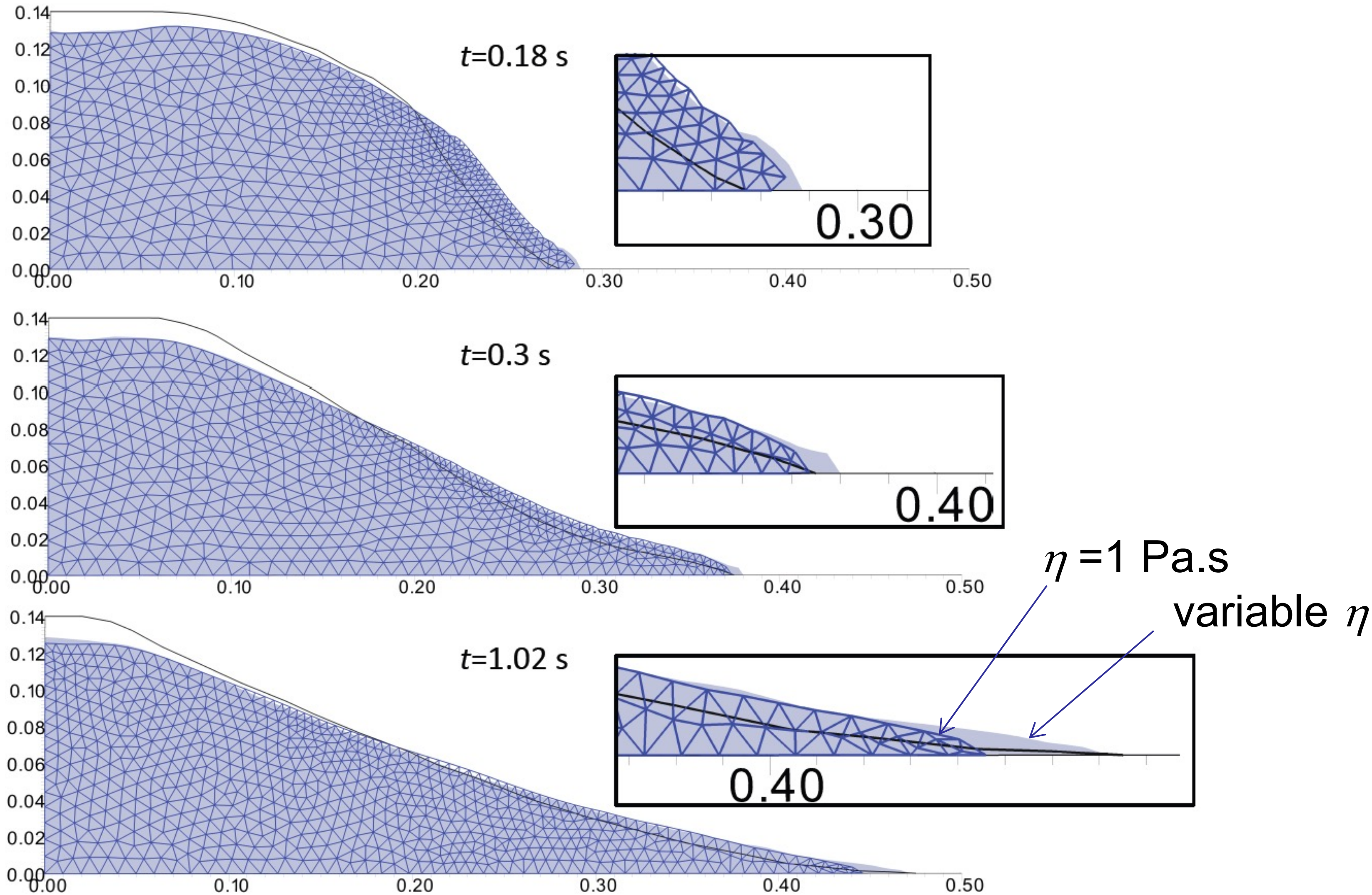

Very similar results with the variable and constant viscosity η =1 Pa.s

Effect of viscosity

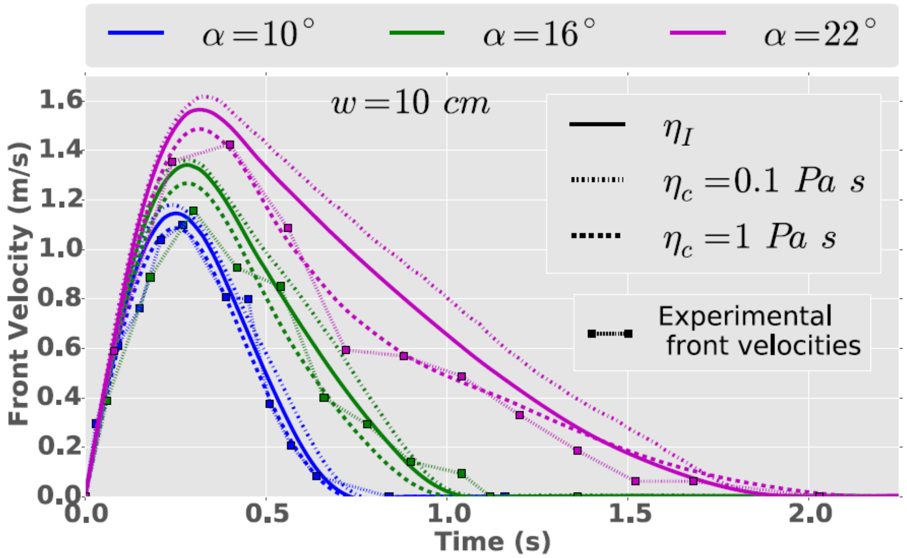

$$2\eta_I(|\boldsymbol{D}|, p) = \frac{k(\mu_2 - \mu_s)p}{k|\boldsymbol{D}| + I_0\sqrt{p}},$$

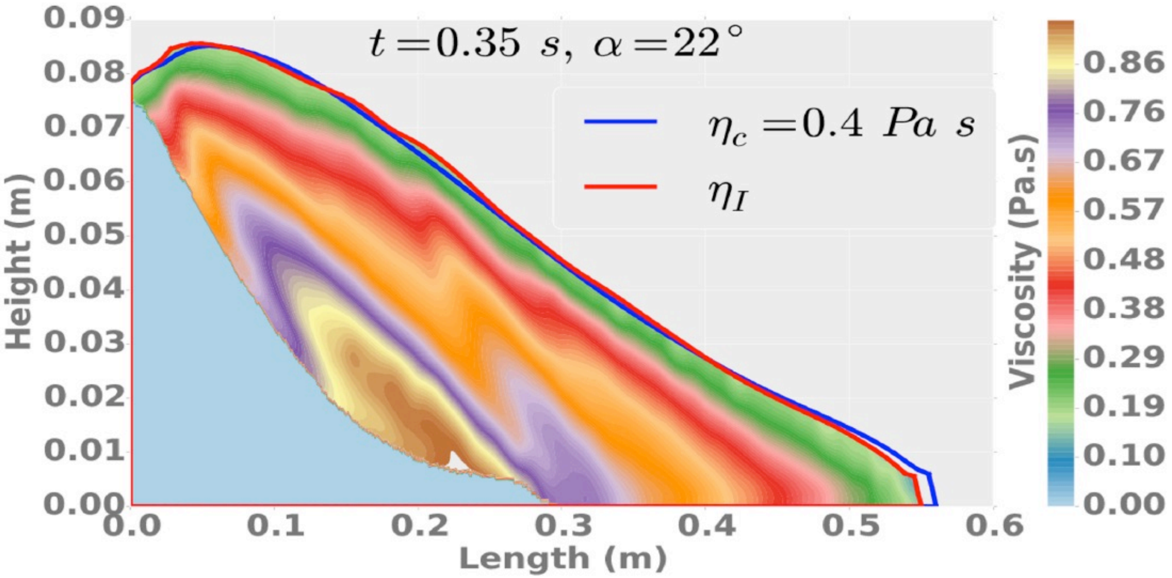

(d)$\alpha = 22^\circ$

Comparison between different numerical methods

Level set method to track the interface granular material - ambient air

$\theta = 0°$

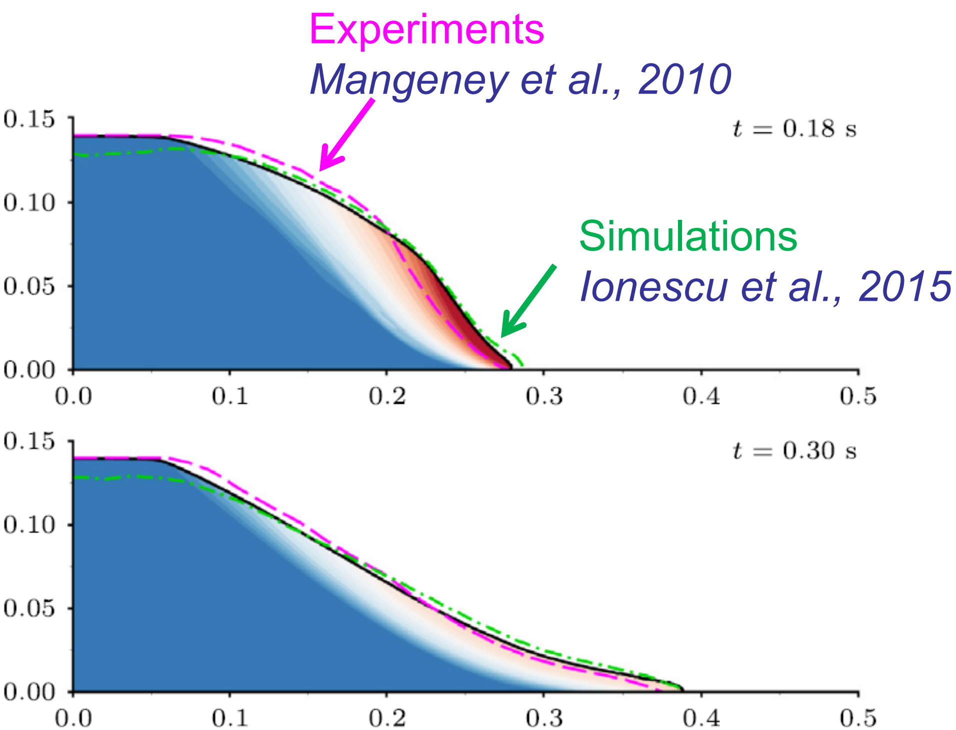

Need for small space steps to well resolve the upper left part of the profile

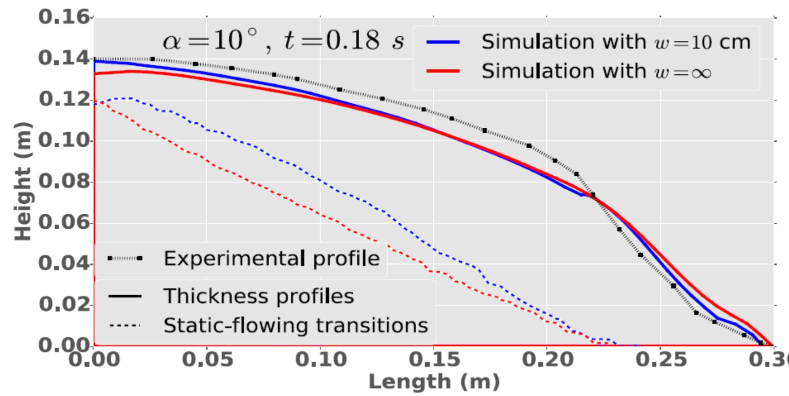

(a) $w = 10$ cm, $t = 0.18$ s

Martin, Ionescu, Mangeney, Bouchut, Farin, 2017

Chupin, Dubois, Phan, Roche, 2021

Ill-posesdness of the model

Hadamard instabilities for models with $\mu(I)$ *Barker et al., 2003*

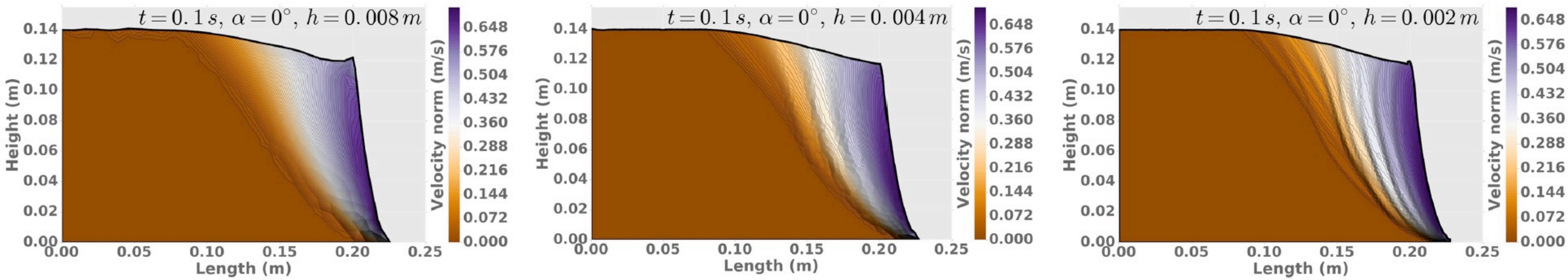

(a)Velocity norm, $h = 0.008$m (b)Velocity norm, $h = 0.004$m (c)Velocity norm, $h = 0.002$m

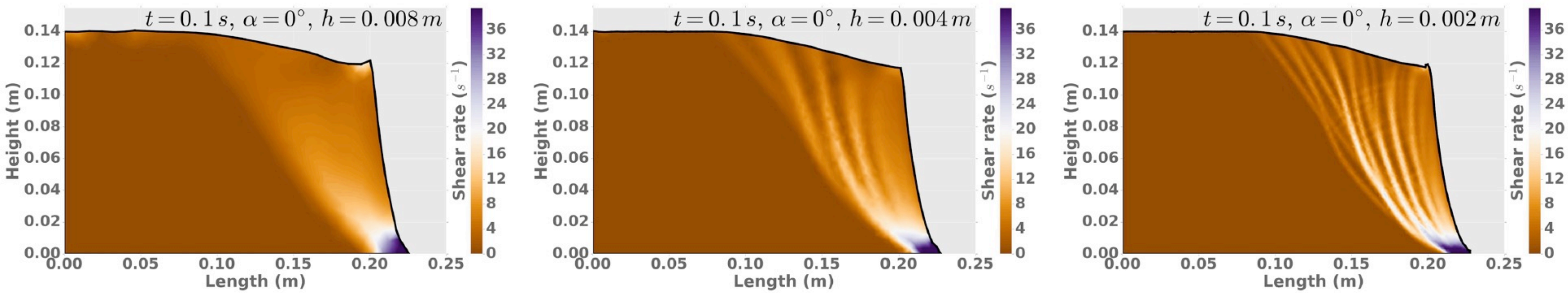

(d)Strain rate, $h = 0.008$m (e)Strain rate, $h = 0.004$m (f)Strain rate, $h = 0.002$m

$\mu(I)$ rheology

Martin, Ionescu, Mangeney, Bouchut, Farin, 2017

Ill-posesdness of the model

Hadamard instabilities for models with $\mu(I)$ *Barker et al., 2003*

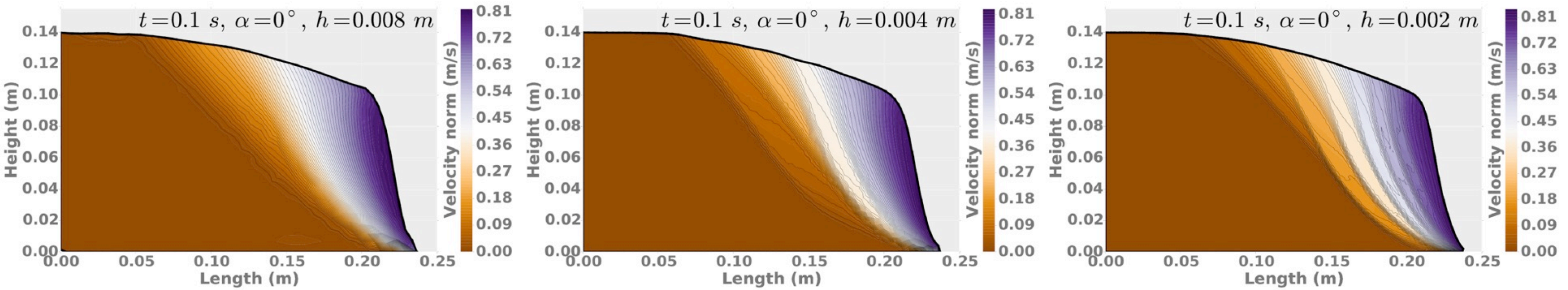

(a)Velocity norm, $h = 0.008$m (b)Velocity norm, $h = 0.004$m (c)Velocity norm, $h = 0.002$m

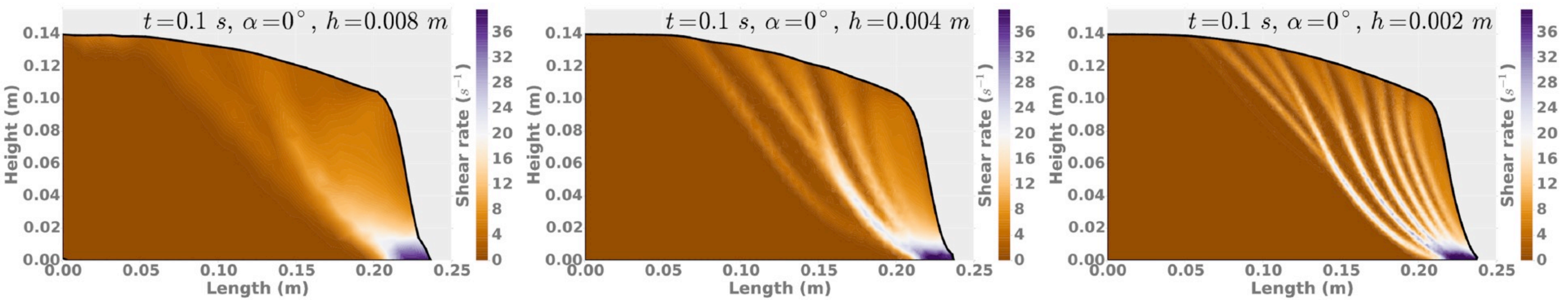

(d)Strain rate, $h = 0.008$m (e)Strain rate, $h = 0.004$m (f)Strain rate, $h = 0.002$m

Drucker-Parger with constant viscosity

Martin, Ionescu, Mangeney, Bouchut, Farin, 2017

Outline

III – Back to lab-scale experiments and simulation

IIIa – Granular column collapse on rigid and erodible beds

IIIb – $\mu(I)$ rheology in 2D models, comparison with other models (DEM, thin-layer)

IIIc – Static-flowing interface (erosion/deposition)

IIId – Grain-fluid mixture model

Discrete Element Method (DEM)

$$m_i \frac{\mathrm{d}\,\mathbf{u}_i}{\mathrm{d}\,t} = m_i\,\mathbf{g} + \sum_{j=i}^{N} \mathbf{f}_{i,j}$$

volume forces

contact forces

- **Molecular Dynamics**

Contact forces are functions

Hertz's contact law

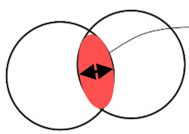

$\delta_{i,j}$

normal stiffness

$$\mathbf{f}_{i,j} \cdot \mathbf{n}_{i,j} = \kappa\ \delta_{i,j}{}^{\frac{3}{2}}$$

unit normal vector

numerical overlap

- **Contact Dynamics**

Contact forces verify contact laws

➡ Constrained optimization problem

Contact forces must be such that beads don't overlap…

Distances between spheres *i* and *j*

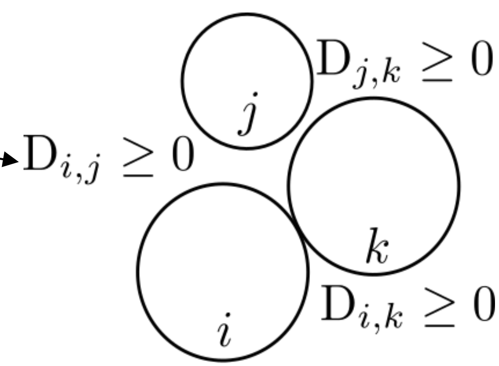

Signorini & Coulomb's contact laws

- **Signorini's law**

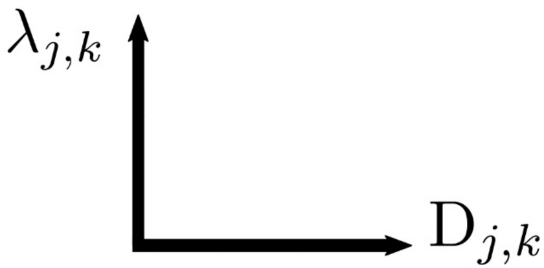

$$\lambda_{j,k} \geq 0$$
$$\mathrm{D}_{j,k} \geq 0$$
$$\lambda_{j,k}\mathrm{D}_{j,k} = 0$$

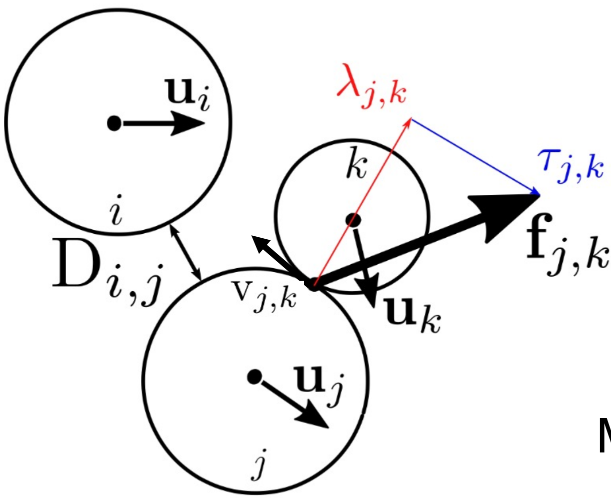

- **Coulomb's law**

Tangential relative velocity

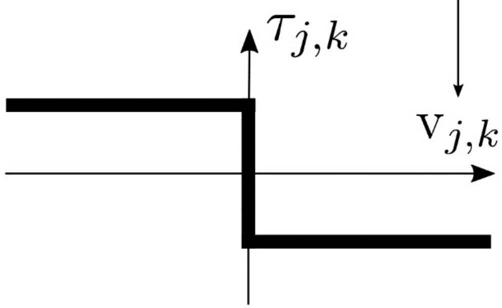

Maximize the dissipated power

$$\max_{\tau_{j,k}} \; -\tau_{j,k} \, \mathrm{v}_{j,k}$$

such that $|\,\tau_{j,k}\,| \leq \mu\lambda_{j,k}$

Discrete Element Method (DEM) : granular collapse

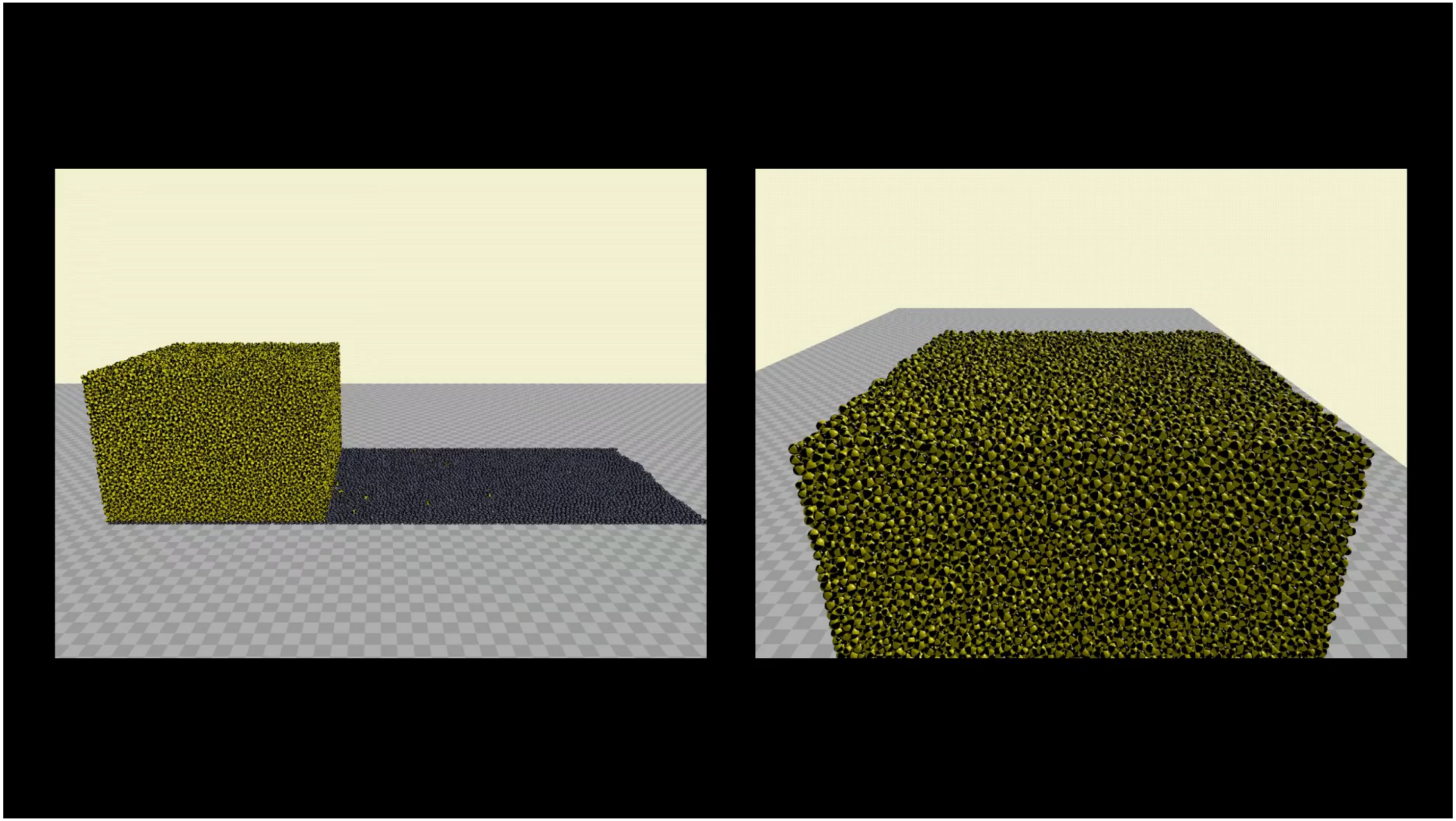

Hugo Martin, A. Mangeney, Y. Maday, B. Maury, A. Lefebvre-Lepot, 2021

for immersed flows see e. g. *Amarsid et al., 2017*

Quantitative comparison with other models and experiments

Comparaison **Contact Dynamics** and **Navier-Stokes** simulations

$\mu = 0.5$ and $e = 0.5$

Lagree et al., 2011

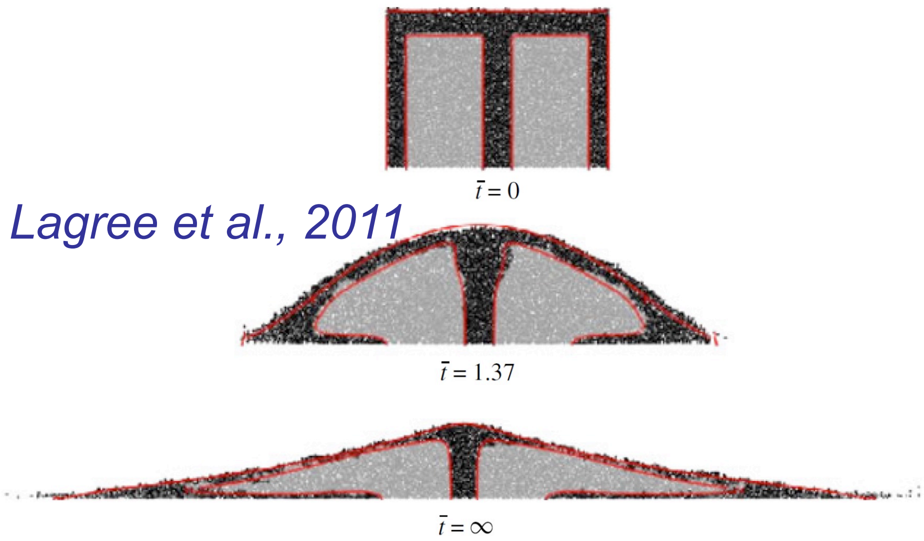

$$\mu(I) = \mu_s + \frac{\mu_2 - \mu_s}{I_0 + I} I$$

$\mu_s = 0.32,\ \Delta\mu = 0.28$ and $I_0 = 0.4$

Very good agreement BUT with parameters smaller than those measured experimentally

$\mu_s = 0.38,\ \Delta\mu = 0.26$ and $I_0 = 0.279$

Jop et al., 2005

2D DEM goes further than experiments if no additionnal dissipation is accounted for !

Quantitative comparison with other models and experiments

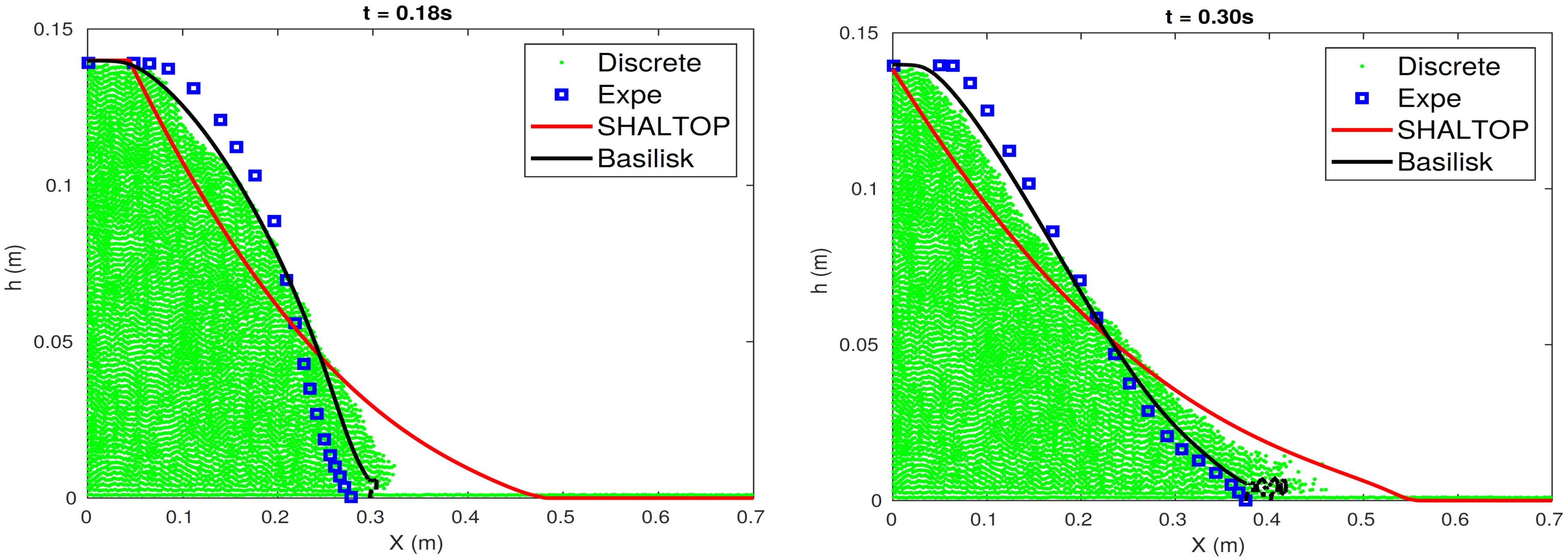

DEM (2h computational time) goes further than experiments

Previous studies used additional dissipation (e. g. rolling friction) *Girolami et al. 2012*

Martin et al., 2021

Outline

III – Back to lab-scale experiments and simulation

IIIa – Granular column collapse on rigid and erodible beds

IIIb – $\mu(I)$ rheology in 2D models, comparison with other models (DEM, thin-layer)

IIIc – Static-flowing interface (erosion/deposition)

IIId – Grain-fluid mixture model

Insight into the static/flowing interface dynamics

A thin flowing layer above a static layer:

Equation for the static/flowing transition $\dot{b}(t)$?

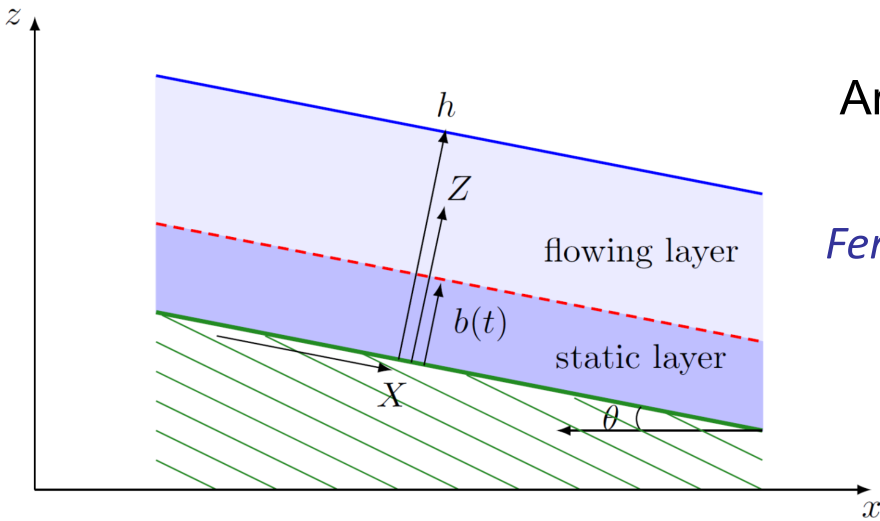

UP TO NOW
Arbitrary closure relations and non-consistent energy in depth-averaged models

Fernandez-Nieto, 2008, Iverson and Ouyang, 2015

⬇

Go back to non-depth-averaged models

Viscoplastic models CONTAIN the static/flowing transition

without having to prescribe arbitrary exchange rates,

velocity profiles (*Capart et al. 2015, Gray et al. 2015*,…), etc…

Bouchut, Ionescu, Mangeney, 2015

Simplified 1D shallow viscoplastic model

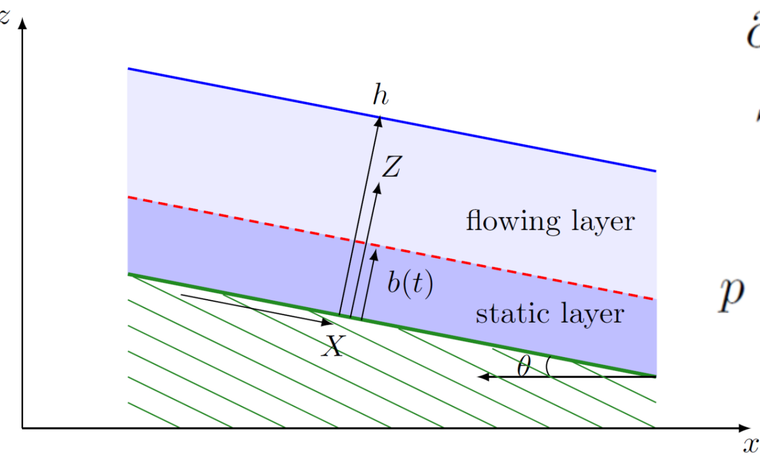

$$\partial_t U(t,Z) + S(t,Z) - \partial_Z\big(\nu \partial_Z U(t,Z)\big) = 0$$

$$S = g(-\sin\theta + \partial_X(h\cos\theta)) - \mu_s \partial_Z p$$

Thin-layer approximation

$$p = g\cos\theta(h - Z) \Rightarrow S = g\cos\theta\,(\tan\delta - \tan\theta + \partial_X h)$$

Boundary conditions

$$\begin{cases} U = 0 & \text{at } Z = b(t), \\ \nu\partial_Z U = 0 & \text{at } Z = b(t), \\ \nu\partial_Z U = 0 & \text{at } Z = h. \end{cases}$$

Initial condition $U(0,Z) = U^0(Z)$

Static/flowing interface

- If $\nu = 0$ and $\partial_Z U(t,b(t)) \neq 0$, then

$$U(t,Z) = \max\Big(U^0(Z) - St, 0\Big)$$

$$\boxed{\dot b(t) = \frac{S(t,b(t))}{\partial_Z U(t,b(t))}}$$

- If $\nu > 0$ and $S(t,b(t)) \neq 0$, then

$$\boxed{\dot b(t,X) = \frac{-\partial^2_{ZZ}(\nu\partial_Z U)(t,X,b(t))}{S(t,X)}\nu.}$$

Lusso, Bouchut, Ern, Mangeney, 2017

Measurements of the static/flowing interface

Laboratory experiments

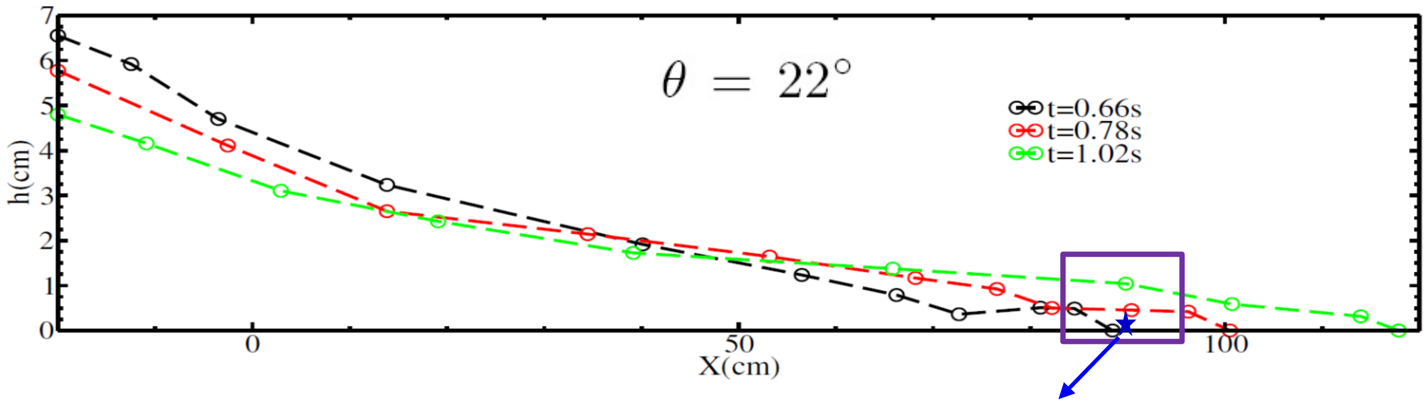

Static/flowing interface at *x*=90 cm

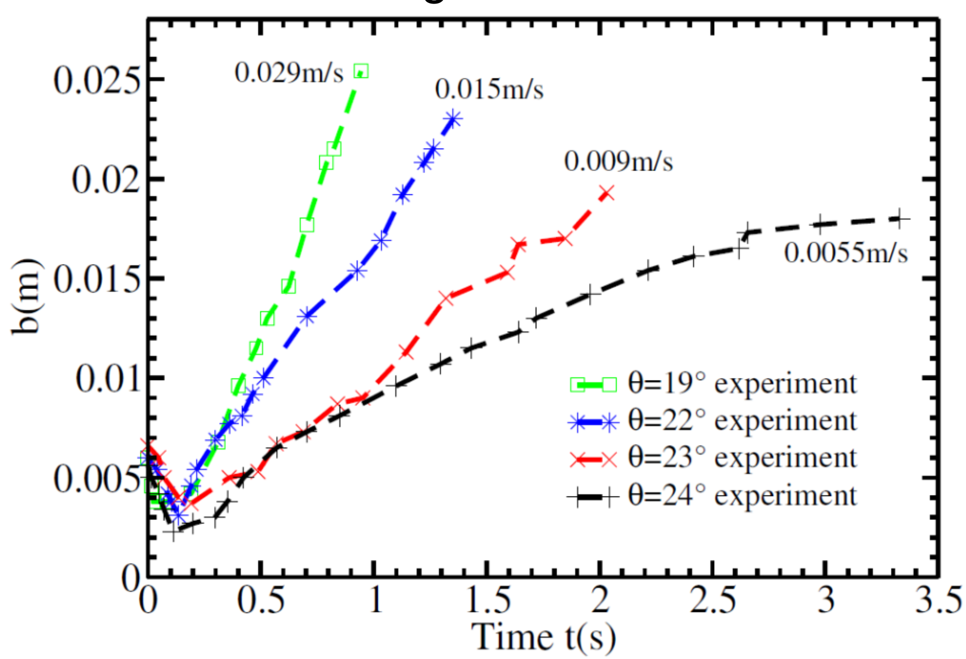

Simplified 1D shallow viscoplastic model

no viscosity (i. e. $\mu(I) = \mu_s$)

Initial linear velocity profile

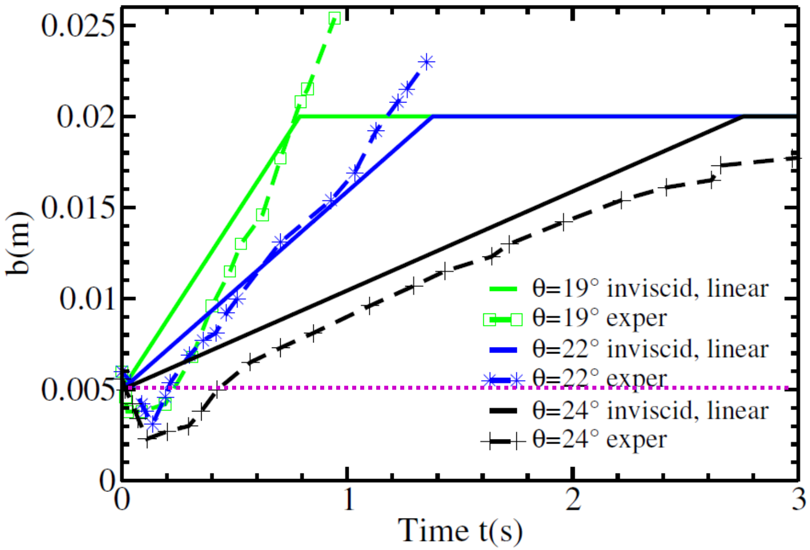

Initial Bagnold velocity profile

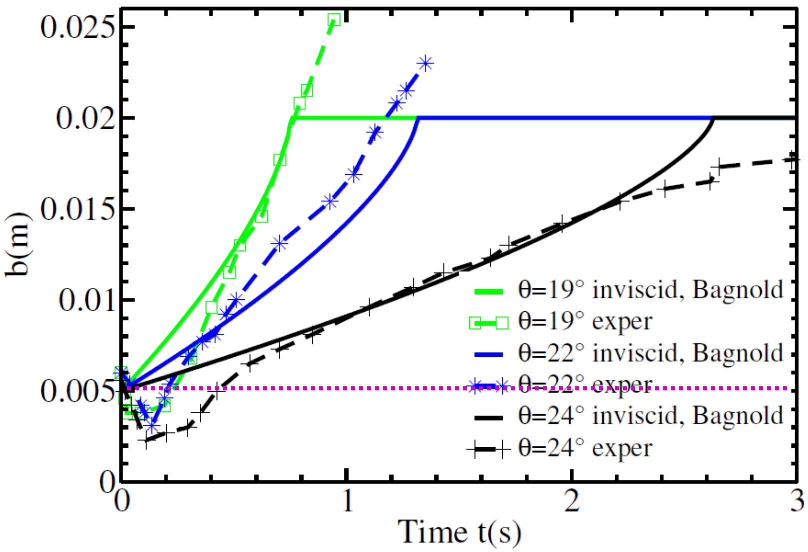

$$U(t,Z) = \max\Big(U^0(Z) - St, 0\Big)$$

$$\dot{b}(t) = \frac{g\cos\theta(\tan\delta - \tan\theta)}{\partial_Z U(t,b(t))} \geq 0$$

➡ the initially static bed is not put into motion

Simplified 1D shallow viscoplastic model

(b) $\nu = 5 \times 10^{-5} \mathrm{m}^2/\mathrm{s}$ η = 0.075 Pa.s

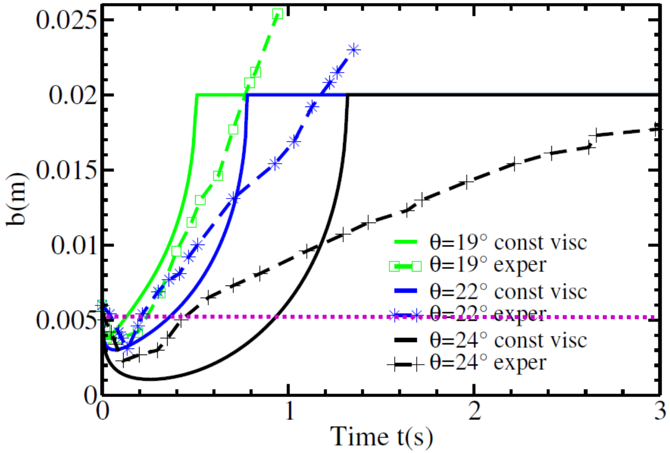

(c) $\nu = 10^{-4} \mathrm{m}^2/\mathrm{s}$ η = 0.15 Pa.s

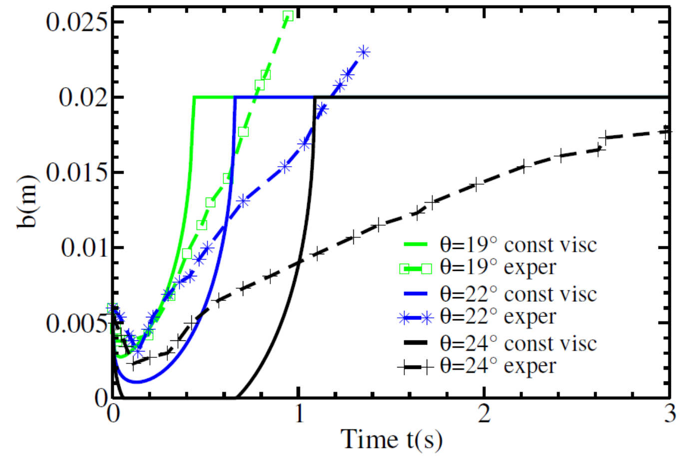

$\mu(I)$ law

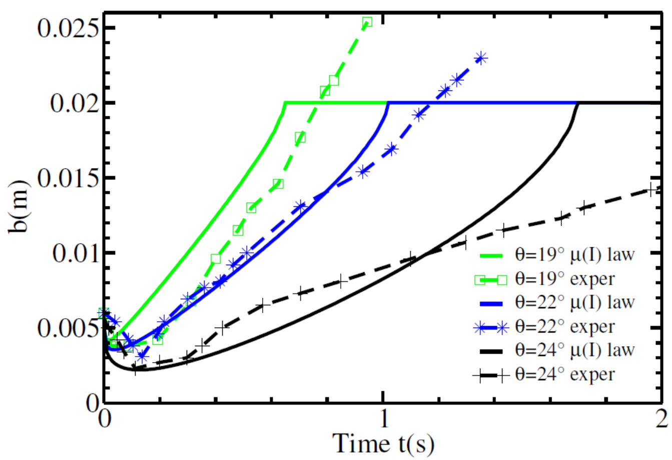

$\theta = 22^o$

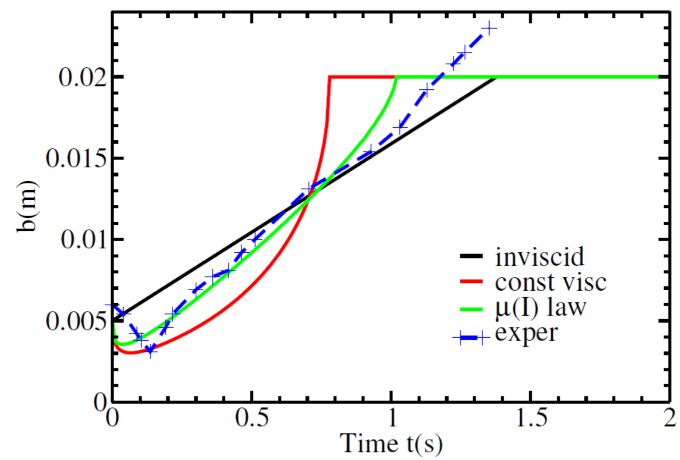

$\mu(I)$ rheology : $2\eta(|\boldsymbol{D}|, p) = \dfrac{k(\mu_2 - \mu_s)p}{k|\boldsymbol{D}| + I_0\sqrt{p}}$

$$\dot{b}(t, X) = \frac{-\partial^2_{ZZ}(\nu \partial_Z U)(t, X, b(t))}{g\cos\theta(\tan\delta - \tan\theta)}\nu.$$

Multilayer Shallow Model

For application to natural flows, equations have to be simplified to lower the computational cost !

➡ Thin-layer (i. e. shallow) approximation $a=h/L<<1$

➡ $p = g\cos\theta(h - Z)$ pression hydrostatique

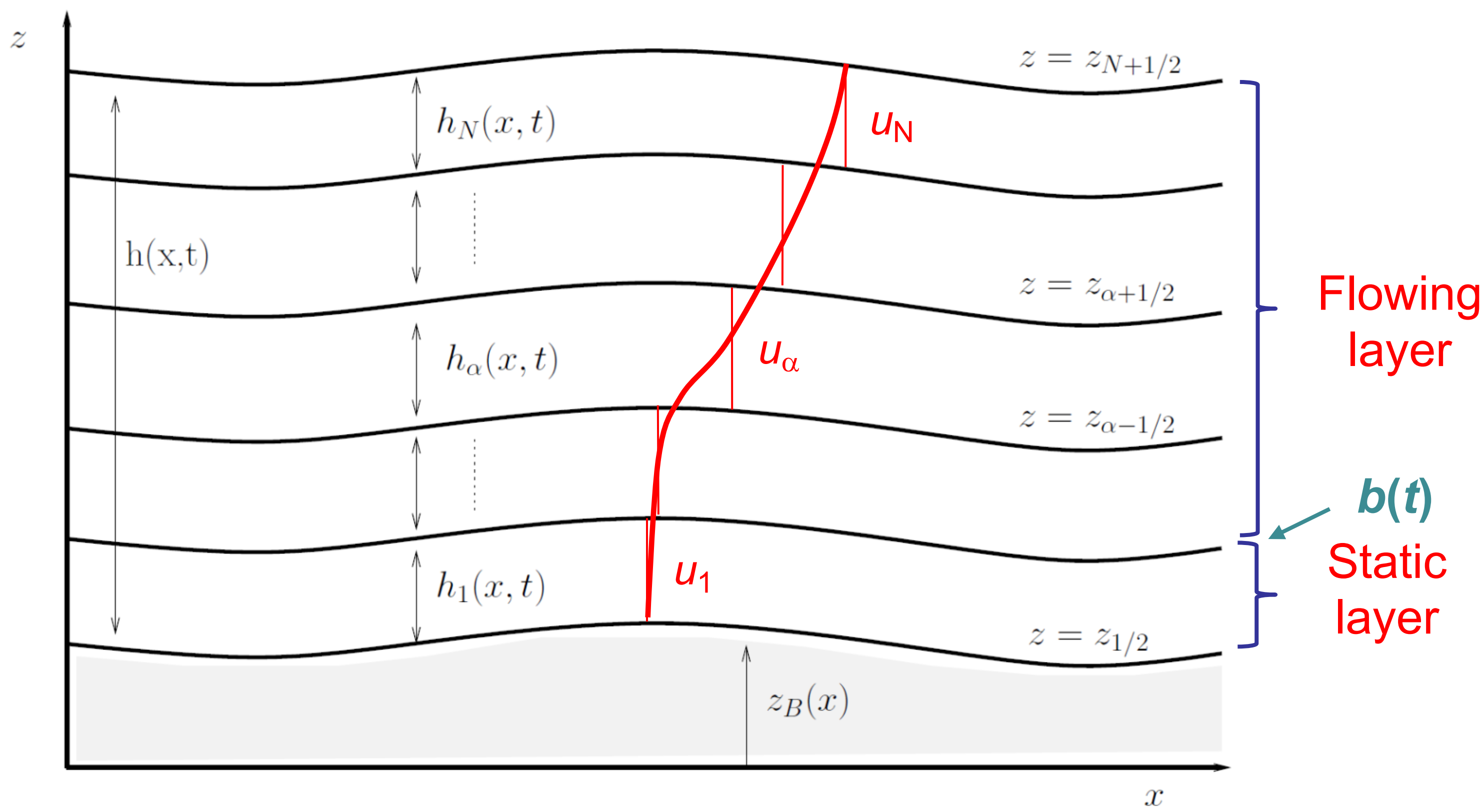

Fernandez-Nieto, Garres, Mangeney, Narbona-Reina, 2015

Multilayer Shallow Model

$$\partial_x \overline{u} + \partial_z \overline{w} = 0,$$
$$\rho\big(\partial_t \overline{u} + \overline{u}\partial_x \overline{u} + \overline{w}\partial_z \overline{u}\big) + \partial_x \overline{p} = -\rho\, g\, \sin\theta + \partial_z \left(\overline{\eta}\frac{\partial_z \overline{u}}{2}\right) - \frac{2}{W}\,\mu_w\,\overline{p}\,\frac{u}{|u|}$$
$$\partial_z \overline{p} = -\rho\, g \cos\theta.$$

Steady uniform flows on inclined planes

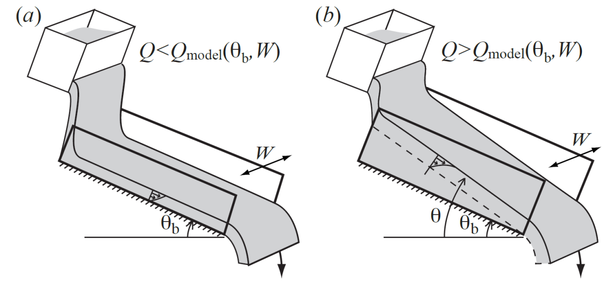

Jop et al., 2005

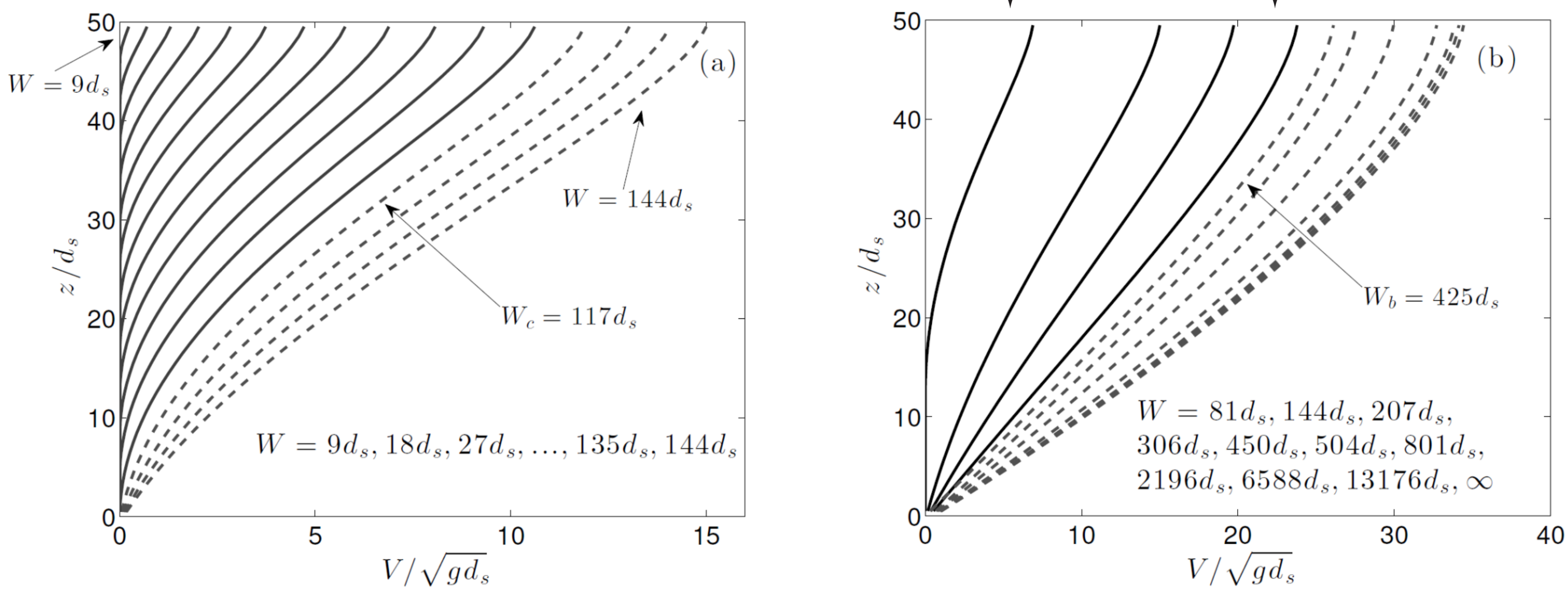

Unsteady flows on inclined planes

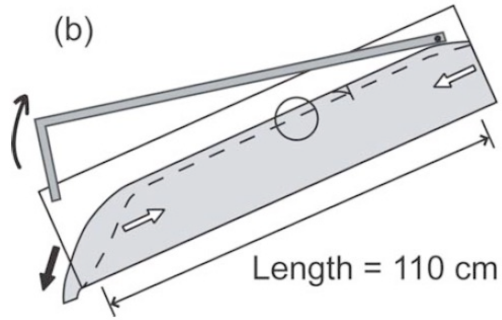

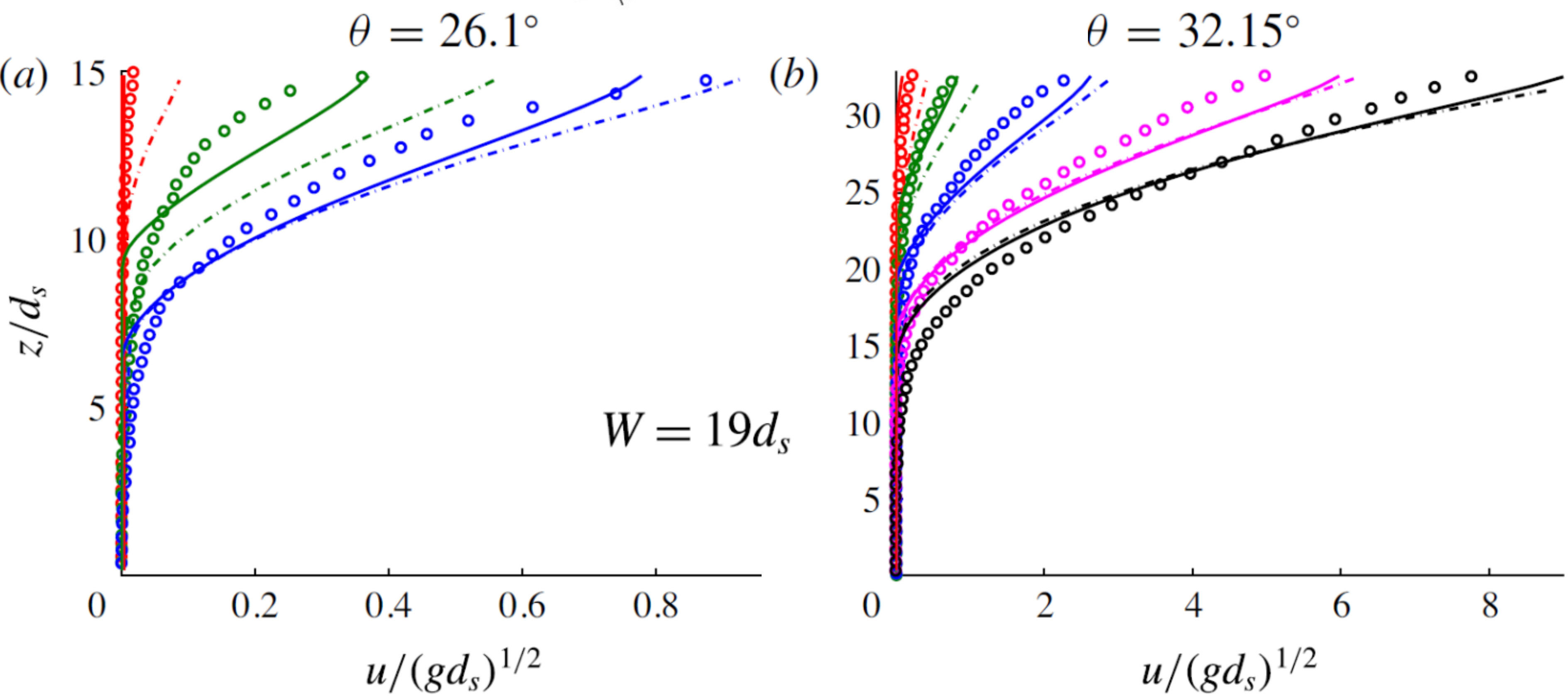

Fernandez-Nieto, Garres, Mangeney, Narbona-Reina, 2017

Monolayer (Saint-Venant) versus Multilayer models

$$\mu_s = \tan(25.5°) \approx 0.48$$

$\theta = 22°$

$\mu(I)$

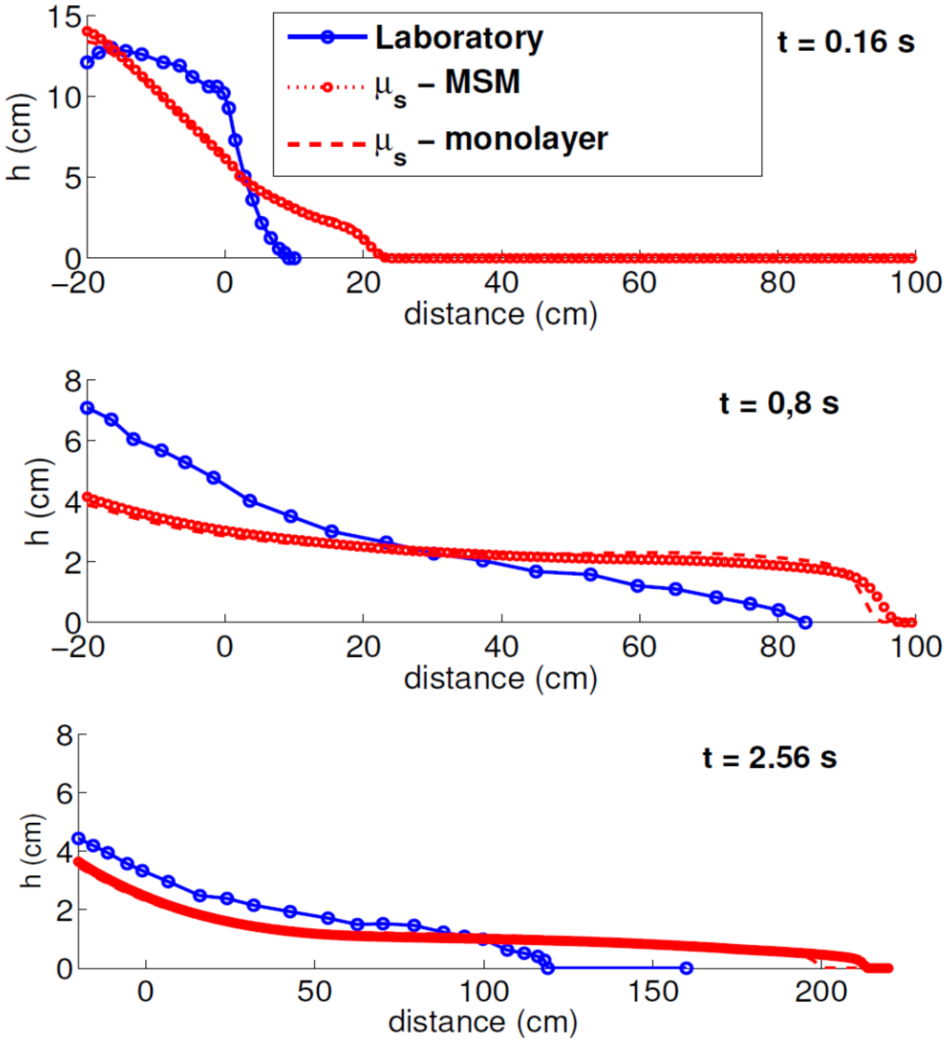

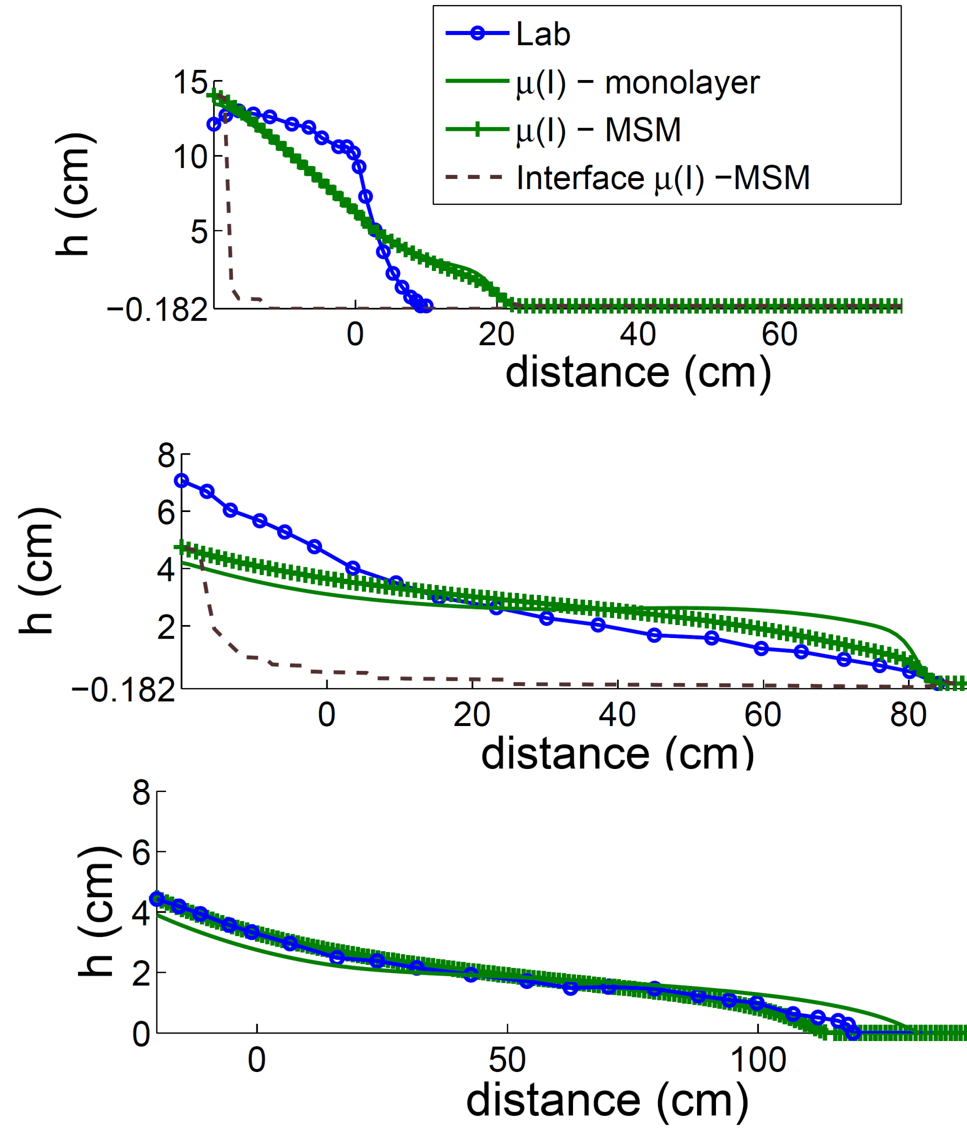

Fernandez-Nieto, Garres, Mangeney, Narbona-Reina, 2016

Multilayer models and wall friction

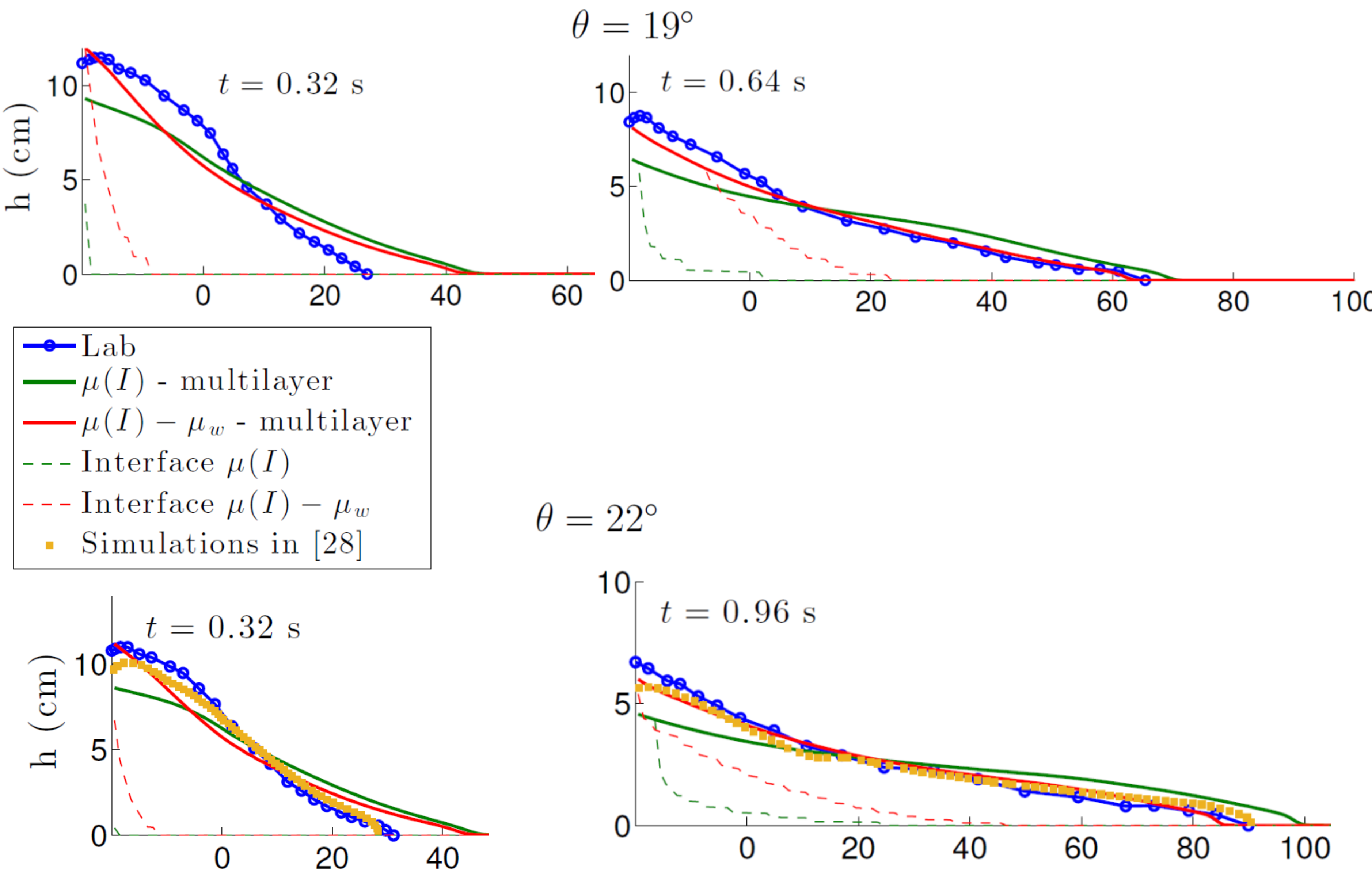

Comparison with shallow visco-plastic model

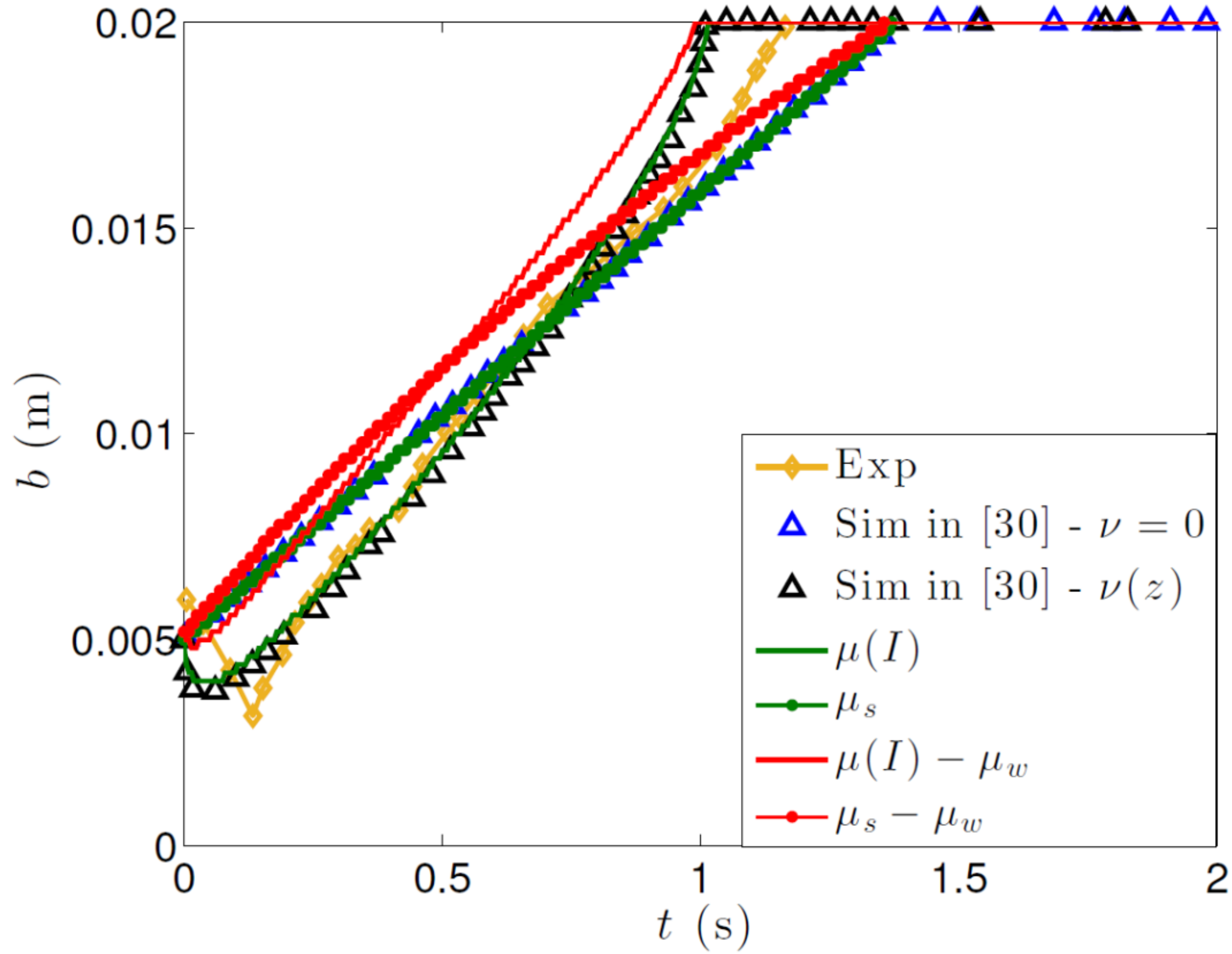

Strong effect of wall friction on the static/flowing interface dynamics

Erosion effects on avalanche runout

$\mu_s = \tan(25.5°) \approx 0.48$

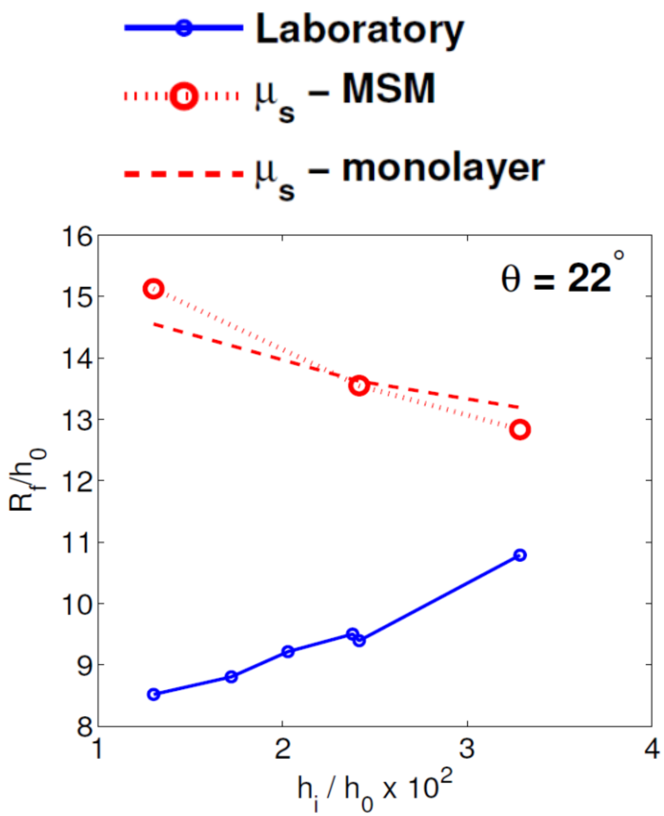

$\mu(I)$

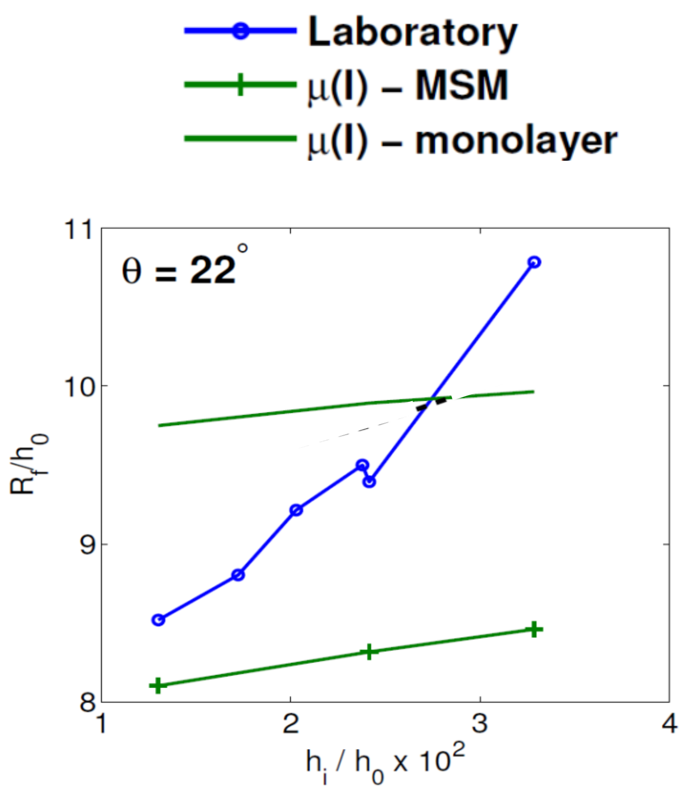

$\mu(I)$ in the Multilayer Shallow Model reproduces qualitatively the increase of runout due to entrainment on sloping erodible beds.

How to get quantitative agreement ?

Non-hydrostatic effects, dilatancy ??

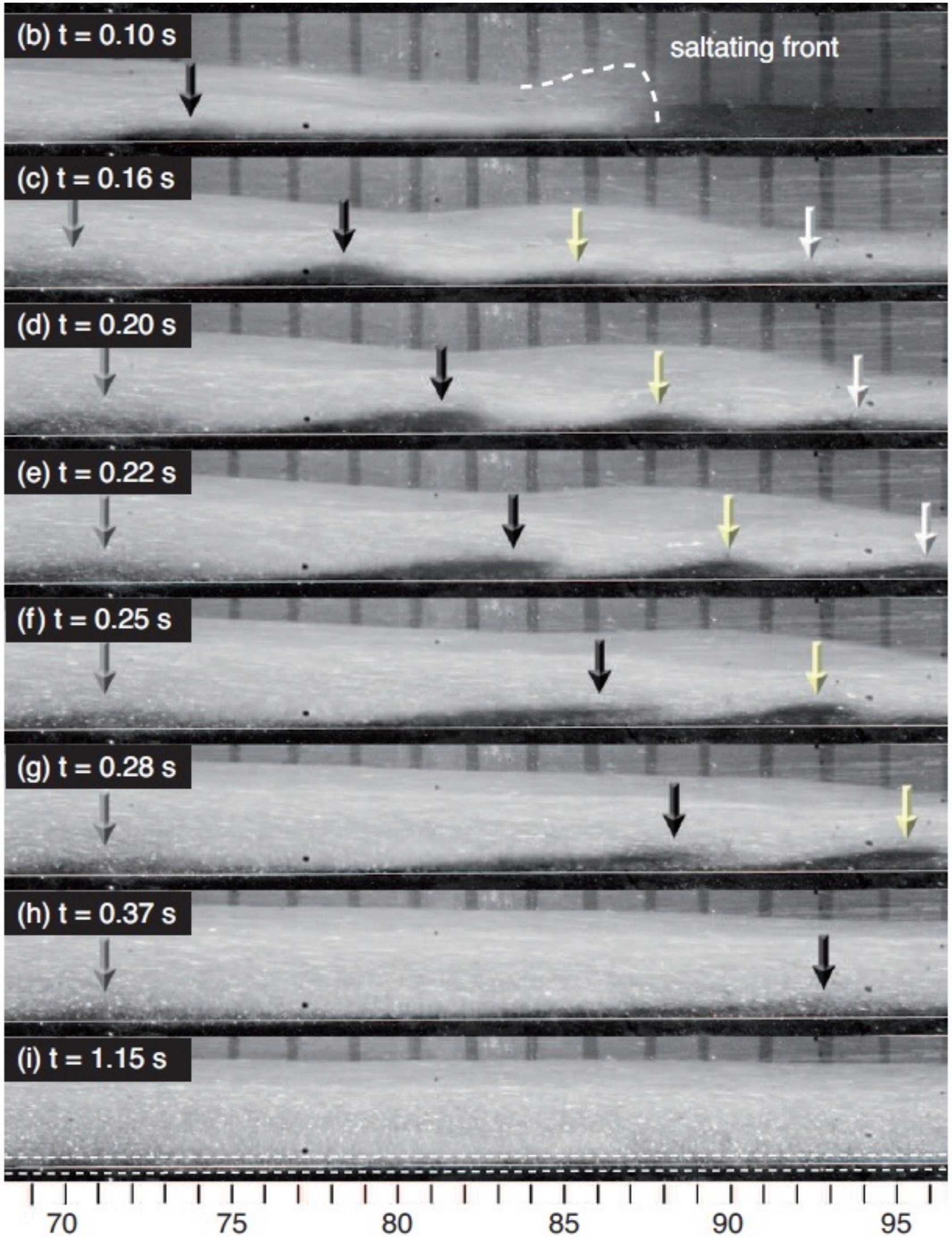

Waves behind the front

$5 \text{ cm} < \lambda < 10 \text{ cm}$

Kelvin-Helmholtz instabilities ?

Force chains ahead of the front

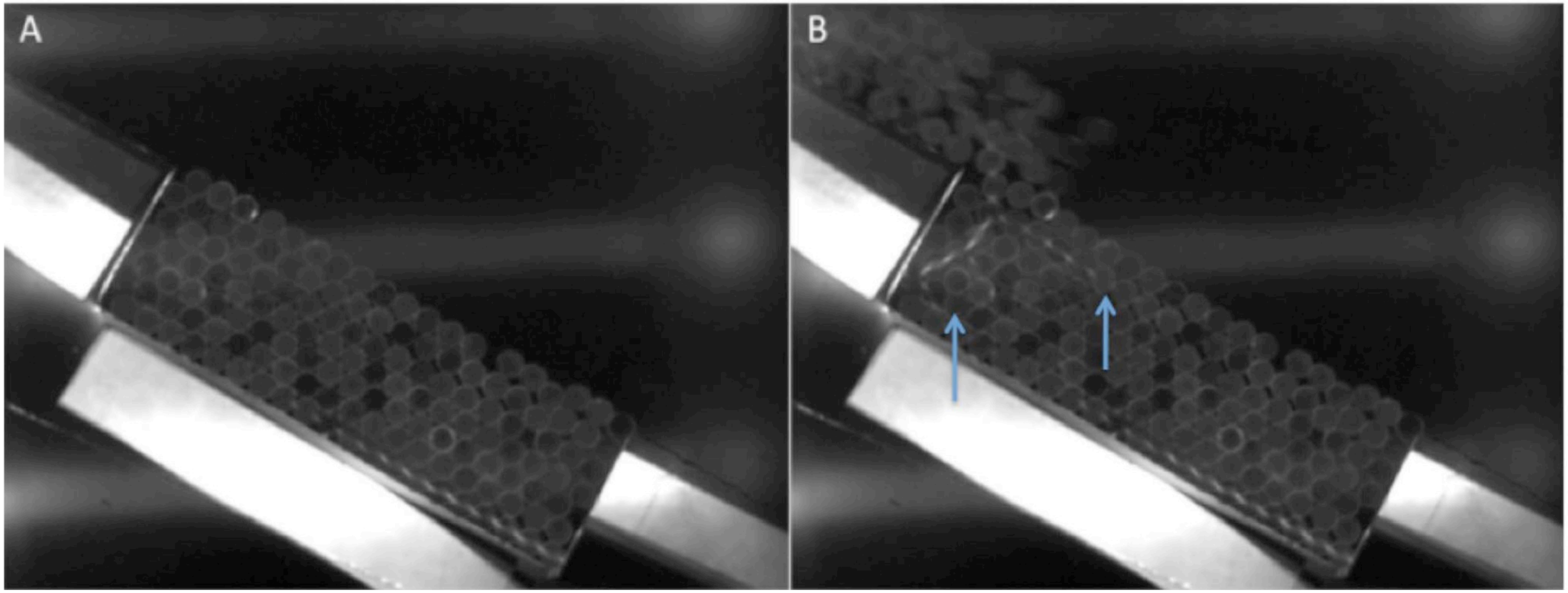

Estep and Dufek, 2012

Film Hugo (VLC)

Erosion waves in granular flows

See *Delannay et al. (2017) for a review*

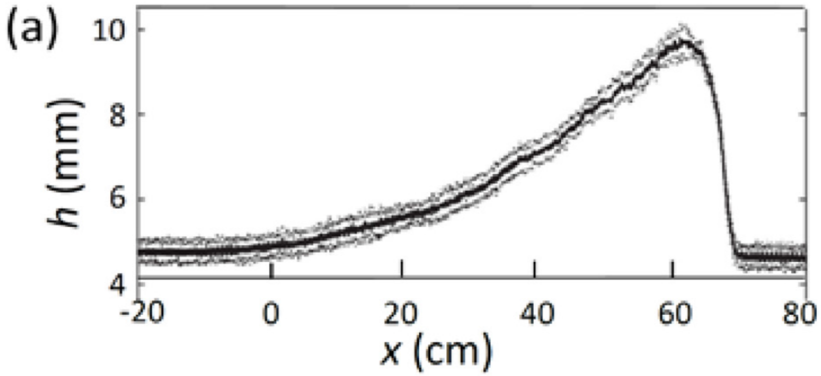

Takagi et al (2011)

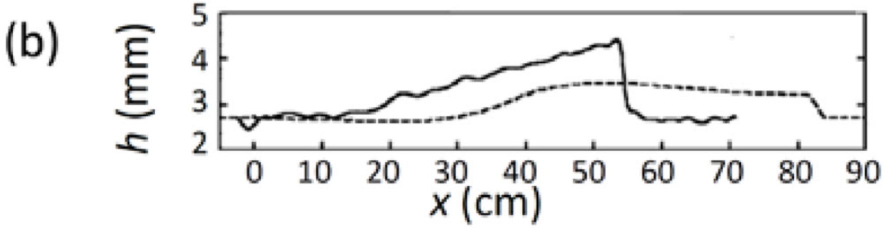

Pouliquen and Forterre (2002)

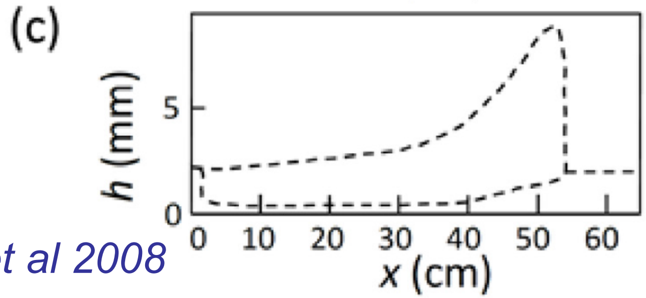

Mangeney et al 2007b

Borzsonyi et al 2008

Forterre and Pouliquen 2003

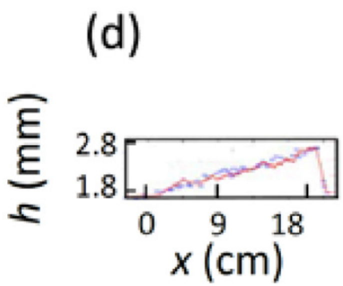

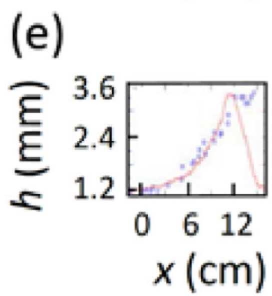

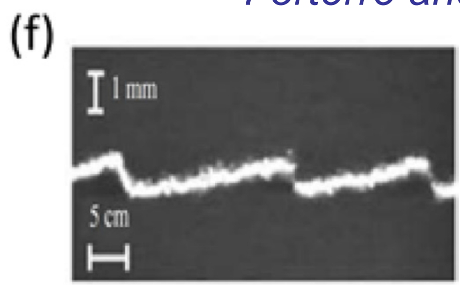

Simulation of the Mt-Steller landslide

no erosion

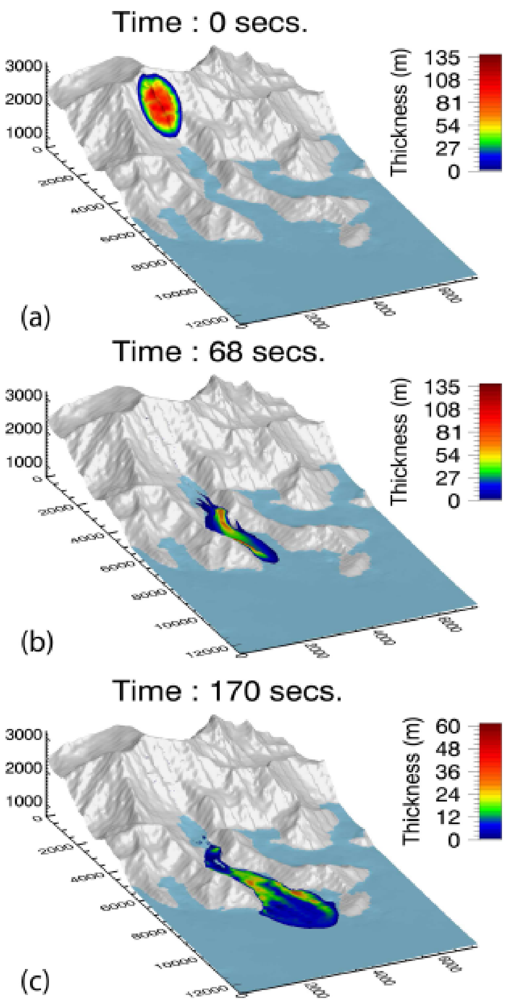

with erosion

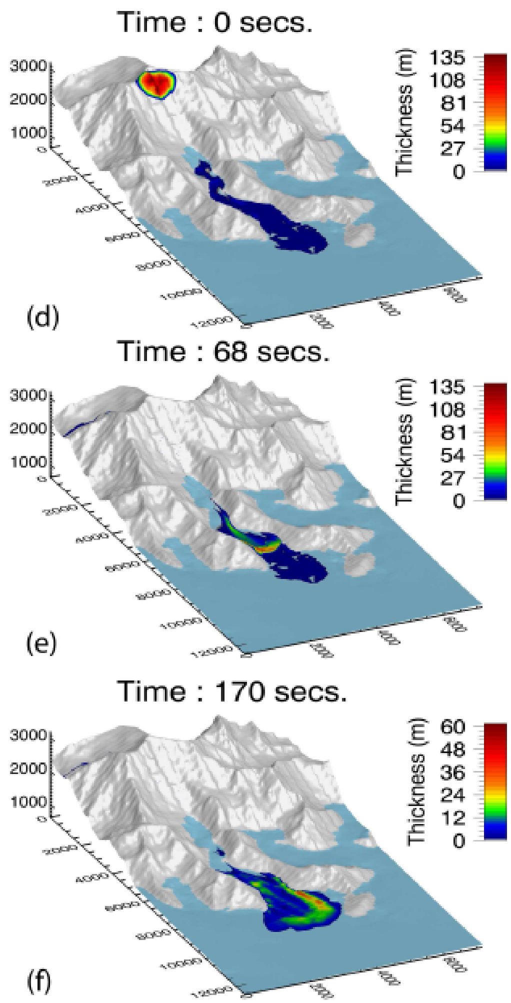

Comparison of deposits

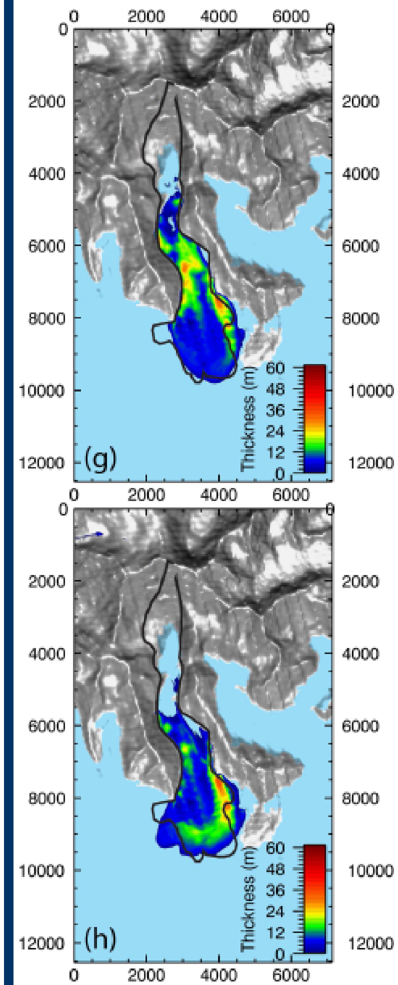

Volume : 40-60 Mm^3

no erosion

with erosion

Moretti et al. 2012

Outline

III – Back to lab-scale experiments and simulation

IIIa – Granular column collapse on rigid and erodible beds

IIIb – μ(I) rheology in 2D models, comparison with other models (DEM, thin-layer)

IIIc – Static-flowing interface (erosion/deposition)

IIId – Grain-fluid mixture model

Modeling of debris flows (grain/fluid)

Solid volume fraction: $0.4 < \varphi < 0.8$

At the field scale

- Thin layer approximation $\frac{h_m}{L_m} = \varepsilon \ll 1$

$$h_m = \mathcal{O}(\epsilon),\ u^{\mathbf{x}} = \mathcal{O}(1),\ u^z = O(\epsilon), \cdots$$

- Depth-averaged model

Mixture model

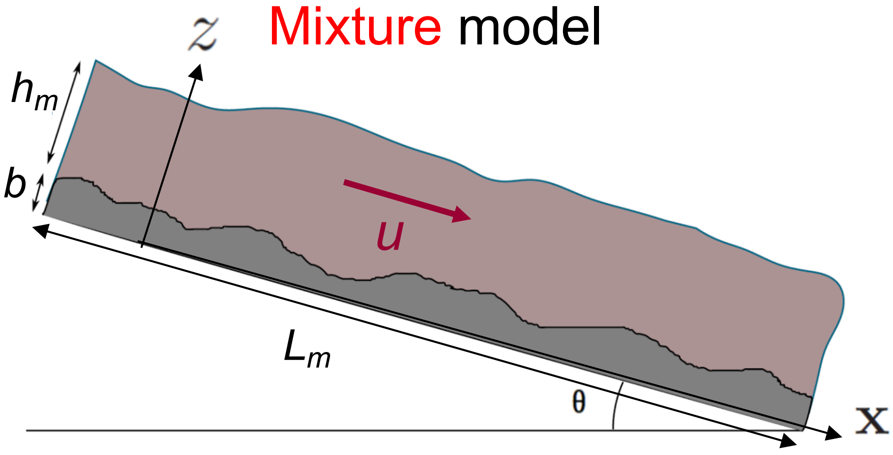

Iverson, Denlinger; Denlinger, Iverson 2001, Iverson, George; George, Iverson 2014

Two-phase model

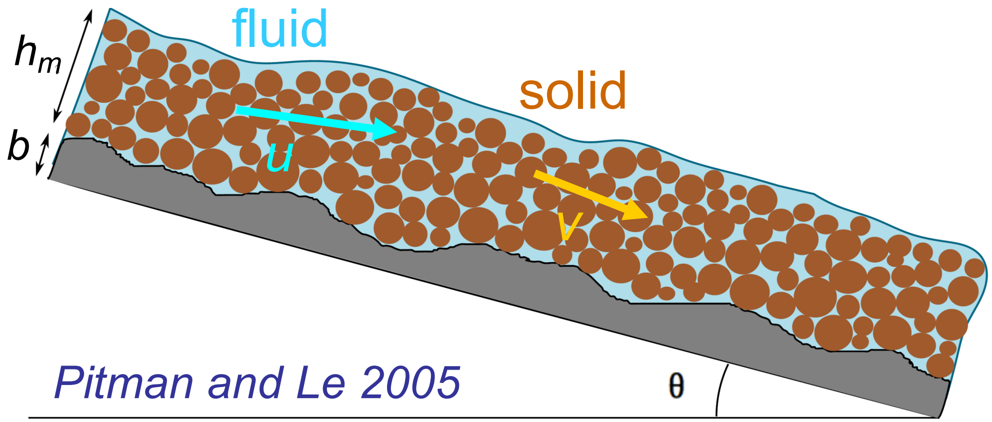

Pitman and Le 2005

Pitman and Le 2005, Bouchut et al. 2016

Modeling of debris flows (grain/fluid)

Solid volume fraction: $0.4 < \varphi < 0.8$

At the field scale

- Thin layer approximation $\frac{h_m}{L_m} = \varepsilon \ll 1$

$$h_m = \mathcal{O}(\epsilon),\ u^{\mathrm{x}} = \mathcal{O}(1),\ u^z = O(\epsilon), \cdots$$

- Depth-averaged model

Mixture model

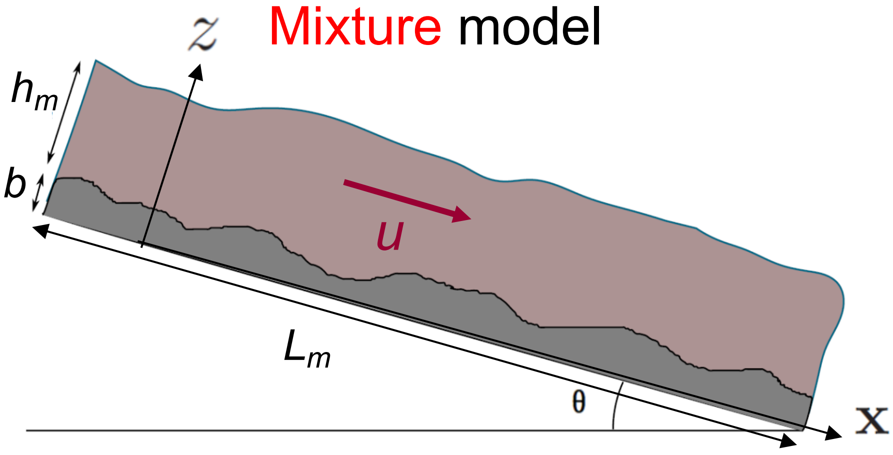

Iverson, Denlinger; Denlinger, Iverson 2001, Iverson, George; George, Iverson 2014

Two-phase model

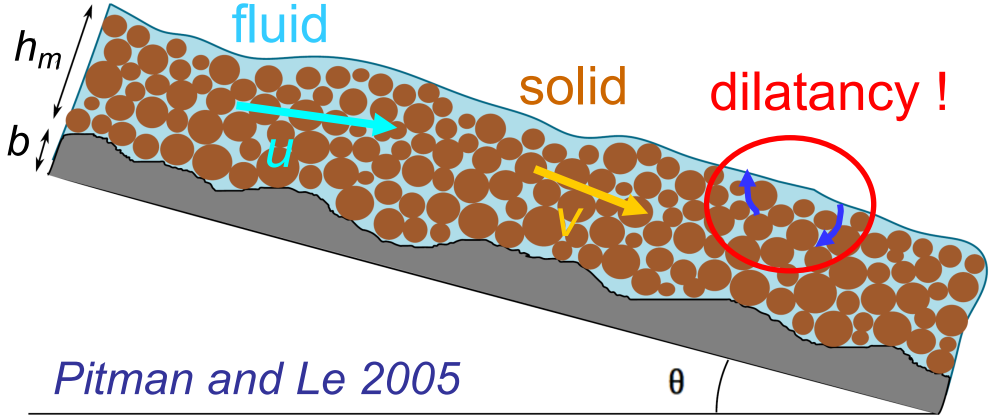

Pitman and Le 2005

Pitman and Le 2005, Bouchut et al. 2016

Jackson's model

Jackson, 2000

φ : solid volume fraction, $1-\varphi$: fluid volume fraction

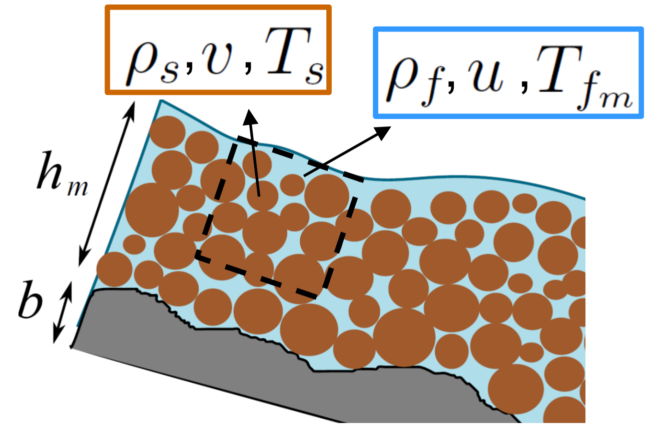

- Mass conservation :

$$\begin{aligned} * \quad \partial_t(\rho_s\varphi) + \nabla\cdot(\rho_s\varphi v) &= 0 \\ * \quad \partial_t(\rho_f(1-\varphi)) + \nabla\cdot(\rho_f(1-\varphi)u) &= 0 \end{aligned}$$

- Momentum conservation :

$$* \quad \rho_s\varphi(\partial_t v + (v\cdot\nabla)v) = -\nabla\cdot T_s - \varphi\nabla p_{f_m} + f + \rho_s\varphi\mathbf{g}$$

$$* \quad \rho_f(1-\varphi)(\partial_t u + (u\cdot\nabla)u) = -\nabla\cdot T_{f_m} + \varphi\nabla p_{f_m} - f + \rho_f(1-\varphi)\mathbf{g}$$

$$T_s = p_s\,\mathrm{Id} + \widetilde{T}_s \qquad T_{f_m} = p_{f_m}\,\mathrm{Id} + \widetilde{T}_{f_m}$$

Friction between the solid and fluid phases : $f = \beta(u-v)$

5 unknowns : φ, v, u, p_s, p_{f_m}, 4 equations

A constitutive equation is required to close the system

Bouchut, Fernandez-Nieto, Mangeney, Narbona-Reina, 2015, 2016

Qualitative explanation of dilatancy effects

Critical state : φ_c^{eq} *when deformed*

$\varphi < \varphi_c^{eq}$ (loose)

Granular medium contracts

⬇

Fluid is expelled ($\mathcal{V}_f$)

⬇

Fluid pore pressure $p_{fm}=p_{hydro}+p^e_{fm}$ increases

⬇

Liquefaction

$\varphi > \varphi_c^{eq}$ (dense)

Granular medium dilates

⬇

Fluid is sucked ($-\mathcal{V}_f$)

⬇

Fluid pore pressure decreases

⬇

Stiffening of the granular matrix

$\mathcal{V}_f$

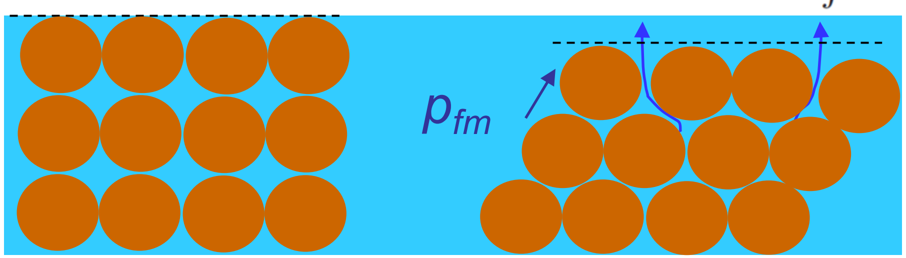

$-\mathcal{V}_f$

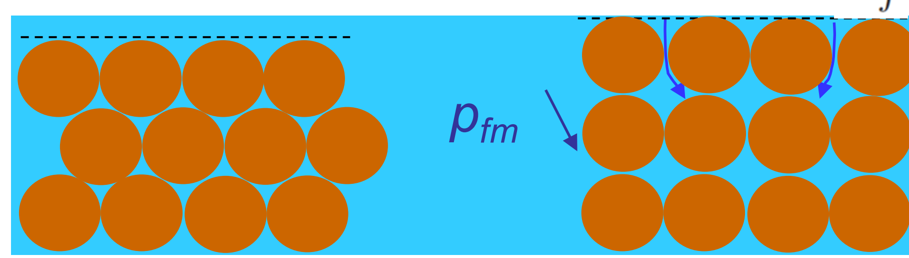

Excess pore pressure $p^e_{fm} \geq 0$

$p^e_{fm} \leq 0$

Coulomb friction: $T^{\mathbf{x}z}_{s\,|b} = \tan\overline{\delta_{\text{eff}}}\left(\bar{\varphi}(\rho_s - \rho_f)g\cos\theta h_m - (p^e_{f_m})_{|b}\right)$

e. g. Schofield and Wroth, 1968, Wood, 1990, Pailha and Pouliquen, 2009

Modeling of dilatancy effects

- Compression/dilatation of the solid phase :

$$\nabla \cdot v = \dot{\gamma} \tan \psi$$ *Roux and Radjai, 1998*

ψ : dilatancy angle, $\dot{\gamma}$: shear strain rate

$$\tan \psi = K(\varphi - \varphi_c^{eq})$$ *Pailha and Pouliquen, 2009*

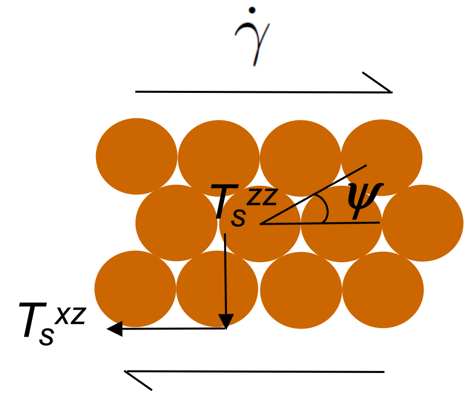

➡ Closure equation : $\boxed{\nabla \cdot v = K\dot{\gamma}(\varphi - \varphi_c^{eq})}$

$$\bar{\varphi}_c^{eq} = \bar{\varphi}_c^{stat} - K_2 \frac{\eta_f \dot{\gamma}}{p_{s|b}}$$

$\varphi < \varphi_c^{eq}$: compression $\qquad$ $\varphi > \varphi_c^{eq}$: dilatation

- Impact of the dilatancy angle on the Coulomb friction force :

$$\boxed{T_s^{xz} = -\underbrace{\tan(\delta + \psi)}_{\delta_{\text{eff}}} \operatorname{sign}(v)\, T_s^{zz}}$$

Compression decreases friction in addition to increase of fluid pore pressure

No need of additional pressure equation !

// George and Iverson 2014

Boundary conditions

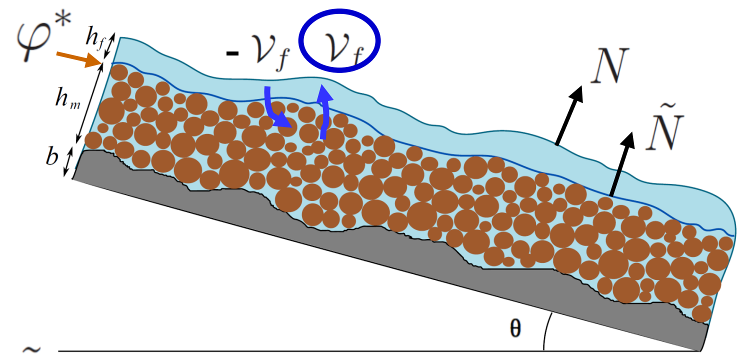

- **At the free surface,** for the fluid:
  - no tension: $T_f N_X = 0$
  - kinematic condition: $N_t + u_f \cdot N_X = 0$
- **At the interface mixture/fluid**:
  - kinematic condition for the solid: $\tilde{N}_t + v \cdot \tilde{N}_X = 0$
  - Rankine-Hugoniot (mass conservation) condition:

$$\tilde{N}_t + u_f \cdot \tilde{N}_X = (1 - \varphi^*)(\tilde{N}_t + u \cdot \tilde{N}_X) \equiv \mathcal{V}_f$$

  - Rankine-Hugoniot (momentum conservation) condition:

$$\rho_f \mathcal{V}_f (u - u_f) + (T_s + T_{f_m})\tilde{N}_X = T_f \tilde{N}_X$$

  - stress transfer condition from the energy balance:

$$T_s \tilde{N}_X = \left(\frac{\rho_f}{2} \left((u - u_f) \cdot \frac{\tilde{N}_X}{|\tilde{N}_X|} \right)^2 + \left((T_{f_m} \tilde{N}_X) \cdot \frac{\tilde{N}_X}{|\tilde{N}_X|^2} - p_{f_m} \right) \frac{\varphi^*}{1 - \varphi^*} \right) \tilde{N}_X$$

  - Navier friction condition for the fluid:

$$\left(\frac{T_{f_m} + T_f}{2} \tilde{N}_X \right)_\tau = -k_i (u_f - u)_\tau$$

Boundary conditions

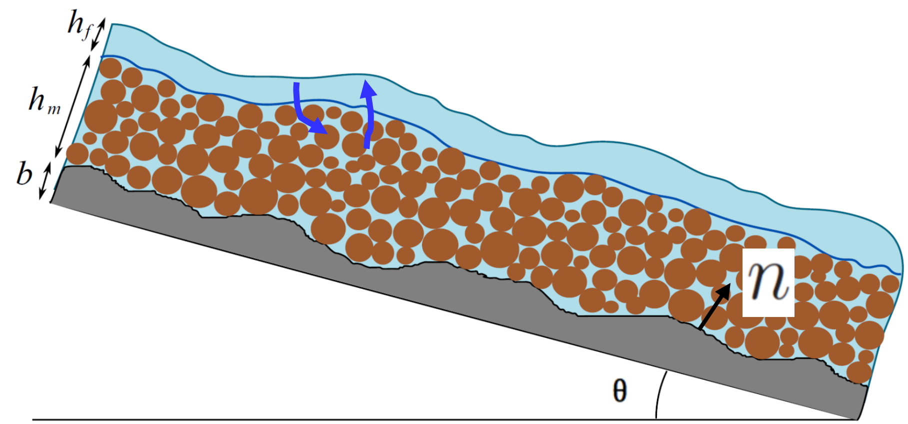

- Bottom boundary conditions:

  ** No penetration condition:

$$u \cdot n = 0, \qquad v \cdot n = 0$$

  * Coulomb friction for the solid:

$$(T_s n)_\tau = -\tan\delta_{\text{eff}}\ \text{sgn}(v)(T_s n)\cdot n$$

  * Navier friction for the fluid:

$$(T_{f_m} n)_\tau = -k_b u$$

Bouchut, Fernandez-Nieto, Mangeney, Narbona-Reina, 2016

Fluid pore pressure

in thin layer depth-averaged models

- From the fluid momentum conservation in the direction normal to the slope

$$\cancel{\varepsilon\rho_f(1-\varphi)(\partial_t u^z + u^{\mathbf{x}}\cdot\nabla_{\mathbf{x}}u^z + u^z\partial_z u^z)} =$$

$$-(1-\varphi)\partial_z p_{f_m} - g\cos\theta\rho_f(1-\varphi) - \beta(u^z - v^z) - \cancel{\varepsilon\nabla_{\mathbf{x}}\cdot T_{f_m}^{\mathbf{x}z}}$$

$$p_{f_m} = \rho_f g\cos\theta(b + h_m + h_f - z) + p_{f_m}^e + O(\epsilon^2)$$

with $$p_{f_m}^e \equiv \frac{\bar\beta}{1-\bar\varphi}\int_z^{b+h_m}(u^z - v^z)(z')dz'$$

using the dilatancy closure equation $\nabla\cdot v = K\dot\gamma(\varphi - \varphi_c^{eq})$

⬇

- Non-hydrostatic (excess) fluid pressure

$$(p_{f_m}^e)_{|b} = \frac{\bar\beta}{1-\bar\varphi}h_m(\overline{u^{\mathbf{x}}} - \overline{v^{\mathbf{x}}})\cdot\nabla_{\mathbf{x}}b - \frac{\bar\beta}{1-\bar\varphi}\frac{h_m^2}{2}\left(\nabla_{\mathbf{x}}\cdot(\overline{u^{\mathbf{x}}} - \overline{v^{\mathbf{x}}}) + \frac{K\bar{\dot\gamma}(\bar\varphi - \varphi_c^{eq})}{1-\bar\varphi}\right)$$

Bouchut, Fernandez-Nieto, Mangeney, Narbona-Reina, JFM, 2016

Our model in the uniform immersed configuration

$$\overline{u_f} = 0, \; h_m(t) + h_f(t,x) + x\tan\theta = cst$$

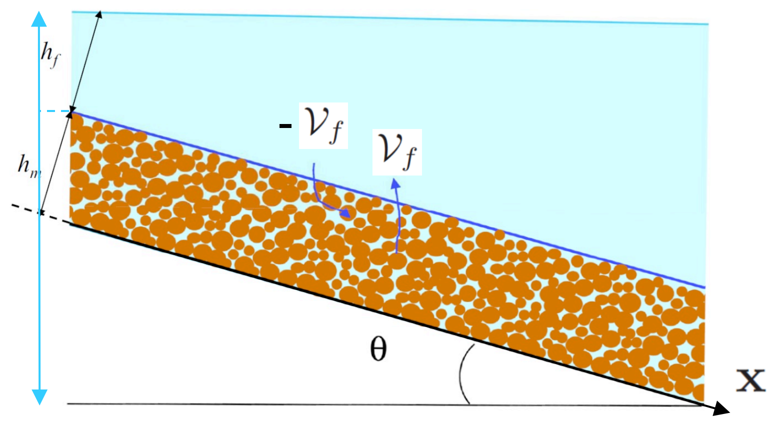

- Mass conservation :
  - $\partial_t(\bar\varphi h_m) = 0$
  - $\partial_t \bar\varphi = -\bar\varphi \bar\Phi$
- Momentum conservation :
  - $\rho_s \bar\varphi \partial_t \overline{v^{\mathbf{x}}} = -\operatorname{sgn}(\overline{v^{\mathbf{x}}})\dfrac{\tau_b}{h_m} + \bar\beta(\overline{u^{\mathbf{x}}} - \overline{v^{\mathbf{x}}}) - \bar\varphi(\rho_s - \rho_f) g \sin\theta$
  - $\rho_f(1-\bar\varphi)\partial_t \overline{u^{\mathbf{x}}} = \left(\dfrac{1}{2}\rho_f \mathcal{V}_f - k_b\right)\dfrac{\overline{u^{\mathbf{x}}}}{h_m} - \bar\beta(\overline{u^{\mathbf{x}}} - \overline{v^{\mathbf{x}}})$

with $\mathcal{V}_f = -h_m \bar\Phi \,, \quad \tau_b = \tan\overline{\delta_{\text{eff}}}\; p_{s|b} + K_1 \eta_f \bar{\dot\gamma}$

$$p_{s|b} = \bar\varphi(\rho_s - \rho_f) g \cos\theta h_m - (p^e_{f_m})_{|b} \,, \quad (p^e_{f_m})_{|b} = -\frac{\bar\beta}{(1-\bar\varphi)^2}\frac{h_m^2}{2}\bar\Phi$$

- Closure related to dilatancy :

$$\bar\Phi = \bar{\dot\gamma}\tan\psi \,, \quad \tan\psi = K(\bar\varphi - \bar\varphi_c^{eq}), \quad \bar\varphi_c^{eq} = \bar\varphi_c^{stat} - K_2 \frac{\eta_f \bar{\dot\gamma}}{p_{s|b}},$$

$$\bar{\dot\gamma} = 3\frac{|\overline{v^{\mathbf{x}}}|}{h_m}\,, \quad \tan\overline{\delta_{\text{eff}}} = \tan\delta + \tan\psi$$

Characteristic time scales

- Our model and *Pailha and Pouliquen's* model :

$t_{crit} = 1/\bar{\dot{\gamma}}$ ≈ 0.2 s : convergence to the critical state

$t_{visc} = \rho_s h_m^2 / 3K_1 \eta_f$ ≈ 4.10^{-2} s : viscous effects

$t_{rel} = \rho_s / \bar{\beta}$ ≈ 5.10^{-5} s : relaxation of the relative velocity: $\overline{u^x} - \overline{v^x} \to 0$

$$Fr^2 \sim t_{visc}/t_{crit} \qquad S \sim t_{visc}/t_{rel}$$

- *Georges and Iverson's* model: due to additional pressure equation

Mixture compressibility α :

$$t_{IG} = \alpha \frac{\bar{\beta} h_m^2}{2(1-\bar{\varphi})^2}$$

≈ 1.5 × 10^{-5} s for $\alpha = 5 \times 10^{-10}\ \mathrm{Pa}^{-1}$

≈ 1.5 s for $\alpha = 5 \times 10^{-5}\ \mathrm{Pa}^{-1}$

see *Bouchut et al., 2016*, *J. Fluid Mech.* for differences between the two models

Model parameters

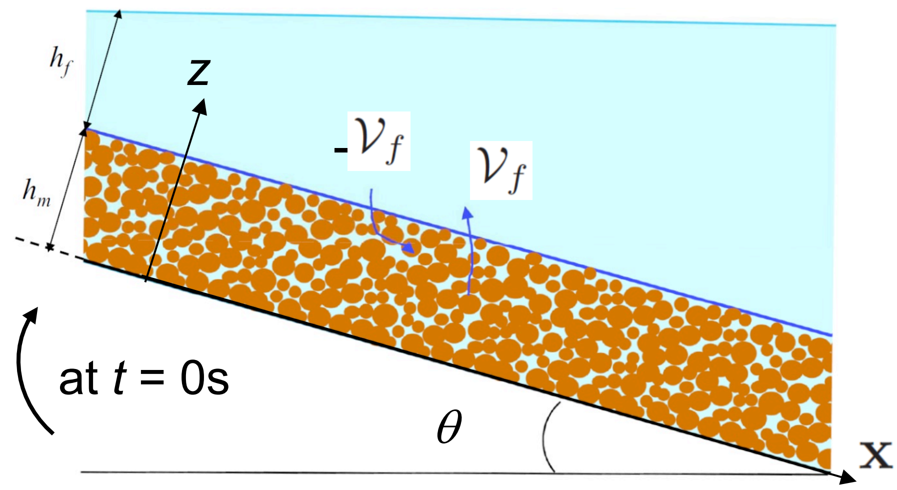

- Parameters for the laboratory experiments of *Pailha et al., 2008* :

$\rho_s = 2500\,\mathrm{kg/m^3}, \quad \bar{\varphi}_c^{stat} = 0.582, \; \delta = 22.5°, \; K_1 = 90.5, \quad K_2 = 25$

- $\eta_f = 96 \times 10^{-3}\,\mathrm{Pa\cdot s}, \; \rho_f = 1041\,\mathrm{kg/m^3}, \; |\theta| = 25^{\mathrm{o}}, \; h_m^0 = 4.9\,\mathrm{mm}$
- $\eta_f = 9.8 \times 10^{-3}\,\mathrm{Pa\cdot s}, \; \rho_f = 1026\,\mathrm{kg/m^3}, \; |\theta| = 28^{\mathrm{o}}, \; h_m^0 = 6.1\,\mathrm{mm}$

Simple tests on submarine granular flows

Laboratory experiments: *Pailha et al., 2008*

viscosity : $\eta_f = 96 \times 10^{-3}\,\mathrm{Pa\cdot s}$

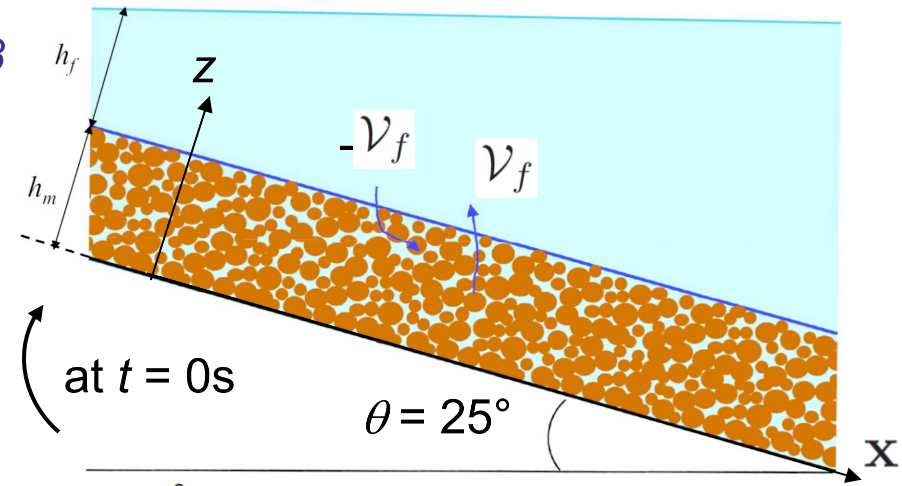

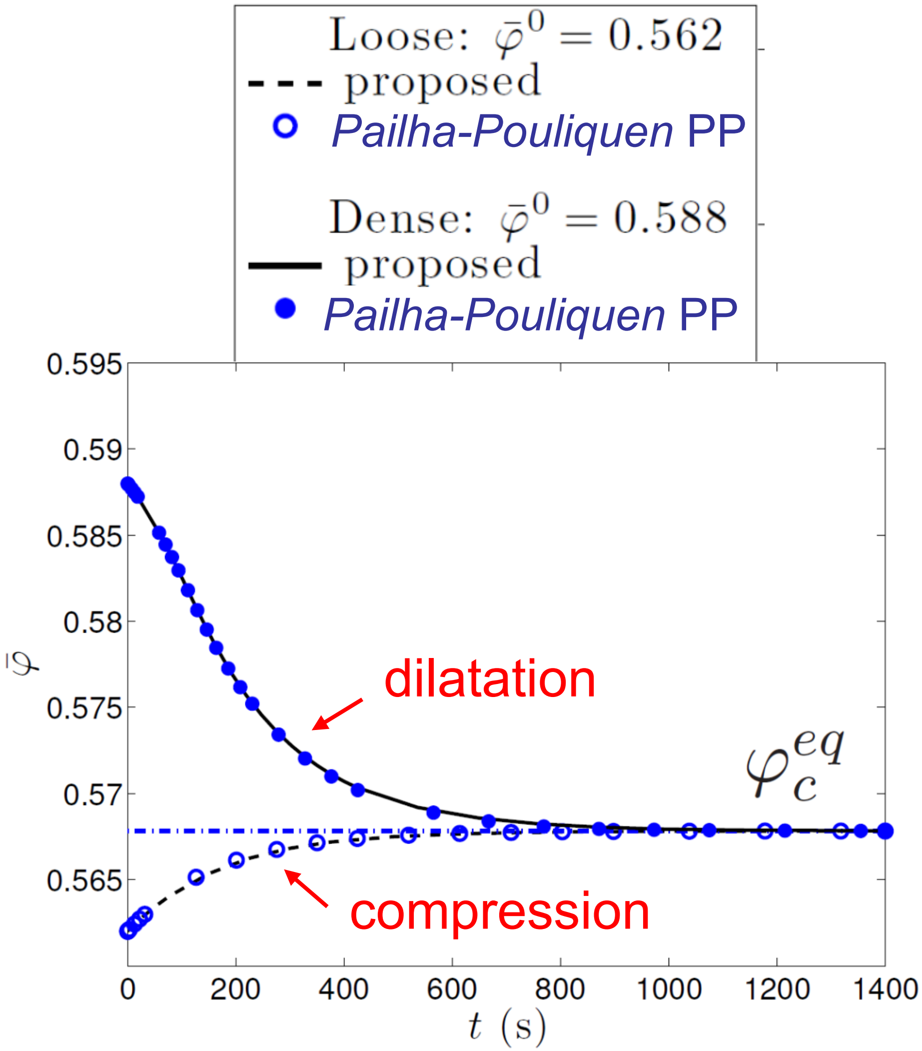

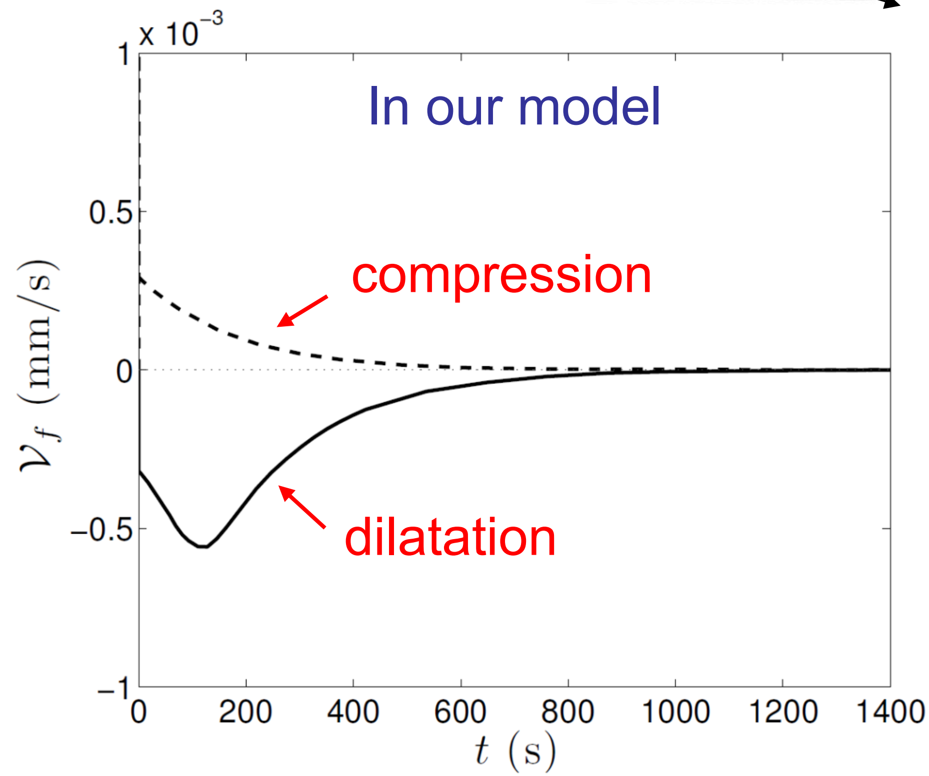

Dry granular column collapse

Simulation of dense laboratory experiments of *Mangeney et al., 2010*

Deposit at θ=0°

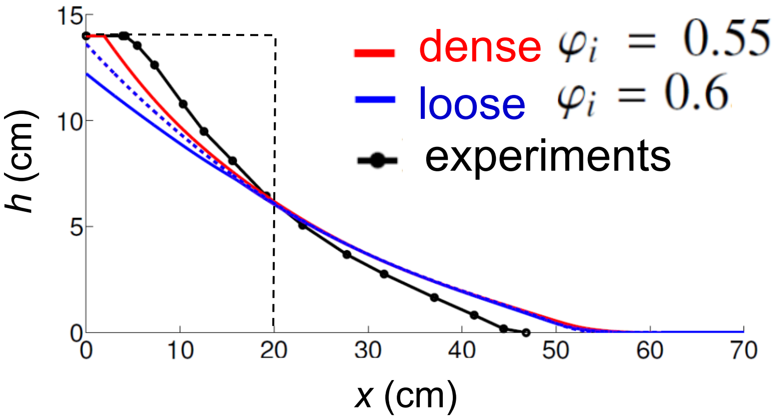

As in DEM *Kermani et al., 2015*

Dry granular column collapse

Simulation of dense laboratory experiments of *Mangeney et al., 2010*

Deposit at $\theta = 0°$

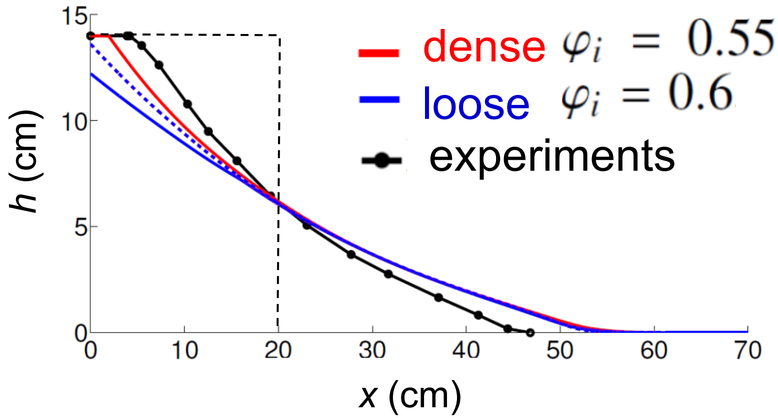

As in DEM *Kermani et al., 2015*

Dilatancy angle

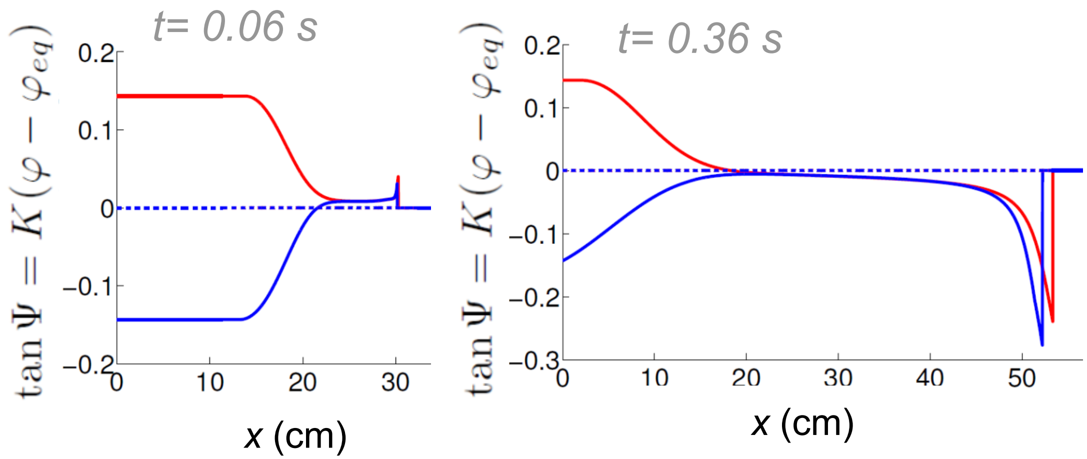

Effective friction coefficient

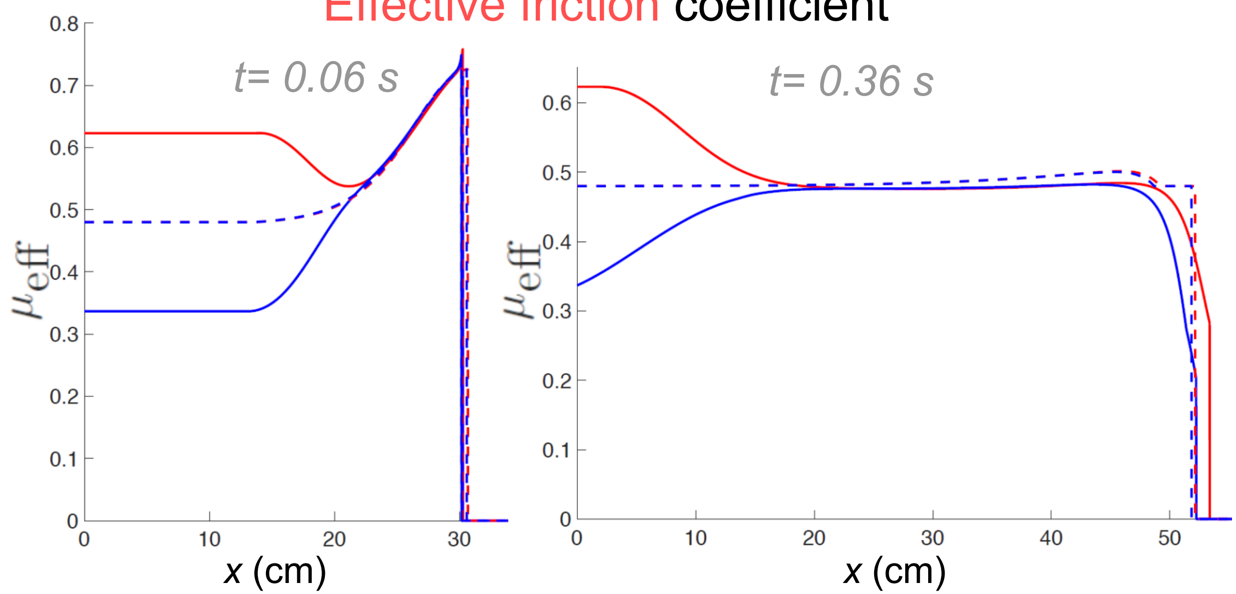

$$\boxed{\tan\delta_{\text{eff}} \approx \underbrace{\mu_1 + \frac{\mu_2 - \mu_1}{I + I_0} I}_{\mu(I)} + \underbrace{\tan\psi}_{\text{dilatancy}}}$$

Bouchut et al., 2019

Submarine granular column collapse

Simulation of laboratory experiments of *Rondon et al., 2011*

Exp. initially dense column

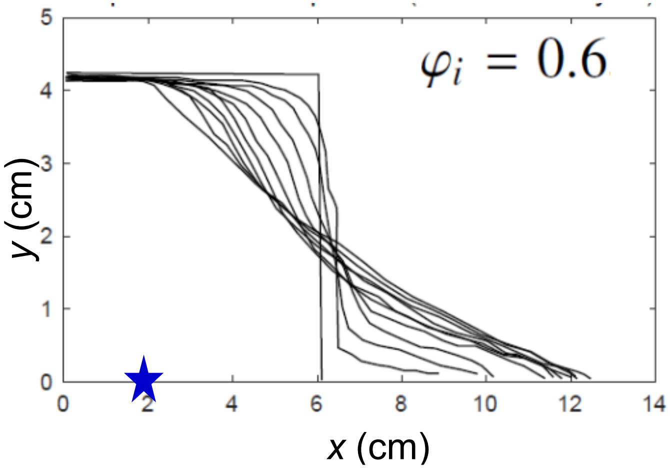

Exp. initially loose column

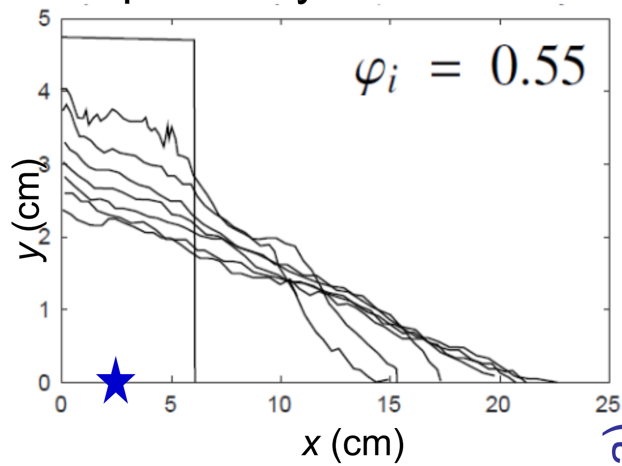

Simulation initially dense

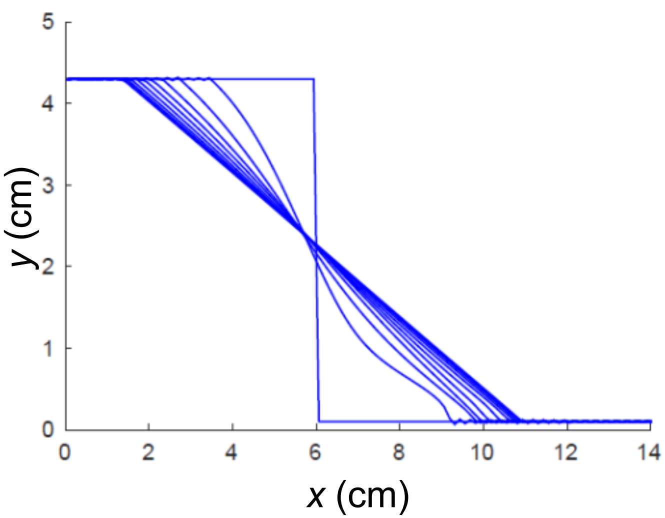

Simulation initially loose

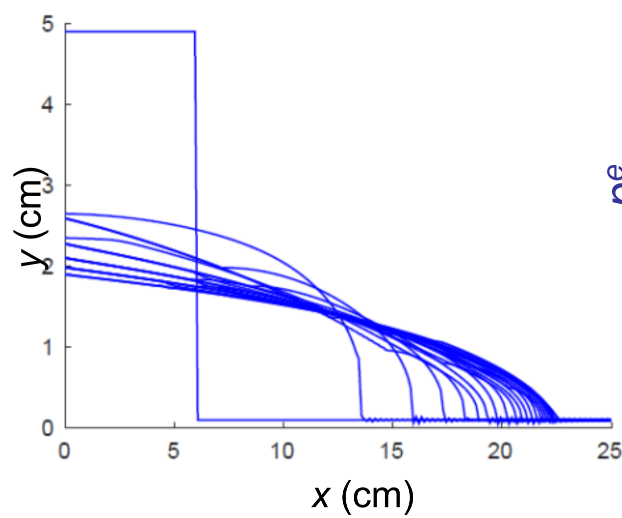

Excess pore fluid pressure

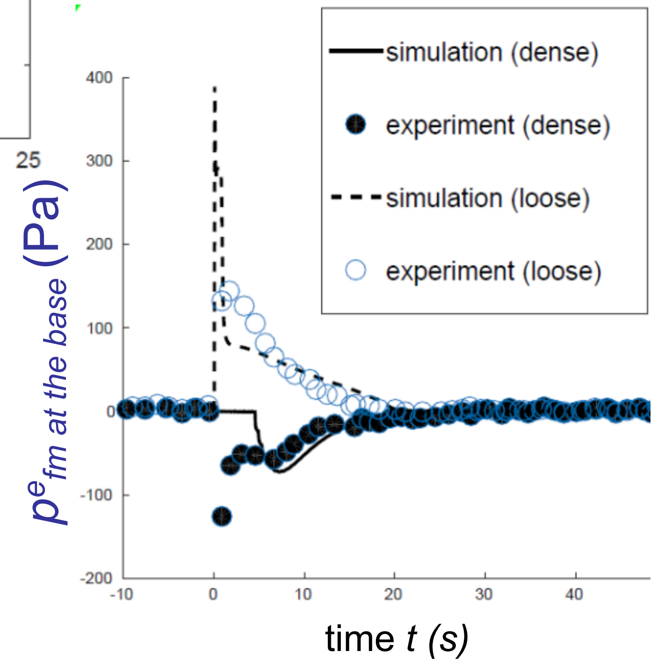

Bouchut et al., 2018

Submarine granular column collapse

Simulation of laboratory experiments of *Rondon et al., 2011*

Exp. initially dense column

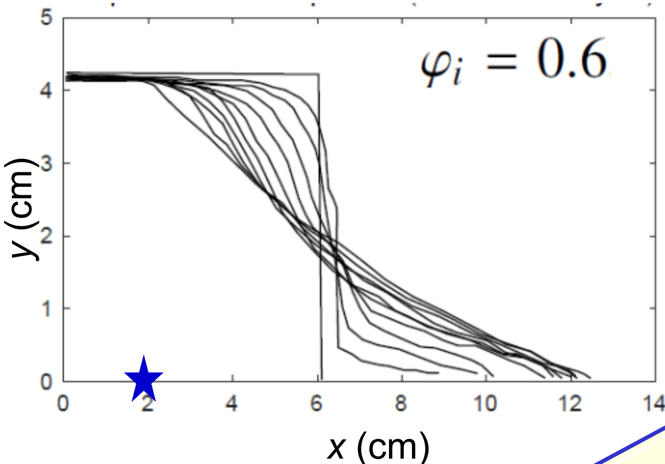

Exp. initially loose column

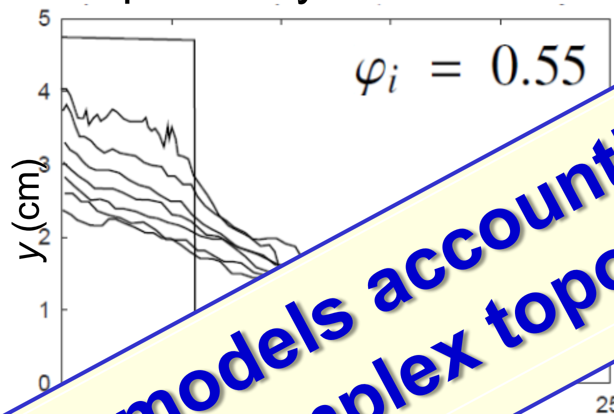

No two-phase flow models accounting for the full tensor of the complex topography!

Simulation initially de

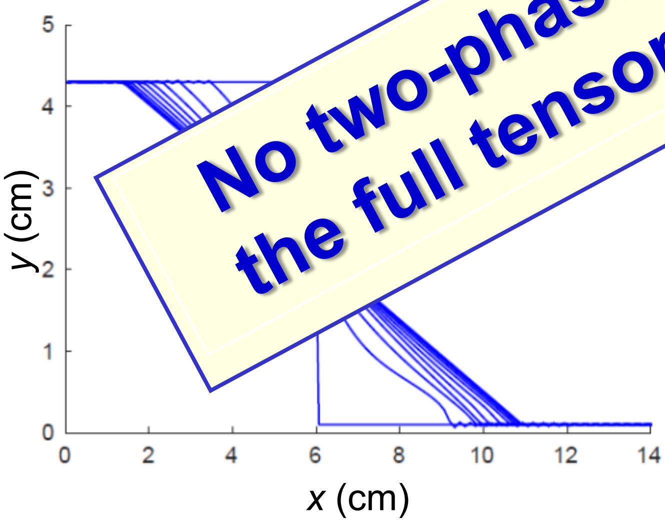

nitially loose

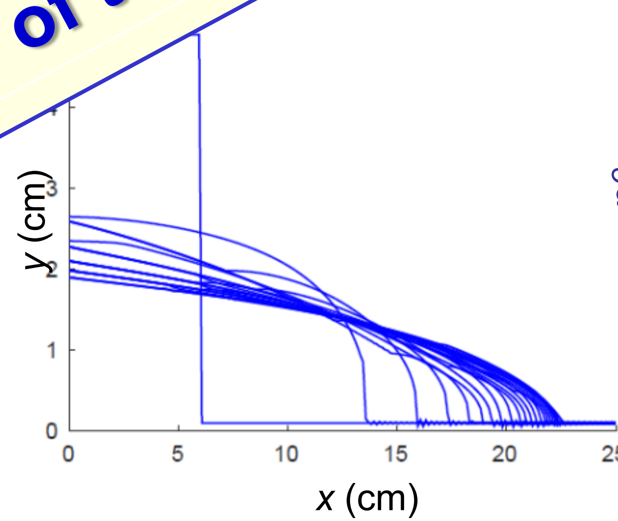

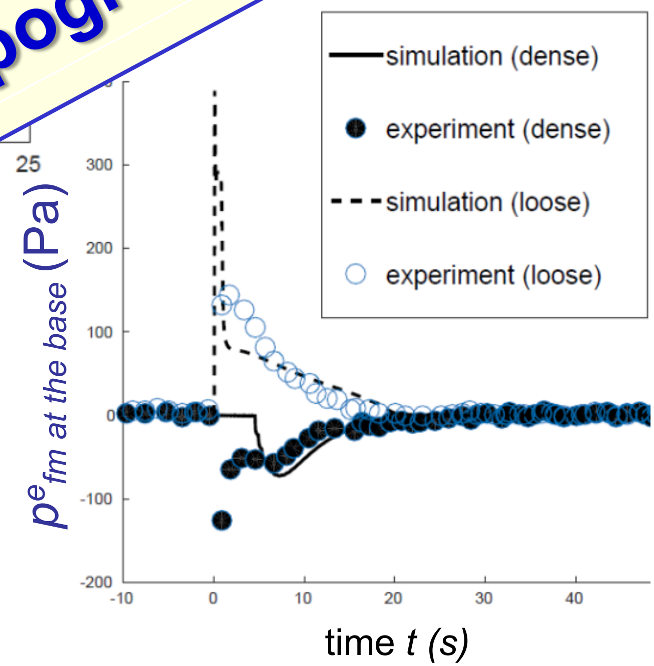

Bouchut et al., 2018